



HAL
open science

Is there still something to eat for trees in the soils of the Strengbach catchment?

Matthias Oursin, Marie-Claire Pierret, Émilie Beaulieu, Damien Daval,
Arnaud Legout

► To cite this version:

Matthias Oursin, Marie-Claire Pierret, Émilie Beaulieu, Damien Daval, Arnaud Legout. Is there still something to eat for trees in the soils of the Strengbach catchment?. *Forest Ecology and Management*, 2023, 527, pp.120583. 10.1016/j.foreco.2022.120583 . hal-04240345

HAL Id: hal-04240345

<https://cnrs.hal.science/hal-04240345v1>

Submitted on 13 Oct 2023

HAL is a multi-disciplinary open access archive for the deposit and dissemination of scientific research documents, whether they are published or not. The documents may come from teaching and research institutions in France or abroad, or from public or private research centers.

L'archive ouverte pluridisciplinaire **HAL**, est destinée au dépôt et à la diffusion de documents scientifiques de niveau recherche, publiés ou non, émanant des établissements d'enseignement et de recherche français ou étrangers, des laboratoires publics ou privés.

Copyright

Is there still something to eat for trees in the soils of the Strengbach catchment?

Matthias Oursin¹, Marie-Claire Pierret¹, Émilie Beaulieu^{1,2}, Damien Daval³, Arnaud Legout⁴

¹ITES Institut Terre et Environnement de Strasbourg - CNRS/Université de Strasbourg - 5 rue Descartes, 67000 Strasbourg. France. Oursin@unistra.fr / marie-claire.pierret@unistra.fr

²ENGEES - École Nationale du Génie de l'Eau et de l'Environnement. 1 quai Koch- 67000 Strasbourg. France. beaulieu@engees.unistra.fr

³Damien Daval – ISTerre Institut des Sciences de la Terre – CNRS/Université Grenoble Alpes 38000 Grenoble damien.daval@univ-grenoble-alpes.fr

⁴INRAE, BEF, rue d'Amance, 54280 Champenoux. France. arnaud.legout@inrae.fr

Corresponding author: Marie-Claire Pierret marie-claire.pierret@unistra.fr

Key words: forested soils, fertility, experimental leaching, Sr isotopes, numerical modelling

Highlights:

- Exchangeable Ca might be only partly available for tree nutrition
- Low Ca release might be due to strong bindings with clay and organic matter
- Sr isotopic composition of leaching solutions helps understanding the Ca reactivity
- Atmospheric deposition and efficient biological cycling sustain tree nutrition

1 **Is there still something to eat for trees in the soils of the Strengbach catchment?**

2 Matthias Oursin¹, Marie-Claire Pierret¹, Émilie Beaulieu^{1,2}, Damien Daval³, Arnaud Legout⁴

3

4 ¹ITES Institut Terre et Environnement de Strasbourg - CNRS/Université de Strasbourg - 5 rue
5 Descartes, 67000 Strasbourg. France. Oursin@unistra.fr / marie-claire.pierret@unistra.fr

6 ²ENGEES - École Nationale du Génie de l'Eau et de l'Environnement. 1 quai Koch- 67000
7 Strasbourg. France. beaulieu@engees.unistra.fr

8 ³Damien Daval – ISTERre Institut des Sciences de la Terre – CNRS/Université Grenoble Alpes
9 38000 Grenoble damien.daval@univ-grenoble-alpes.fr

10 ⁴INRAE, BEF, rue d'Amance, 54280 Champenoux. France. arnaud.legout@inrae.fr

11 Corresponding author: Marie-Claire Pierret marie-claire.pierret@unistra.fr

12

13 **Abstract**

14 The global demand for wood is growing and the sustainability of forests has become an
15 increasingly important issue. The first metre of soil represents the reserve of nutrients cations
16 (K, Ca, Mg) for trees. The depletion of these elements in the soil gradually leads to a decrease
17 in soil fertility, which can have a strong impact on the development and health of forests.

18 The aim of this study was to better understand the source and dynamics of nutrients in forested
19 soils from a base poor environment by combining mineralogic, chemical, isotopic and
20 numerical tools through an experimental approach. We designed batch experiments to follow
21 the leaching of soils from two experimental plots (under spruce and under beech from the
22 Strengbach catchment, Vosges Mountain, NE France). The studied elements show highly
23 contrasting behaviours. Mg release results from a mixing between cationic exchange, mineral
24 dissolution (mainly smectite) and organic matter mineralization. The dynamics of K are
25 underestimated by modelling, which may be attributed either to an unknown source of K or to
26 an overestimation of the secondary phase precipitation. The Sr isotopic approach, used as a
27 proxy to identify the sources of Ca, shows that the exchangeable complex supplies nutrients
28 first and rapidly to the solution, followed by the clay compartment and at the very end, the bulk
29 soils. Na is mainly controlled by albite dissolution.

30 The release of Ca is significantly lower than that of other cations as Mg or K. Our results suggest
31 that the exchangeable Ca, estimated through classical extractions, is only partly available for
32 plants, due to strong chemical binding with organic matter and/or the occurrence of Ca-
33 chemical bridges between clay and organic matter. Sustainable management should thus
34 consider that exchangeable Ca, conventionally determined, does not necessarily provide an
35 accurate picture of the real availability of Ca and therefore of the fertility of soils, with a risk
36 of overestimation of nutrient reservoir for trees. Calcium tree nutrition at these sites has to rely
37 on the long term on atmospheric deposition and an efficient recycling through biological
38 cycling. This is also true for the other nutrient cations, but to a lesser extent since soil intrinsic
39 fluxes (i.e., weathering, mineralisation of OM...) are not null and may thus supply the
40 exchangeable pools and participate substantially to tree nutrition. Harvesting and biomass
41 exportation could rapidly impact the biological cycle and threaten the sustainability of these
42 ecosystems, similar to changing tree species that may influence the nature of the litter, its
43 turnover and the input of nutrients to the soil.

44

45 **Key words:** forested soils, fertility, experimental leaching, Sr isotopes, numerical modelling

46

47 **Highlights:**

- 48 • Exchangeable Ca might be only partly available for tree nutrition
- 49 • Low Ca release might be due to strong bindings with clay and organic matter
- 50 • Sr isotopic composition of leaching solutions helps understanding the Ca reactivity
- 51 • Atmospheric deposition and efficient biological cycling sustain tree nutrition

52 1. Introduction

53 Increased human activities (both industrial and transport) has led to the emission of atmospheric
54 pollutants such as SO₂ and NO_x, which were maximal in Europe during the 1970s (Klimont et
55 al., 2013). The transformation of these contaminants in the atmosphere generated atmospheric
56 acid deposits that are able to modify and impact, sometimes strongly, natural ecosystems,
57 through soil and stream water acidification (Probst et al., 1999; Lucas et al., 2011; Tian and
58 Niu, 2015), reduction of stream (Guerold et al., 2000) or soil (Wei et al., 2017) biodiversity,
59 and damage to vegetation (Cape, 1993) such as forest decline (Reichle, 1981; Paces, 1985;
60 Schulze, 1989; Probst, Fritz, and Stille, 1992; Dambrine et al., 2000; Poszwa et al., 2000;
61 Thimonier, Dupouey, and Le Tacon, 2000; van der Heijden et al., 2011; Cohen et al., 2016;
62 Legout et al., 2020).

63 Although soil acidification is a natural process that plays a key role in pedogenesis and the
64 supply of nutrients for plants, an excessive input of protons can significantly modify the soil
65 equilibrium between microorganisms, weathering, and exchangeable phases, and therefore
66 impact vegetation in forest ecosystems (Rodhe et al., 1995; Calace et al., 2001; Bolan, Adriano,
67 and Curtin, 2003; Qiu et al., 2015). Proton input may be balanced by cationic exchange and/or
68 weathering of soil minerals (Ulrich, 1986; Li et al., 2018), but strong soil acidification can result
69 in the loss of nutrient cations and soil desaturation with the dominance of H⁺ and Al³⁺ on the
70 cationic exchangeable capacity (CEC), making nutrient cations less available for plants. The
71 decrease of the bioavailability of these essential cations may result in plant chlorosis, leaf and
72 needle yellowing and/or loss (Mehne-Jakobs, 1995; DeHayes et al., 1999; Siefertmann-Harms
73 et al., 2004), and may ultimately lead to forest decline (Durka et al., 1994; Likens, Driscoll and
74 Buso, 1996; De Vries et al., 2014).

75 The global emission of acid rain precursors, especially SO₂, has declined since the 1980s,
76 resulting in a decrease in the acidity of atmospheric deposits recorded in many places around

77 the world (Smith, Pitchera, and Wigley, 2001; Khokhar et al., 2005; Kopáček and Veselý, 2005;
78 Lu et al., 2010; Klimont, Smith, and Cofala, 2013; Sudalma, Purwanto, and Santoso, 2015;
79 Pierret et al., 2018; 2019). Despite this decline, numerous forest ecosystems show very little
80 sign of recovery (Stoddard et al., 1999; Sverdrup et al., 2006; Jonard et al., 2012), especially
81 in the Vosges Mountain (northeast France) mainly due to base poor bedrock and chemically
82 poor soils (Landmann, 1995; van der Heijden et al., 2011; Legout et al., 2020). Acidification
83 may also be reinforced by other pressures such as forest management, especially through the
84 choice of tree species and the exportation of biomass (Augusto, Bonnaud, and Ranger, 1998;
85 Augusto et al., 2002; Berger, Köllensperger, and Wimmer, 2004; Legout et al., 2016), which
86 may jeopardize the recovery of these forest ecosystems.

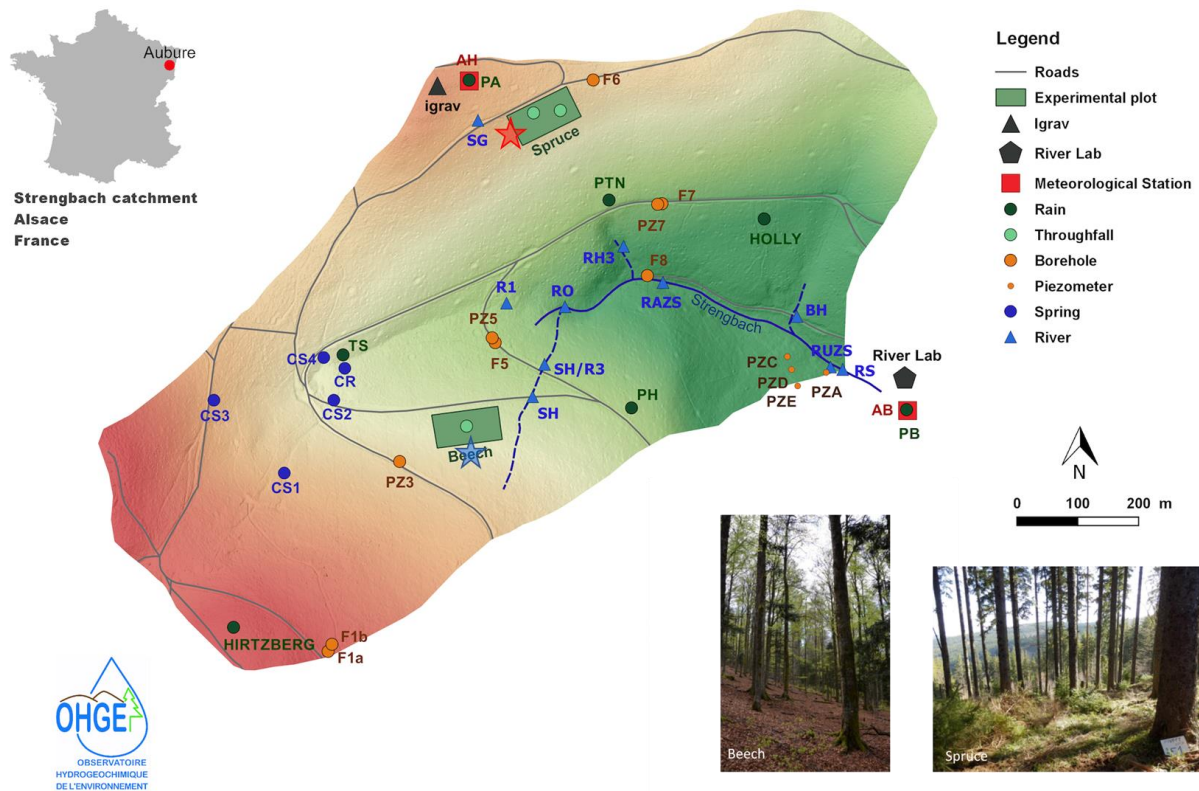
87 In soil, Ca, Mg, and K are present in different forms with different levels of bioavailability:
88 entrapped within organic matter (available through mineralization), within primary and
89 secondary minerals (available through weathering) or adsorbed on the cationic exchangeable
90 capacity (available by ionic exchange). The true bioavailability of Mg and Ca for plants is
91 difficult to define, measure and accurately assess and is still not clearly understood (Jandl,
92 Alewell, and Prietzel, 2004; Jonard et al., 2009; van der Heijden et al., 2011; Hansson et al.,
93 2020). Usually, the chemical fertility of forested soil is investigated from the determination of
94 the global CEC and its composition in Mg, Ca, K and Na. However, atmospheric deposits and
95 weathering of soil minerals have to be considered because they are the main sources of nutrient
96 cations in forest ecosystems, and the recycling by plants also plays an important role in
97 maintaining and optimizing these nutrients in the soil-plant system (Cole, 1986; van der Heijden
98 et al., 2013; Dessert et al., 2020; Turpault, Calvaruso, and Dincher, 2019). However, in
99 chemically poor soils widely affected by strong past acidification, we may question the
100 remaining capacity of soils to supply nutrient cations for plant growth, especially through the
101 weathering of soil minerals. Numerous environmental and societal issues including

102 development of sustainable forestry, the use of wood as a renewable energy or as a way to store
103 CO₂ depend on forest healthiness, practices and management (Chum and Overend, 2001; Viana
104 et al., 2010; Ellabban, Abu-Rub, and Blaabjerg, 2014; Pang et al., 2019). Currently, we need to
105 provide a better characterization of the actual availability of nutrient cations in soils, their
106 origins and their dynamics to provide forest managers and policy makers with the most accurate
107 picture of the potential of forest ecosystems and associated threats.

108 The main objectives of this study were to evaluate the potential contribution of this chemically
109 poor soil to tree nutrition through the supply of nutrient cations in the mid- to long-term. For
110 this purpose, Here, we developed a new approach based on laboratory experiments to study the
111 interactions between water and natural acidic soils from a well-monitored field site
112 characterized by low pools of nutrient cations (Strengbach catchment, Vosges Mountains,
113 France). We designed batch experiments with soil samples from two plots characterized by
114 different soil and vegetation types.

115 2. Site descriptions

116 To better understand the relationship between forest decline and acid rain, several investigations
117 have been conducted since the 1980s in the Strengbach catchment (Dambrine, Le Goaster, and
118 Ranger, 1991; Probst, Fritz, and Stille, 1992; Probst et al., 1992; 1999; Pierret et al., 2018).



119

120 Fig. 1: Strengbach catchment map with different equipment and monitoring stations (see
 121 legend). The red star corresponds to the soil pit at the SP site (SP: Spruce plot), and the blue
 122 star corresponds to the soil pit at the BP site (BP: beech plot).

123

124 Located in the Vosges Mountains (Northeast of France), the Strengbach catchment covers an
 125 area of 80 ha with altitudes ranging from 883 to 1146 m. Since 1986, the catchment has been
 126 highly equipped allowing a continuous monitoring of meteorological, geochemical and
 127 hydrological data.

128 Today, the Strengbach catchment is monitored by OHGE (Observatoire hydrogéo chimique de
 129 l'environnement, <http://ohge.unistra.fr>) and is involved in the French critical zone observatories
 130 network OZCAR (<http://www.ozcar-ri.org>) (Gaillardet et al., 2018).

131 Approximately 90% of the catchment is covered by commercially managed forest, principally
 132 dominated by conifers (80%, *Piceas Abies L.*) and beeches (20%, *Fagus Sylvatica*). Plantations

133 are between 70 and 175 years old (Pierret et al., 2018). The stands are managed by the National
134 Forestry Office and are exploited for the municipality of Aubure. Wood represents a significant
135 economic resource for the municipality and the health of the forests is therefore a major issue
136 in mountain areas. The climate type is oceanic mountainous. The annual temperature is 6 °C
137 and the mean annual precipitation and discharge are 1370 mm and 760 mm respectively for the
138 period 1986-2015 (Pierret et al., 2018). Due to a north exposition, the southeast side is colder,
139 more humid and rainier than the south-exposed northwest side (Pierret et al., 2018).

140 The main bedrock of the catchment is a Hercynian base-poor granite (cordieritic granite) with
141 low Ca and Mg contents (Bonhomme, 1967). The granite on the northern slope is more
142 hydrothermally altered than that on the southern slope (El Gh'Mari, 1995). Hydrothermal
143 events caused the alteration and transformation of albite, K-feldspar and muscovite into fine-
144 grained illite and quartz; biotite and albite disappeared to a large extent (Pierret et al., 2014).

145 The soils range from ochreous podzolic to brown acidic soils and are approximately 1 metre
146 thick (Lefèvre, 1988). The brown acidic soils are mainly located in the northern part of the
147 catchment whereas the podzolic soils are mainly in the southern part. The soils of the
148 Strengbach catchment are acidic, with pH ranging from 3.4 at the top of the profiles to 4.9 at 1-
149 metre depth. The humus is generally moder or mor.

150 Two experimental forested plots were deeply monitored to investigate the atmosphere/soil/plant
151 interactions by regular monitoring and sampling of throughfalls, soil solutions, soils, litters or
152 plants (Pierret et al. 2019). Each parcel is representative of the two main ecosystems: one under
153 spruce on brown acidic soil and on the northern slope (SP site), and the second one under beech
154 on ochreous soils and on the southern slope (BP site; cf. Fig. 1). The soils sampled and studied
155 in the present work came from these two plots.

156 The long-term monitoring of the Strengbach catchment showed the following trends:

- 157 - There was a significant decrease in the concentrations of H^+ , SO_4^{2-} , Cl^- , and Ca^{2+} in
158 precipitation and throughfalls. These decreases are linked to the decrease in anthropic
159 SO_2 emissions, and of particles from industrial processes (Pierret et al. 2019).
- 160 - A continuous decrease in Ca and Mg in soil solution since 1986 under spruces and
161 beeches is probably due to modification of cation exchange processes (Prunier et al.,
162 2015; Schmitt et al., 2017; Dambrine et al., 1998; Beaulieu et al., 2020)
- 163 - Ca and Mg deficiencies in the needles of spruce are attributed to the low contents in the
164 soils, with a 30% needle loss and needle yellowing (Dambrine et al., 1991; Landmann,
165 1995).

166 3. Methods and analytical procedures

167 3.1. Sample collection

168 Two soil profiles were collected in April 2017: one at the SP site (under spruce), and one at the
169 BP site (under beech; Fig. 1). In the field, we dug pits with a surface of about 1 x 2 m with a
170 mechanical shovel. For each horizon we evaluated the proportions of coarse elements and roots.
171 The profiles were divided into the following horizons: 00-05 cm; 05-10 cm; 10-20 cm; 20-40
172 cm; 40-60 cm and 60-80 cm. The surface differentiation (0-20 cm) is finer because of the higher
173 contents of organic matter and clays which are important and dynamic reservoirs of nutrients.
174 Under 20 cm depth, we studied layers of 20 cm thickness. The soil samples were sequentially
175 sieved (4 cm and 4 mm) in the field. For each soil layer, approximately 1 kg of the fraction
176 between 4 mm and 4 cm was collected and 2 kg for the fraction lower than 4 mm from a big
177 box that has been carefully homogenized. For each horizon, the roots were also separated and

178 weighed. We work with the fine soil i.e. the fraction < 2mm, as it is classically the case in
179 pedology.

180

181 3.2. Litter analyses

182 Two different levels of humus were collected:

- 183 - OL, anything that falls to the ground and is still almost intact
- 184 - OH-OF, characterized by an absence of any recognizable plant structure.

185 The litter was then several times washed and rinsed with ultrapure water to remove impurities
186 and small rock fragments (the heavier soil particles settle to the bottom and can be separated
187 from the litter). The chemical concentrations in litter were determined by alkaline fusion with
188 LiB_2O_4 . The solution obtained was analysed by ICP-OES (ICP-OES 6500 radial ThermoFisher)
189 for major elements with an accuracy of $\pm 2\%$ and by ICP-MS (X7 ThermoFisher) for trace
190 elements with an uncertainty of 10 %. The accuracy was controlled using a spinach Standard
191 Reference Material® 1570a (Carignan et al., 2001).

192 3.3. Soil analyses

193 Each soil sample was dried at 50°C and all the analyses were performed with the fine soil
194 fraction (<2 mm). In the laboratory we carefully homogenized this initial fraction, then we
195 carefully divided it into sub-samples with a sample splitter until we obtained the mass necessary
196 for our experiments. We thus obtained several aliquots of the same initial homogeneous soil
197 that we used for the different analyses and for the 3 experiments.

198 This methodology allows us to work in a repeatable way. The pH_{water} was determined according
199 to the standard NF ISO 10390. The composition of the exchangeable phase (Al, Fe, Na, Mg,
200 Ca, K and H) and the CEC were determined following cobaltihexamine extraction, with an
201 uncertainty of 10%, according to the standard NF X 31-130 and described by Ciesielski et al.
202 (1997a; 1997b).

203 Clay (grain size $< 2\mu\text{m}$), fine silt (2 – 20 μm), coarse silt (20-50 μm), fine sand (50-200 μm)
204 and coarse sand (200-2000 μm) size fractions were determined according to the standard NF X
205 31-107. All these analyses were performed at INRA LAS (Arras, France).

206 The mineralogical composition of the soil samples was determined by X-ray diffraction (XRD)
207 using a Bruker AXS D5000 X-ray diffractometer at LHYGES (Strasbourg, France). The clay
208 fraction was extracted by sedimentation, using the Stokes law, according to Robert and Tessier
209 (1974). To remove organic matter, a pretreatment with hydrogen peroxide was realized for the
210 soil sample with high OM contents (all samples above 20 cm depth). Four different treatments
211 allow the identification of the different clay minerals: air drying without treatment; drying at
212 490°C for 4 hours; 24 h under an ethylene glycol saturated atmosphere; and 24 h under a
213 hydrazine monohydrate saturated atmosphere (Larque and Weber, 1978; Thiry et al., 2013).

214 The chemical composition of bulk soils and clay fractions were determined by alkaline fusion
215 with LiB_2O_4 following the protocol described in Carignan et al. (2001). The major and trace
216 elements were analysed at the CRPG, Nancy, France, using the same methods as described in
217 the previous section for litter. The uncertainties are 2% for major elements and 10% for Sr
218 concentrations.

219 3.4. Leaching experimental set up

220 To avoid contamination by materials, all the laboratory equipment used was washed beforehand
221 with the following protocol: 24 h 10%-HCl bath, double rinsing, two sequential 24 h water
222 baths and double rinsing. Ultrapure water (resistivity $< 18 \text{ M}\Omega \cdot \text{cm}$) was used for this purpose.
223 Discontinuous batch experiments between soils and acidic solutions were conducted. For each
224 experiment, after a homogeneous splitting, 5 g of soil from the 6 horizons of the two soil profiles
225 (SP and BP) was put into a 50 mL conical centrifuge tube (Falcon™) with 40 mL of ultrapure
226 hydrochloric acid at pH 3.5. The pH of the solution was chosen to mimic the pH of the
227 superficial soil solution (Pierret et al. 2019). After a variable time of experimentation ΔT during

228 which the reactors were continuously stirred, each tube was centrifuged at 4700 rpm for 40 min,
 229 allowing the soil to flocculate at the bottom of the cone. Then, the supernatant was recovered
 230 for chemical and isotopic analyses. The reactors were then refilled with 40 mL of fresh solution,
 231 thus the soils are resuspended in the solution, for an additional step of solution-soil interactions.
 232 Eleven successive steps were conducted over 150 days in total, according to an increasing
 233 period of reaction (Table 1). At the final step of the experiments, the soils were dried and fully
 234 characterized for comparison with the initial soils. Each experiment was run in triplicate,
 235 representing 36 tubes at each time step.
 236

Number of step	T1	T2	T3	T4	T5	T6	T7	T8	T9	T10	T11
Name of the step (Nb of days)	D0.6	D1	D3	D5	D8	D12	D18	D28	D48	D96	D152
Δt	14 h	10 h	2 d	2d	3 d	4 d	6 d	10 d	20 d	48 d	56 d
Duration	14 h	1 d	3 d	5 d	8 d	12 d	18 d	28 d	48 d	96 d	152 d

237 Table 1: Time between each step (between T_i and T_{i-1}) and total duration (D_a ; d corresponding
 238 to the number of days) for each iteration of the batch experiments. In the figure the times will
 239 be represented with in index the total number of days of corresponding experiment.

240

241 3.5. Solution analyses

242 The pH of the solution was measured using a pHM210 meterLab pH-meter (Radiometer
 243 Analytical) fitted with a Mettler HA406-DXKS8 electroded. The precision of the pH-meter was
 244 ± 0.02 . The conductivity of the solution was measured using a CDM210 MeterLab (analytical
 245 radiometer) with a CDC 745-9 conductivity cell with a precision of 0.1 $\mu\text{S}/\text{cm}$.

246 The concentration of major elements was determined by ICP-AES (Thermo Scientific iCAP
 247 6000 SERIES – Thermo Fisher Scientific©) with an uncertainty of $\pm 2\%$. Trace elements were

248 analysed using ICP-MS (Thermo Fisher X Serie II – Thermo Fisher Scientific©) with indium
249 as an internal standard and with $\pm 10\%$ uncertainties.

250 3.6. Sr isotopes

251 Sr does not play a major role in plant nutrition, unlike Ca (Capo, Stewart, and Cahdwick, 1998).
252 However, Sr is often considered as a calcium analogue because of its similar chemical structure
253 (similar ionic charge, radius, electron configuration, etc...). Thus, the combination of $^{87}\text{Sr}/^{86}\text{Sr}$
254 and Ca/Sr ratios can be used to characterize the different Ca pools in ecosystems as atmospheric
255 deposits, soil solutions, litter, soil minerals, exchangeable fractions (Miller, Blum, and
256 Friedland, 1993; Bailey et al., 1996; Blum et al., 2002; Kennedy, Hedin, and Derry, 2002;
257 Bullen and Bailey, 2005; Pett-Ridge, Derry, and Barrows, 2009; Meek et al., 2016), and then
258 to discuss the signature of experimental solutions.

259 Solid samples (bulk soil and clays) were digested using a mix of HCl, HNO₃ and HF. Litter
260 samples were digested by microwaves with HNO₃/H₂O₂.

261 The experimental solutions and the exchangeable fractions were first evaporated and then
262 dissolved in two steps, with a mix of HCl/HNO₃ and then with HF.

263 The purification of Sr was performed with 0.05 N HNO₃ on an Eichrom Sr spec resin, 50-10
264 mesh using the protocol established by Horwitz, Dietz, and Fisher (1991) and Philip, Chiarizia,
265 and Dietz (1992). The yield of this purification step was between 88 and 92%. Isotopic ratios
266 were determined by MC-ICP-MS (Thermo Finnigan Neptune) at LHyGeS, France (Pierret et
267 al., 2014; Prunier et al., 2015; Brazier, 2018). The repeatability of the Sr isotopic analyses was
268 tested by regular measurements of standard NBS 987 (prepared following the methods used for
269 the samples). The resulting mean value of NBS 987 $^{87}\text{Sr}/^{86}\text{Sr}$ was 0.710256 ± 0.00003 (n = 62).

270 3.7. Numerical modeling of the reactivity of soil samples

271 - Description:

272 The WITCH code is a geochemical box model that can be used to calculate the evolution of the
 273 soil solution composition as a function of time in a given soil profile (Godd ris et al., 2006,
 274 2010; Beaulieu et al., 2012). Here, the code was used as a tool to single out the sources of the
 275 release of several key elements over the course of the experiments. The code accounts for
 276 dissolution/precipitation processes and the exchange fluxes with the exchange complex surface.
 277 The mass balance is solved in each box at each time step and for each chemical species as
 278 follows:

$$279 \frac{d(z.\theta.C_i)}{dt} = F_{in} + F_{out} + \sum_{j=1}^{n_m} F_{diss,i}^j - \sum_{j=1}^{n_m} F_{prec,i}^j \pm F_{exch} \quad (1)$$

280 where C , z and θ are the concentration of chemical species i , the thickness and the water content
 281 in the considered soil box, respectively. The F_{in} and F_{out} parameters represent the input and
 282 output fluxes of chemical species estimated from vertical drainage. F_{diss} and F_{prec} are the fluxes
 283 resulting from dissolution and precipitation processes of minerals j in the considered box,
 284 calculated using kinetic rate laws derived from laboratory experiments, and based on the
 285 transition state theory. The cation flux exchange (F_{exch}) between the soil solution and the clay-
 286 humic complex is calculated according to the Fick's second law of diffusion (Sverdrup et al.,
 287 1995) and could be either negative or positive. The values of selectivity coefficients associated
 288 with the reactions of cation adsorption have been previously calibrated on the measured soil
 289 solutions of the Strengbach catchment and fixed at $10^{-2.7}$ for Ca^{2+} and 10^{-3} for Mg^{2+} , K^+ , and
 290 Al^{3+} (Beaulieu et al., 2020). These values are of the same magnitude as the values estimated in
 291 other studies (Ludwig et al., 1999; Cosby et al., 2001; Zetterberg et al., 2014). The selectivity
 292 coefficient is described as:

$$293 k_{H/BC} = \frac{H_{surf} \cdot E_{BC}}{BC_{surf}^{1/n} \cdot E_H} \quad (2)$$

294 where E_{BC} and E_H are the fractions of sites on the exchange complex occupied by a given cation
 295 BC (Ca^{2+} , Mg^{2+} , Al^{3+} , or K^+) and by H^+ respectively, BC_{surf} is the concentration of BC at the

296 exchange surface (with n the cation charge), and H_{surf} is the concentration of H^+ at the exchange
297 surface.

298 Two simulations were performed with soil samples from each site (HP and VP) with the
299 WITCH code in order to simulate the evolution of the soil solution in two soil layers: 0-5 cm
300 depth and 40-60 cm depth. The results of these simulations were then compared with the results
301 obtained from batch experiments for the same depths.

302 - Model inputs and outputs:

303 The parameters required for the simulations were chosen to be as close as possible to the
304 mineralogical, physical and chemical features of the reacted powders and the experimental set-
305 up. We used the mineralogical composition of the two soil layers (0-5 cm and 40-60 cm depths)
306 estimated from XRD (see #3.3). The measurements of exchangeable cation contents (see #3.3)
307 were used to set the initial fraction of the CEC sites occupied by each cation for each soil layer.
308 The initial water content of each soil layer was set at its maximum (θ_{sat}), corresponding to solids
309 fully immersed in aqueous solution. Last, the specific surface area of minerals was fixed to 10
310 m^2/g for secondary phases and to 0.1 m^2/g for the primary phases (Hayes et al., 2020).

311 At the end of the simulation, the WITCH code allows to estimate the evolution of the
312 concentration of each cation in the solution of the considered box, the fluxes resulting from the
313 exchange between the solution and the clay-humic complex, the solution saturation index with
314 respect to each mineral and the fluxes resulting from mineral dissolution/precipitation.

315 4. Results

316 4.1. Soil analyses

317 4.1.1. Litters

318 For the two sites, the chemical concentrations were higher in the OF-OH layers than in the OL
319 layer, except for Ca (Table 2). The litters of the beech plot BP were enriched in Si, Al, Na and
320 K as opposed to Ca compared to the spruce plot SP (Table 2).

	Si	Al	Mg	Ca	Na	K	Sr	⁸⁷ Sr/ ⁸⁶ Sr	err (2σ)
	μg/g	μg/g	μg/g	μg/g	μg/g	μg/g	μg/g		
BP OL	12200	1231	549	3945	356	2515	11	0.753399	0.000003
BP OF-OH	55672	8402	772	2409	2411	7164	19	0.729347	0.000004
SP OL	11312	773	549	5618	<d.l.	1212	11	0.730029	0.000003
SP OF-OH	15800	2006	537	3473	215	2133	12	0.724282	0.000003

321
322 Table 2: Composition of the two litter layers for spruce (SP) and beech (BP) plots in μg/g. OL
323 corresponds to the horizon of recognizable remains, and OF-OH contains degraded materials
324 and humic components.

325

326 4.1.2. Characteristics of the soils and exchangeable phase

327 The soils are mainly sandy, with an average of 65% for the sandy fraction, except for the 00-05
328 cm horizon, which had lower values (45% on average) at both sites. Clay proportions decreased
329 with depth from 30% to 9% under BP, and from 30% to 16% under SP. The soils under spruces
330 had higher clay contents than those under beeches, especially below 20 cm depth (Table 3). For
331 both sites, the pH_{H2O} increases with depth, from 3.52 (respectively, 3.85) at the surface to 4.59
332 (respectively, 4.33) for the deepest horizon on BP (respectively, SP). SP soils are more acidic
333 than BP soils below 5 cm depth (Table 3).

334 The surface horizon is significantly more concentrated in organic matter due to the
335 decomposition of litter with almost 23% of C at 00-05 cm. C decreases with depth and reaches
336 1.6% and 0.6% in BP and SP deepest horizons, respectively. Below 10 cm depth, the BP soils
337 have higher OM contents than those of the SP site (Table 3).

338

339

	Depth	C	pH _{H2O}	Clay	Silt	Sand	CEC	Ca _{exch}	Mg _{exch}	K _{exch}	Na _{exch}	Al _{exch}	H _{exch}	CEC	Ca _{exch}	Mg _{exch}	K _{exch}	Na _{exch}	Al _{exch}	H _{exch}
	cm	%		%	%	%	cmol/kg						cmol/kg							
	Initial values													After experimentation						
Beech Plot	0-5	22.9	3.52	29.9	25.1	45	16.1	3.09	0.86	0.73	0.07	5.62	5.87	14.00	2.22	0.51	0.25	0.05	5.00	4.3
(BP)	5-10	4.2	3.56	16.8	22.7	60.5	8.49	0.31	0.16	0.19	0.03	6.21	2.24	7.15	0.18	0.09	0.34	0.1	5.04	0.96
	10-20	4.4	3.69	15	19.7	65.3	7.64	0.1	0.08	0.12	0.02	7.04	1.1	6.93	0.08	0.07	0.28	0.08	5.71	0.36
	20-40	2.6	4.12	15.5	20.5	64	8.35	0.07	0.04	0.09	0.03	8.93	<0.05	5.44	0.04	0.04	0.25	0.06	4.77	<0.05
	40-60	2.3	4.45	13.8	23.1	63.1	4.09	0.05	0.02	0.05	0.03	4.7	<0.05	3.04	0.03	0.02	0.17	0.04	2.83	<0.05
	60-80	1.6	4.59	8.6	26.7	64.7	2.41	0.03	0.01	0.03	0.02	2.68	<0.05	<1.5	0.03	0.02	0.16	0.04	1.72	<0.05
Spruce Plot	0-5	22.8	3.85	30.4	20.9	48.7	17.9	3.31	1.05	0.77	0.11	5.52	4.88	16.1	2.84	0.9	0.36	0.03	6.36	4.32
(SP)	5-10	8.1	3.54	18.9	17.3	63.8	9.97	0.69	0.25	0.22	0.03	6.53	2.89	10.8	0.56	0.28	0.45	0.04	7.31	1.62
	10-20	2.2	3.79	15.2	13.4	71.4	8.85	0.2	0.09	0.11	0.04	7.66	0.79	8.04	0.09	0.16	0.49	0.04	6.34	0.13
	20-40	1.3	4.04	19.5	19	61.5	8.8	0.16	0.05	0.1	0.02	8.93	0.21	8.86	0.07	0.12	0.49	0.03	7.47	<0.05
	40-60	0.8	4.17	17.8	16.5	65.7	7.99	0.09	0.03	0.1	0.02	8.61	0.27	7.81	0.04	0.13	0.52	0.03	6.71	<0.05
	60-80	0.6	4.33	16	16.1	67.9	7.13	0.07	0.03	0.1	0.02	7.81	0.13	6.93	0.05	0.18	0.64	0.04	5.75	<0.05

340

341 Table 3: Soil description (particles smaller than 2 mm diameter) from the beech and spruce
342 plots at the Strengbach catchment. CEC: Cation Exchange Capacity, determined with
343 cobaltihexamine. Data from the initial soils before leaching and after the end of the
344 experimentation.

345

346 CEC ranges from 16.1 to 2.4 and from 17.9 to 7.1 $\text{cmol}^+\cdot\text{kg}^{-1}$ with increasing depth, for soils
347 from the BP and SP sites, respectively (Table 1). The CEC corresponds mainly to the total
348 exchangeable sites in the clay humic complex and is related to the clay and OM concentrations.
349 As OM and clays, the CEC decreases with depth in both profiles, with higher values in SP soils.
350 These greater values are consistent with the higher clay contents in the SP than in the BP plots
351 (Table 3).

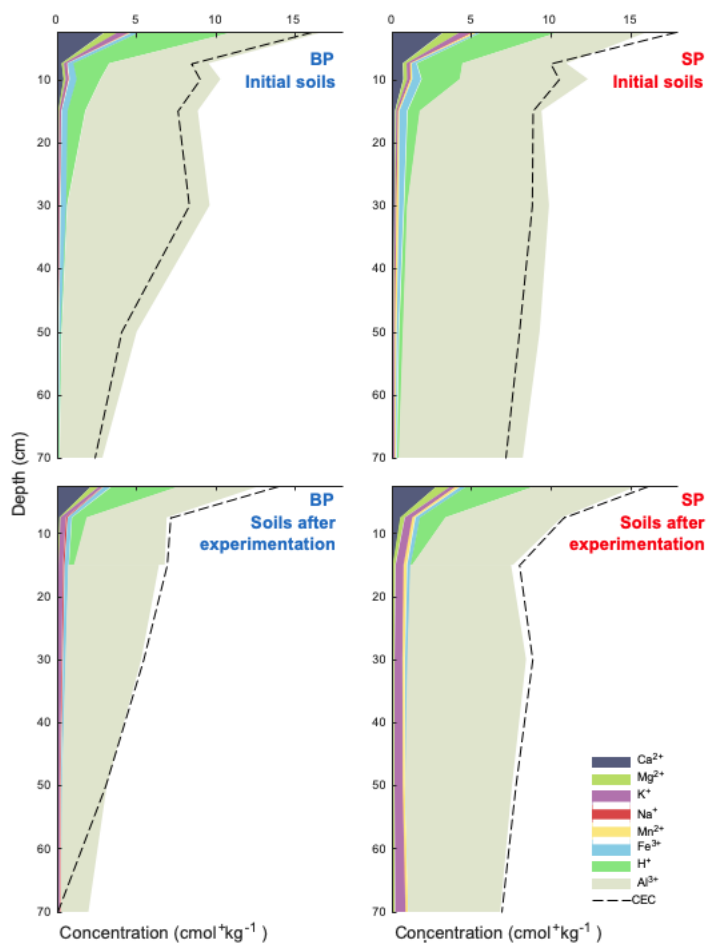
352 The CEC determined with cobaltihexamine was lower than the sum of the measured
353 exchangeable cation concentrations, except at 00-05 cm for the SP soil (Fig. 2; Table 3). The
354 difference between the CEC and the sum of exchangeable cations is on average 12% on both
355 sites, which may correspond to the uncertainty of the analyses (about 10%, see 3.3).

356 The chemical composition of the exchangeable pool presents similar evolution with depth for
357 both soil profiles, but with higher Ca, Mg, K, Mn and H concentrations in SP soils, having also
358 higher CEC than that in the BP soils (Fig. 2).

359 The exchangeable pool of the top 5 cm of soil strongly differs from the other layers, with higher
 360 Ca, Mg, K, Mn and H concentrations. Conversely, the Al and H concentrations are similar, each
 361 corresponding to approximately one-third of the CEC (Fig. 2). The 5-10 cm depth layers have
 362 intermediate chemical concentrations of Ca, Mg, K or protons. Below 10 cm depth, Al strongly
 363 dominates the exchangeable chemistry, representing more than 90% of the total pool (Fig. 2)
 364 and Ca, Mg, K and Na become minor elements.

365 The CEC and the concentration of exchangeable cations were also determined in the soil after
 366 the experiment (Table 3). Above 5 cm depth, Na, Mg in some cases and mainly K enriched the
 367 exchangeable fraction underlining changes in the nature of the exchangeable reservoir (Fig. 2;
 368 Table 3).

369



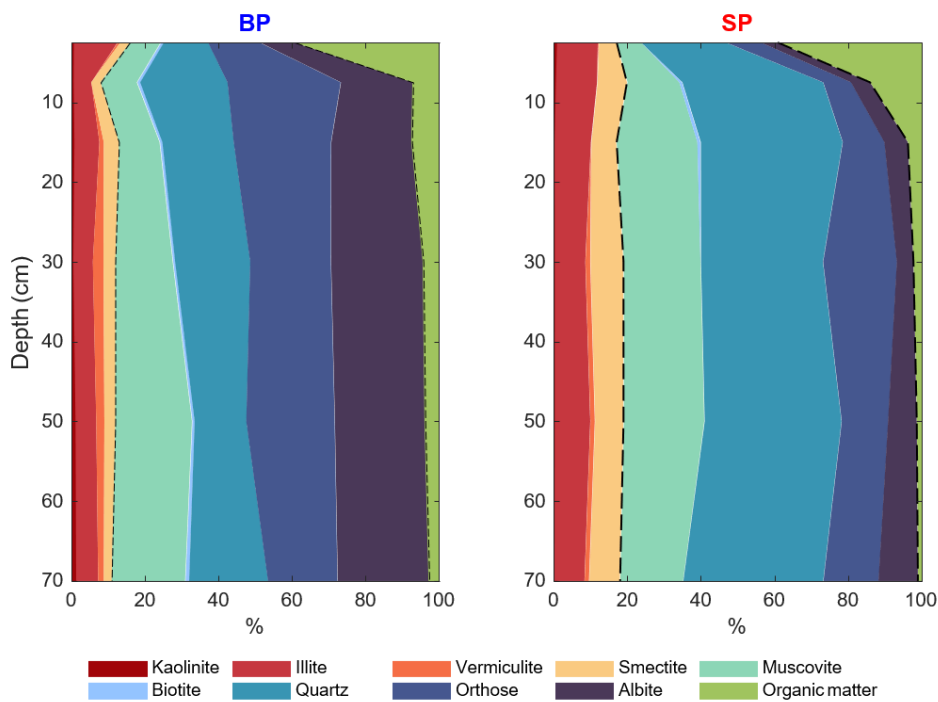
370

371 Fig. 2: Composition of the exchangeable phase for both BP (under beech) and SP (under spruce)
 372 soils at various depths, in initial soils and in soils after experimentation. Compositions were
 373 determined by cobaltihexamine extraction protocol.

374

375 4.1.3. Mineral and chemical composition of bulk soil and clay

376 The soils are composed mainly of a mix of organic matter, clays (kaolinite, illite, vermiculite
 377 and smectite) and primary minerals (muscovite, biotite, K-feldspar, albite and quartz). Since
 378 the proportions of organic matter and clays in each soil sample were already determined (cf.
 379 3.3), the proportion of primary minerals was simply deduced from the residual phase and
 380 quantified by XRD (cf. 3.3).



381

382 Fig. 3: Mineral composition in % of the soils from BP (left) and SP (right) profiles. Reddish
 383 parts correspond to clays, blueish parts correspond to primary minerals and greenish parts to
 384 organic matter (data in appendix A - supplementary material).

385 For both sites, organic matter dominates the soil composition at the surface (40% for the 0-5
 386 cm depth sample). Below 10 cm, the mineralogical composition remains rather stable along
 387 the soil profile. The proportions of kaolinite and biotite are very low for both sites. BP has a
 388 higher level of organic matter, K-feldspar and albite than SP. The soils from the SP site are
 389 characterized by higher clay contents in general, as well as higher quartz, illite and smectite
 390 contents than the BP site, especially in the 5-10 cm range (Fig. 3).

391

	Depth	Si	Al	Na	K	Mg	Ca	Sr	⁸⁷ Sr/ ⁸⁶ Sr	err (2σ)
	cm	mg/g	mg/g	mg/g	mg/g	mg/g	mg/g	μg/g		
Bulk soil										
Beech Plot (BP)	0-5	167.48	21.76	7.40	21.87	1.22	1.13	31.34	0.789114	0.000014
	5-10	290.94	36.94	13.23	39.32	1.79	0.89	45.51	0.806601	0.000016
	10-20	297.9	39.13	13.52	41.91	1.99	0.86	46.70	0.809622	0.000012
	20-40	303.32	40.62	13.79	41.73	1.97	0.84	48.29	0.806266	0.000012
	40-60	303.65	40.63	13.13	41.7	1.97	0.82	43.67	0.811786	0.00001
	60-80	295.84	44.96	14.83	40.62	2.54	1.11	43.12	0.809955	0.000026
Spruce Plot (SP)	0-5	182.3	20.09	2.10	18.90	1.78	0.79	35.40	0.757335	0.000014
	5-10	292.95	33.35	3.23	31.36	2.80	0.33	53.87	0.764484	0.000012
	10-20	332.91	33.93	3.26	34.40	2.75	0.36	51.24	0.764455	0.00001
	20-40	310.43	43.29	4.40	40.00	3.53	0.29	76.23	0.764404	0.000014
	40-60	314.68	43.31	4.61	41.80	3.42	0.32	72.43	0.768632	0.000016
	60-80	315.43	44.02	4.73	42.54	3.49	0.41	73.80	0.768716	0.000012
Clays										
Beech Plot (BP)	0-5	188.53	73.65	8.29	27.52	2.90	0.96	52.50	0.771566	0.000004
	5-10	241.73	135.13	6.44	42.12	6.15	0.61	42.65	0.83199	0.000003
	10-20	190.77	115.65	4.55	33.57	5.40	0.39	28.38	0.845975	0.000004
	20-40	207.95	139.78	1.33	45.37	7.83	0.07	32.20	0.848006	0.000006
	40-60	177.89	124.7	4.47	30.52	5.27	0.34	28.52	0.8329	0.000004
	60-80	167.53	128.25	4.38	27.62	5.33	0.39	26.04	0.825962	0.000004
Spruce Plot (SP)	0-5	171.55	85.19	2.48	31.62	4.46	0.69	72.17	0.751935	0.000004
	5-10	228.57	133.1	2.11	48.87	7.24	0.39	67.07	0.745304	0.000007
	10-20	198.52	128.35	1.25	44.55	7.24	0.07	32.99	0.836336	0.000003
	20-40	192.59	123.8	4.44	33.67	5.72	0.40	30.27	0.84285	0.000003
	40-60	204.07	136.65	1.22	44.03	7.74	0.07	29.34	0.857096	0.000003
	60-80	208.74	140.79	1.24	45.43	7.98	0.23	30.24	0.862445	0.000003

392

393 Table 5: Chemical and Sr isotopic composition of bulk soils and clays from the beech and
 394 spruce plots at the Strengbach catchment.

395

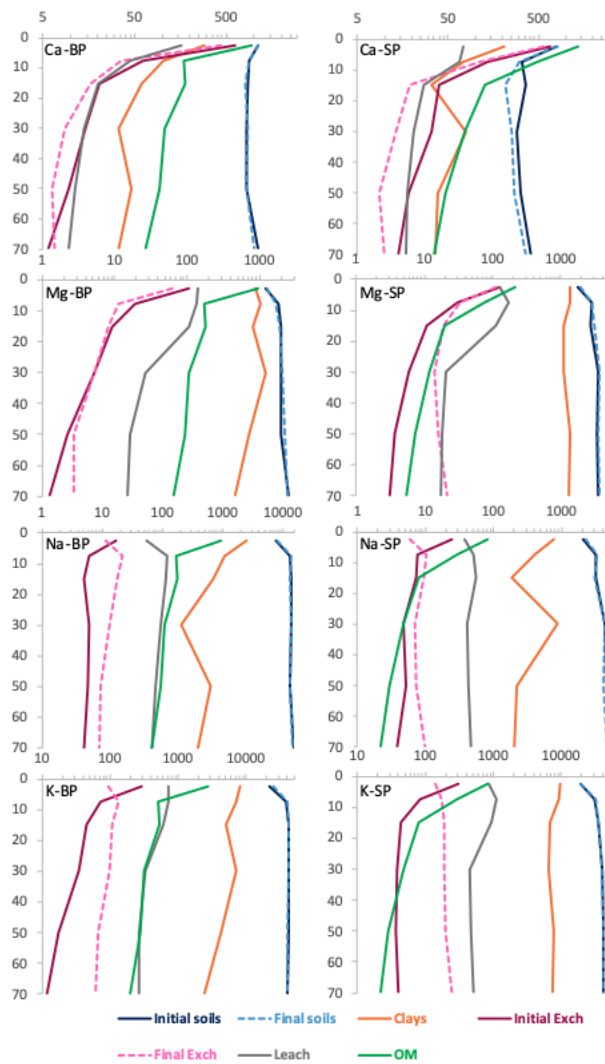
396 The chemical compositions in both plots were dominated by Si with overall values of 300 and
 397 200 mg/g for soils and clays respectively, except at the top profile characterised by the lowest
 398 values (Table 5). Bulk soil geochemical compositions vary little along the profile for each of
 399 the two sites, while those of the clays are more heterogeneous. Calcium is the least concentrated
 400 nutrient in bulk soils and clays. On the other hand, Ca is the only element with a higher surface

401 content in both profiles, with concentrations ranging from about $1 \text{ mg}\cdot\text{g}^{-1}$ in uppermost horizons
402 to 0.3 and $0.07 \text{ mg}\cdot\text{g}^{-1}$ in deeper compartments, for bulk soils and clays respectively. Except for
403 Ca, the uppermost horizon generally has the lowest concentrations, due to the high content of
404 organic matter.

405 In addition, significant chemical variations were observed between the two sites, especially for
406 bulk soils (Table 5). The sodium concentrations in BP bulk soils ($\approx 12 \text{ mg}\cdot\text{g}^{-1}$ on average) are
407 strongly higher those in SP soils ($3.7 \text{ mg}\cdot\text{g}^{-1}$ on average), consistent with the highest albite
408 content in BP profiles (Table 4, 5; Fig. 3). In contrast, Mg concentration was the highest in SP
409 soils (Table 5). In detail, the samples from the BP site exhibit slightly but significantly higher
410 Ca and K and lower Al and Sr contents in bulk soils than those from the SP site.

411 The proportions of the different reservoirs (organic matter, exchangeable phases, clays,
412 minerals) in the soil are represented on the same figure by element (Fig. 4), to compare the
413 contributions of the different soil constituents. Each reservoir is thus related to its proportion in
414 the bulk soil, and each elemental concentration expressed is normalized to one gram of soil
415 (Fig. 4, Appendix A-Supplementary material). The initial and final (after experiment)
416 concentrations of bulk soils and exchangeable pool are also represented in the same Figure, as
417 well as, the total cumulative concentrations of the experimental leachate solution (sum of the
418 quantities of each element leachate during the 11 steps of the experiment). The chemical
419 concentration of organic matter has been approximated from the proportion of organic matter
420 in the soils and the chemical composition of the degraded litter (OF-OH layer; Table 2) for each
421 type of soil profile (BP or SP). No significant variations ($p \text{ value} > 0.05$) were observed between
422 the initial and final concentrations in bulk soils, which was confirmed by the two very similar
423 blue curves in Fig. 4.

424



425

426 Fig. 4: Variation versus depth of chemical compositions (expressed in $\mu\text{g/g}$ of soil) for initial
 427 and final (after experimentation) bulk soils, compare with the contribution of different
 428 reservoirs as clay minerals, initial and final exchangeable pool, organic matter as total
 429 cumulated experimental leachate calculated for 1 g of soil (see text; Appendix A-
 430 Supplementary material) for two sites: BP-Beech Plot and SP-Spruce Plot.

431

432 4.2 Results of the leaching experiments

433

433 4.2.1 Chemistry of experimental solutions

434

434 4.2.1.1. Reproducibility of triplicates

435 The concentrations were monitored in each experiment run in triplicate (see 3.4). A standard
436 deviation was then estimated for all parameters at each step between the three results (Appendix
437 B. Supplementary material). Overall, the standard deviations calculated on the chemical
438 concentrations reveal good reproducibility.

439 The standard deviation varies with time and type of element. For example, calcium and sodium
440 have a low standard deviation of 5% on average while Si, Al and Mg have a standard deviation
441 of 10.4, 13.5 and 15.5% on average. Then the discussion will be based on the average values of
442 the three triplicates.

443

444 4.2.1.2. Temporal variation of concentration

445 The chemical concentrations were determined at 11 time steps during about 5 months of the
446 experiment (152 days; Table 1). The temporal variations show different patterns, depending on
447 the elements, site or depth (Fig. 5), which are:

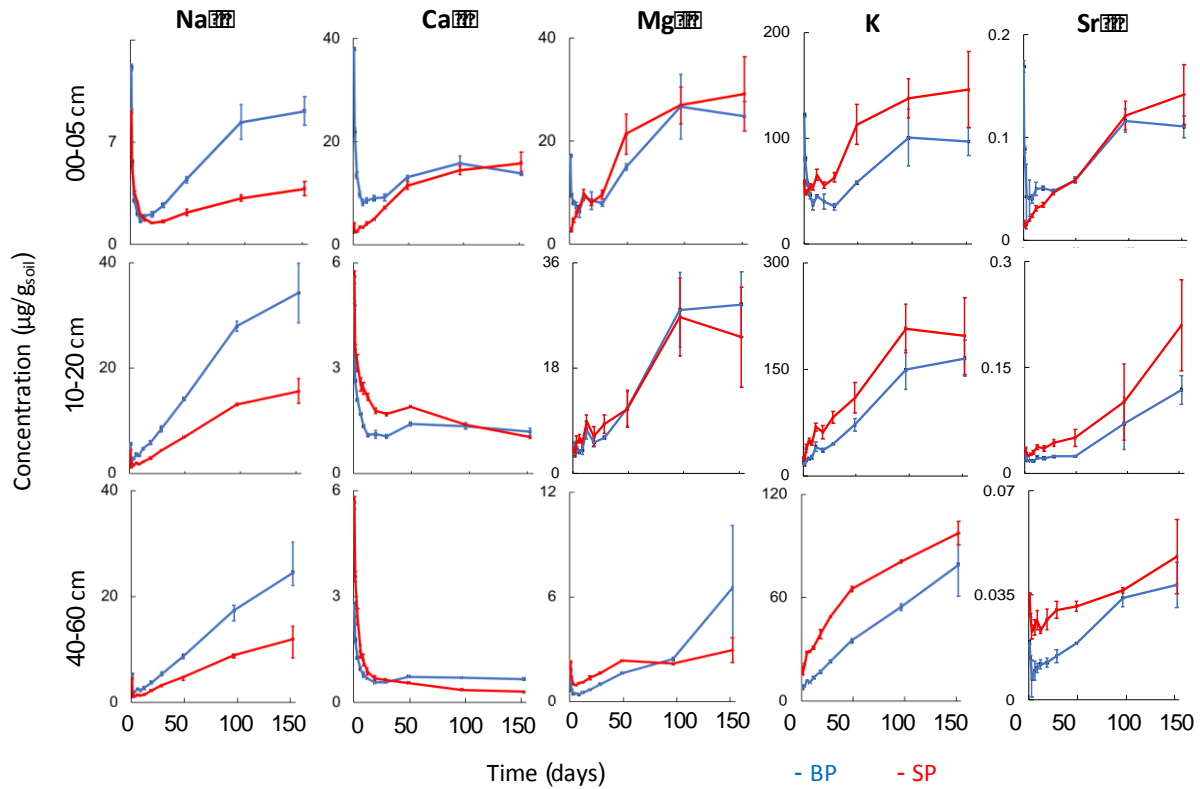
- 448 - Sharp decreases in concentration during the first steps followed by a regular increase
449 (e.g., Na in all cases and pH between 10 and 20 cm depth).
- 450 - Global increases in concentrations with different slopes (e.g., K in SP and BP profiles
451 below 20 cm depth).
- 452 - Sharp decreases in concentration at the beginning of the experiment, followed by an
453 increase prior to levelling off to a plateau value (e.g., Ca below 10 cm depth in BP
454 profile) or a decrease to lower values (Ca below 10 cm depth in SP profile).
- 455 - Sharp decreases, followed by a scattered increase for about 960h (40 days) (Mg, K
456 above 20 cm depth, pH in uppermost soils).

457 The main differences observed between the two profiles are as follows:

- 458 - Significantly higher Na and lower K concentrations in experiments conducted with BP
459 samples compared to experiments conducted with SP samples from all depths;

460 - Higher Mg, pH and lower Ca in experiments conducted with SP samples from uppermost
 461 soils and vice versa for samples from deeper levels.

462



463

464 Fig. 5: Na, Ca, Mg, K and Sr concentrations leached over time for experiments conducted with
 465 soils from three representative different depths (0-5; 10-20 cm; 40-60 cm). Concentrations are
 466 expressed in µg of element per g of soil. The concentrations for the BP and SP profiles are in
 467 blue and red, respectively. The symbols represent the average concentrations from triplicate
 468 measurements and the vertical bars indicate the standard deviation.

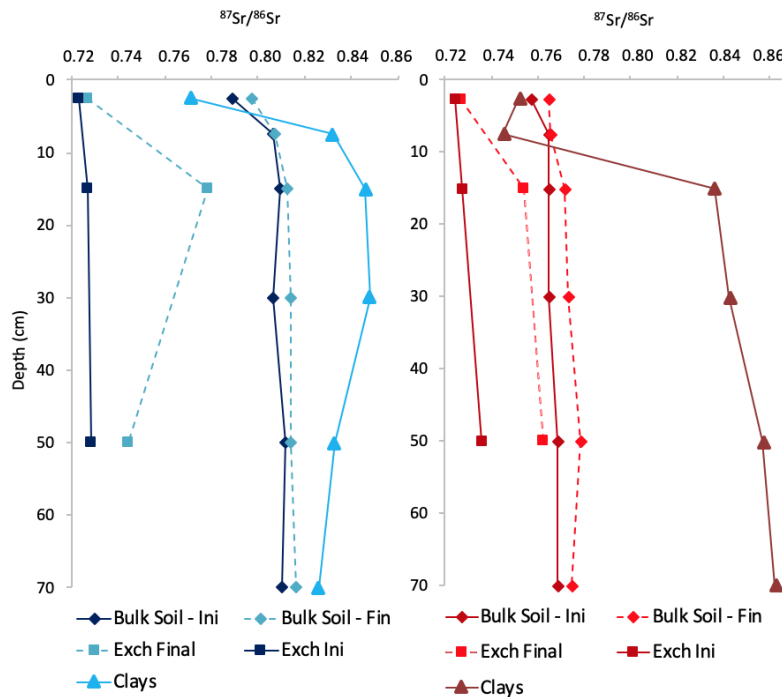
469

470 4.2.2. Sr isotopes

471 The bulk soils, as well as the litter samples from the BP sites have higher Sr isotopic ratios than
 472 those from the SP soils (Tables 2, 5, Fig. 6). The clays below 10 cm depth represent the most
 473 radiogenic materials with $^{87}\text{Sr}/^{86}\text{Sr}$ ranging from 0.82 to 0.86 (Fig. 6). The lowest Sr isotopic

474 ratios were measured in the topsoil exchangeable pool and in litter (Appendix A-supplementary
475 material; Fig. 6).

476 In general, the Sr isotopic ratios of bulk soils, clays and exchangeable pools increase with depth
477 in the SP profile and exhibit a maximum between 15 and 40 cm depth in the BP profile (Fig.
478 6).



479
480 Fig. 6: Evolution versus depth of the isotopic ratio $^{87}\text{Sr}/^{86}\text{Sr}$ of the clays, the bulk soils and the
481 exchangeable fraction (Exch.) before (init) and after leaching (final) in the BP profile (left) and
482 the SP profile (right).

483
484 For both bulk soils and the exchangeable pool, the isotopic signatures obtained after
485 experimentation are shifted towards higher values than the initial materials (Fig. 6), underlining
486 the preferential leaching of Sr with lower $^{87}\text{Sr}/^{86}\text{Sr}$ during experiments.

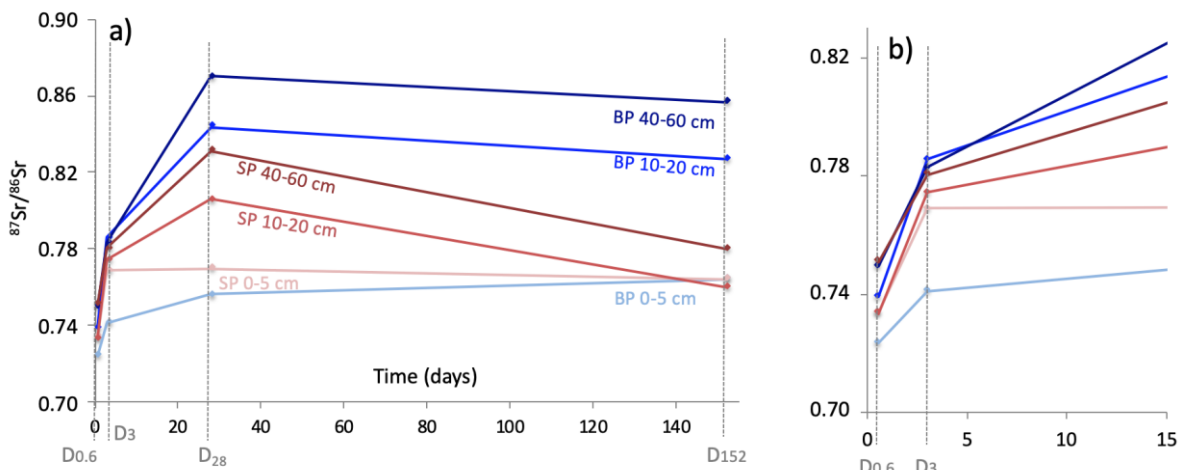
487 Four output solutions from the experiments were selected to study the evolution of isotopic
488 release over time: at $D_{0.6}$ (14 h), D_3 (3 days), D_{28} (28 d) and D_{152} (152 d) (Table 1). These times
489 are representative of the global dynamic, with two early times ($D_{0.6} = 14$ hours and $D_3 = 2$ days)

490 when the variations of concentration are the most important (Fig. 5) one intermediate and one
491 final time.

492 For each selected depth, the temporal evolutions of the experimental output solutions
493 systematically show the lowest Sr isotopic composition at $D_{0.6}$, a significant increase to D_3 and
494 then to D_{28} for both profiles. Between D_{28} and D_{152} , the values decrease or remain similar (Fig.
495 7)

496

497



498

499 Fig. 7: Variation of the $^{87}\text{Sr}/^{86}\text{Sr}$ isotopic ratios versus time for experimental BP and SP leached
500 solutions a) at 4 steps $D_{0.6}$ (14 h), D_3 (3 days), D_{28} (28 d) and D_{152} (152 d) and b) with a zoom
501 for the first 15 days, for 3 different soil horizons (0-5 cm; 10-20 cm and 40-60 cm).

502

503 5. Discussion

504 5.1. Strontium isotope variations to trace the origin of calcium

505 The Sr isotopic compositions allow tracing the origin of elements because of the lack of isotopic
506 fractionation during water/mineral interactions and biogeochemical reactions. It has been

507 frequently used to study the dynamics of Ca in atmosphere/soil/water/vegetation systems
508 (Graustein, 1989; Capo, Stewart, and Chadwick, 1998; Probst et al., 2000; Aubert et al., 2002;
509 Poszwa et al., 2004; Bélanger et al., 2012; Gangloff et al., 2014; Bedel et al., 2016; Blotevogel
510 et al., 2019; Novak et al., 2020).

511 5.1.1. Characterization of the different end-members:

512 Characterization of the different sources of Sr in the soils is essential to discuss the signature of
513 the leachates and their evolution during the experiments. This explains why we separately
514 analysed the exchangeable fractions, clays, soils and litters, in the present study.

515 Previous studies focused on tree samples from the two plots of the same catchment showed
516 $^{87}\text{Sr}/^{86}\text{Sr}$ ratios ranging from 0.72433 to 0.72577 at the BP site and from 0.71653 to 0.72349 at
517 the SP site for leaves and litters (Prunier, 2008; Prunier et al., 2015). With this data set and
518 those from the present study, we can define a mean biological end-member with $^{87}\text{Sr}/^{86}\text{Sr}$ ratios
519 of 0.7268 and 0.7230 for BP and SP, respectively. Based on the same studies, the mean Ca/Sr
520 ratios of tree samples (leaves and litters) were 418 and 447 for BP and SP, respectively. The
521 biological end-members shown in Fig. 8 correspond to these averages.

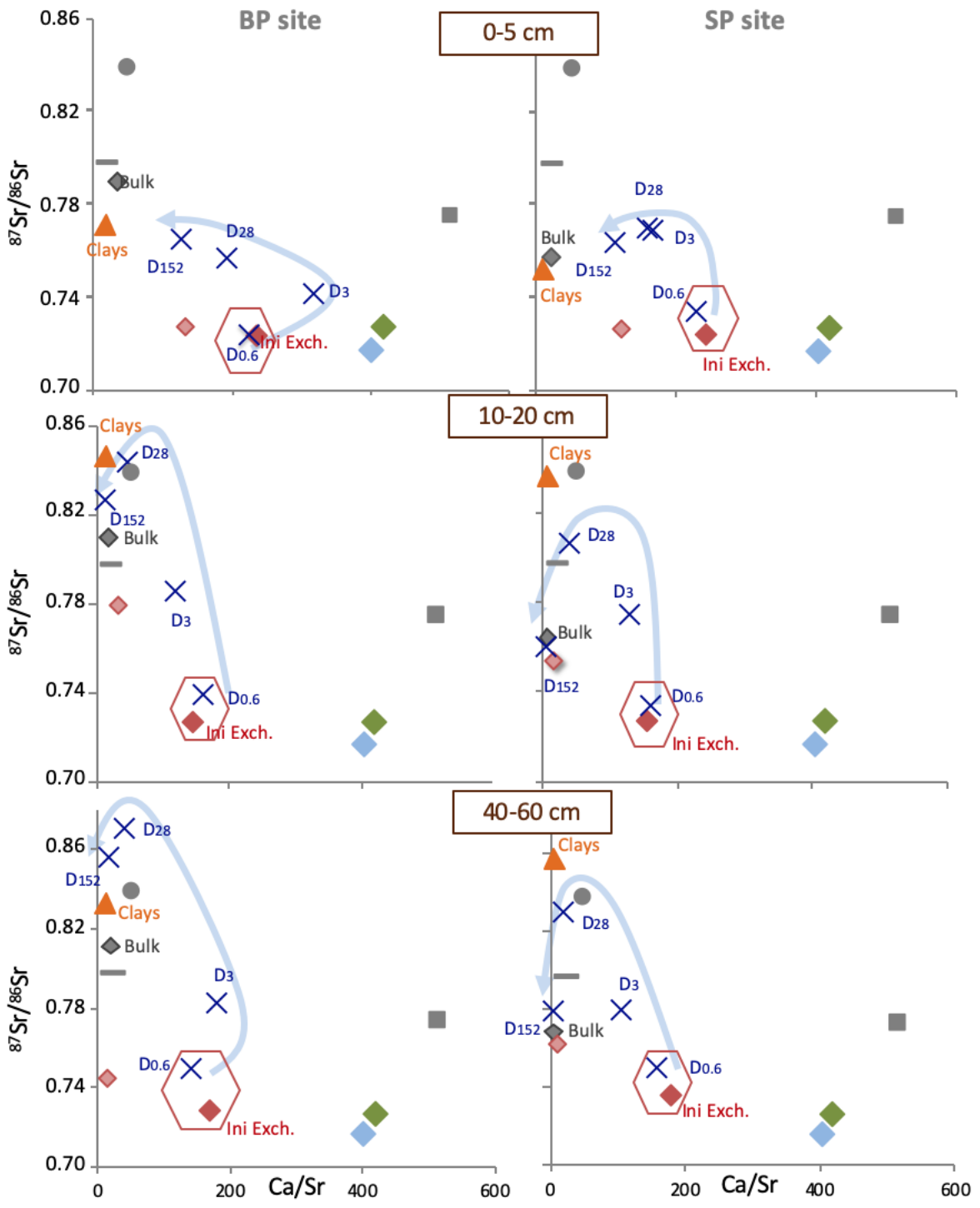
522 The atmospheric end-members have been determined from throughfalls sampled at both sites
523 and correspond to $^{87}\text{Sr}/^{86}\text{Sr} = 0.71327$ (respectively 0.71664) and $\text{Ca}/\text{Sr} = 438$ (respectively
524 402) for SP and BP (Prunier et al., 2015; Pierret et al., 2019).

525 The Sr from exchangeable fraction showed low $^{87}\text{Sr}/^{86}\text{Sr}$ ratios (from 0.723 to 0.736; Table 3),
526 which may be attributed to mixing between organic matter and atmospheric inputs. This
527 assumption is supported by the work of Van der Heijden et al. (2014), who showed that
528 atmospheric inputs represent a major source of Ca and Mg in exchangeable and total pools of
529 base-poor soils and that the litter layer played an essential role in the retention of throughfall
530 Mg and Ca. In addition, Bedel et al., (2016) indicated that the Sr isotopic compositions of

531 exchangeable soil are controlled by the mixing of litter Sr and throughfalls Sr in two acidic
532 soils, in superficial and deep horizons (down to 1 metre depth).

533 The more radiogenic materials are the clays and the primary minerals of granite. However, the
534 $^{87}\text{Sr}/^{86}\text{Sr}$ ratios of clays show contrasting values (Table 5; Fig. 7; 8) with low ratios in the
535 superficial horizons. The clay content is at a maximum in topsoil (about 30% in the 0-5 cm
536 samples), and decreases with depth to 9% and 16% in BP and SP profiles, respectively (Table
537 3). Clay minerals can have two origins: either primary (i.e., from bedrock) or pedogenetic (i.e.,
538 resulting from the soil formation). We can hypothesize that the proportion of pedogenetic clays
539 increases at the superficial oldest soils, in agreement with the measured increase in clay
540 proportion. The precipitation of secondary phases occurred from solutions containing
541 atmospheric and biological Sr, resulting in a less radiogenic signature. Conversely, clays from
542 bedrock, coming from the weathering/hydrolysis of primary minerals preserved their initial Sr
543 isotopic composition. Thus, the evolution of the clay Sr isotopic signature along both
544 weathering profiles (Fig. 10) is the result of variable proportions of radiogenic primary clays
545 and less radiogenic pedogenetic clays. Kaolinite, for example, results from the hydrolysis of K-
546 feldspar and its proportion within the clay fraction increases with depth in BP profile. Illite can
547 precipitate from solution (Godderis et al., 2006; 2009; Beaulieu et al., 2020), and its highest
548 proportion was recorded in the uppermost soil (about 70% in 0-5 cm depth soils).

549



◆ Bulk Soil ▲ Clays ◆ Biol ◆ Atmo ◆ Ini Exch ◆ Fin Exch ● Granite — orthose ■ albite

550

551 Fig. 8: $^{87}\text{Sr}/^{86}\text{Sr}$ isotopic ratio versus Ca/Sr ratios (mass ratio) for the different end-members

552 (defined in text), and the exchangeable fraction in initial and final soils. The leached solutions

553 obtained during the experiment at four different time steps D_{0.6} (14 h-0.6d), D₃ (3 days), D₂₈

554 (28 d) and D₁₅₂ (152 d) (see Table 1) are represented by the dark blue cross and for soils at three

555 representative horizons (0-5 cm; 10-20 and 40-60 cm). The signatures of bulk soil and clay are
556 specific for each corresponding depth. Granite and primary mineral signatures are from Aubert
557 et al., (2002). BP (under beech) and SP (under spruce) represent the two studied plots.

558

559 The contrasting Sr isotopic signatures between soils from the two plots (more radiogenic for
560 BP site; Fig. 6) have already been observed (Aubert et al, 2002; Pierret et al., 2014; Prunier et
561 al., 2015) and can be explained by the contrasting bedrocks, the northern slope being
562 characterized by strongly hydrothermally altered granite.

563

564 5.1.2. Evolution of Sr isotopic signature during the experiments

565 The temporal Sr isotopic evolutions of leachate during the experiments are shown in Fig. 7,
566 with the different potential end-members. For the six studied samples of the SP and BP sites,
567 the composition of the D_{0.6} leachate is very close to the initial exchangeable pool in terms of Sr
568 isotopic composition as well as Ca/Sr ratios (Fig. 8). It can therefore be deduced that the Ca or
569 Sr released at the beginning of the experimentation results mainly from the exchangeable stock,
570 even at deep horizons where the CEC is the lowest and the proportion of exchangeable Ca or
571 Sr in the bulk soils is weak (less than 0.2% for the Sr; Table 3, 5). Thus, the exchangeable
572 compartment is very quickly mobilized while other sources are still negligible.

573 At D₃ (3 days) the ⁸⁷Sr/⁸⁶Sr ratios of each leached solution increase and deviate from the initial
574 exchangeable pool, suggesting an additional leaching of elements from other sources, such as
575 clays (Fig. 8).

576 The contribution of clay end-members (each having their specific signature, extracted from
577 each studied soil) to the solution composition increases at D₂₈ (Fig. 8), suggesting that the
578 weathering of clay minerals represents an important source of Sr during the experiments for all
579 studied soils. At D₁₅₂ (152 days), the Sr concentrations reach their highest values (Fig. 5) and

580 the isotopic composition is close or tends towards that of the bulk soils or a mixture of clays
581 and bulk soils (Fig. 8). In summary, the results show that the first mobilized reservoir is the
582 exchangeable pool, followed by the clay compartment and at the very end, the bulk soils, which
583 can control the Sr isotopic signature especially in deep horizons of the spruce plot.

584 In addition, the exchangeable pool Sr signature is more radiogenic at the end of the experiment
585 compared to the beginning, with lower Ca/Sr ratios than in the initial sample (Table 3; Fig. 6,
586 8). Thus, in addition to chemical changes in the exchangeable fraction, the sources from which
587 they originate also change during the experiments: the initial poorly radiogenic Sr derived from
588 biological materials and atmospheric inputs is partly replaced by more radiogenic Sr coming
589 from mineral dissolution, released in solution during the experiments. In addition, the Ca/Sr
590 ratios of the exchangeable pool at the end of the experiment are very close to those of final
591 leaching solution (D_{152} ; Fig. 8) for each depth and profile. We suggest that in the final
592 experimental steps, a chemical equilibrium occurs between the experimental solution and the
593 exchangeable pool. The lower Sr isotopic composition of the exchangeable fraction compared
594 to the final experimental solution (D_{152}) in some case, may be explained by the fact that part of
595 the initial Sr remains in the final exchangeable pool.

596 To conclude, time-resolved analyses of Sr isotopic ratios revealed that the exchangeable
597 complex supplies Sr (and therefore, supposedly, Ca) first and rapidly. Then the contribution of
598 mineral dissolution, especially clays, increases. The Ca content of the exchange complex
599 decreases during experiment, while its radiogenic Sr signature increases.

600 5.2. Reservoirs of nutrient cations in the soil profiles

601 5.2.1. Initial reservoirs of nutrient cations in soils

Plot	Depth <i>cm</i>	Ca		Mg		Na		K	
		<i>kg · ha⁻¹</i>	%	<i>kg · ha⁻¹</i>	%	<i>kg · ha⁻¹</i>	%	<i>kg · ha⁻¹</i>	%
Beech Plot	00-05	199	54.8	34	8.6	5	0.2	92	1.3
(BP)	05-10	20	7.0	6	1.1	2	0.1	23	0.2
	10-20	13	2.4	6	0.5	3	0.04	30	0.1
	20-40	22	1.7	8	0.3	9	0.04	53	0.1
	40-60	12	1.2	3	0.1	7	0.04	22	0.04
	60-80	6	0.5	1	0.1	6	0.03	13	0.03
	<i>Total</i>	<i>272</i>		<i>58</i>		<i>32</i>		<i>233</i>	
Spruce Plot	00-05	142	83.6	27	7.2	5	1.2	65	1.6
(SP)	05-10	30	42.2	6	1.1	2	0.2	18	0.3
	10-20	17	11.0	5	0.4	3	0.2	19	0.1
	20-40	39	11.5	7	0.2	6	0.1	46	0.1
	40-60	24	5.7	5	0.1	7	0.1	49	0.1
	60-80	15	3.4	3	0.1	4	0.1	41	0.1
	<i>Total</i>	<i>267</i>		<i>53</i>		<i>27</i>		<i>238</i>	

602

603 Table 6: Evaluation of the stock of exchangeable cation per soil layer (expressed in kg/hectare)

604 and proportion of exchangeable pool in the bulk soils for Ca, Mg, Na, and K (expressed in %).

605 The total corresponds to the sum over the whole soil profile.

606

607 The total pools of nutrients in bulk soil provide important information regarding the long-term

608 fertility of ecosystems because they could be released by weathering over time (Schlesinger,

609 1997; Ghiel and von Wiren, 2014; Legout et al, 2020). Our results suggest that Ca is the most

610 limiting nutrient cation among K, Mg or Na, in the Strengbach soils in terms of total stock

611 (especially at the SP site with only 1.6 t of Ca in the whole profile until 80 cm depth; Appendix

612 C. Supplementary material) and a large proportion of Ca is in exchangeable form, especially in

613 the topsoil of the two sites (Table 6). The proportion of Na, K and Mg in an exchangeable form

614 is also the highest in the 0-5 cm layer, which may be attributed to the highest CEC (Table 3)

615 and to biological cycling (Jabagy and Jackson, 2001).

616

617 5.2.2. Evolution of the nutrient cation reservoirs during the experiment

618 The composition of the exchangeable phase varied with time during the experiment (Table 3).

619 The soil CEC decreased during the leaching experiment and the variations were more important
620 with samples from the BP site (- 9 to -35%) than from the SP site (1 to -10%), especially below
621 20 cm depth (Table 3). These changes may be partly explained by the mineralization of organic
622 matter and by the weathering and/or the interlayer aluminization of clay minerals (Mareschal
623 et al, 2009) during the 5 months of the experiment.

624 The 0-5 cm depth layers are characterized by a general loss of all elements in parallel to a
625 decrease of CEC indicating that there is no recharge of the exchangeable phase, with a net loss
626 of nutrients over time.

627 Regarding deeper soil layers, the composition of the CEC also varies during the leaching
628 experiment with an enrichment in Mg, K and Na (up to 570%, 530% and 260% of the initial
629 value respectively; Table 5), and a depletion of Ca (-20 to -60% of the initial values) over time.
630 Thus, part of the Mg, K and Na released in solution during the experiments by exchange,
631 mineral dissolution or organic matter mineralization contribute to the supply of the
632 exchangeable pools, which are considered as available for plants (van der Heijden et al, 2018).
633 Conversely, the exchangeable phase was significantly and systematically depleted in calcium
634 at the end of the experiment (Table 5; Fig. 4), highlighting the fact that the bioavailable Ca
635 reserve in soils decreased with time.

636

637 5.3. Dynamics/mobilization of elements and processes

638 5.3.1. Model calibration and hypotheses used in the simulations

639 Several hypotheses have been tested in order to represent the experimental conditions and to
640 determine the optimal set of parameters to simulate the evolution of the measured
641 concentrations of all major cations in the leachate (Table 6). The simulations with the final

642 parameter set are thought to reflect for the actual processes that control the evolution of the
643 concentrations of major elements, and to single out processes that cannot be captured by the
644 simulations because such processes are not included in the model.

645 In the figures we have chosen to represent two horizons. These two depths represent two
646 characteristic horizons of superior scientific interest.

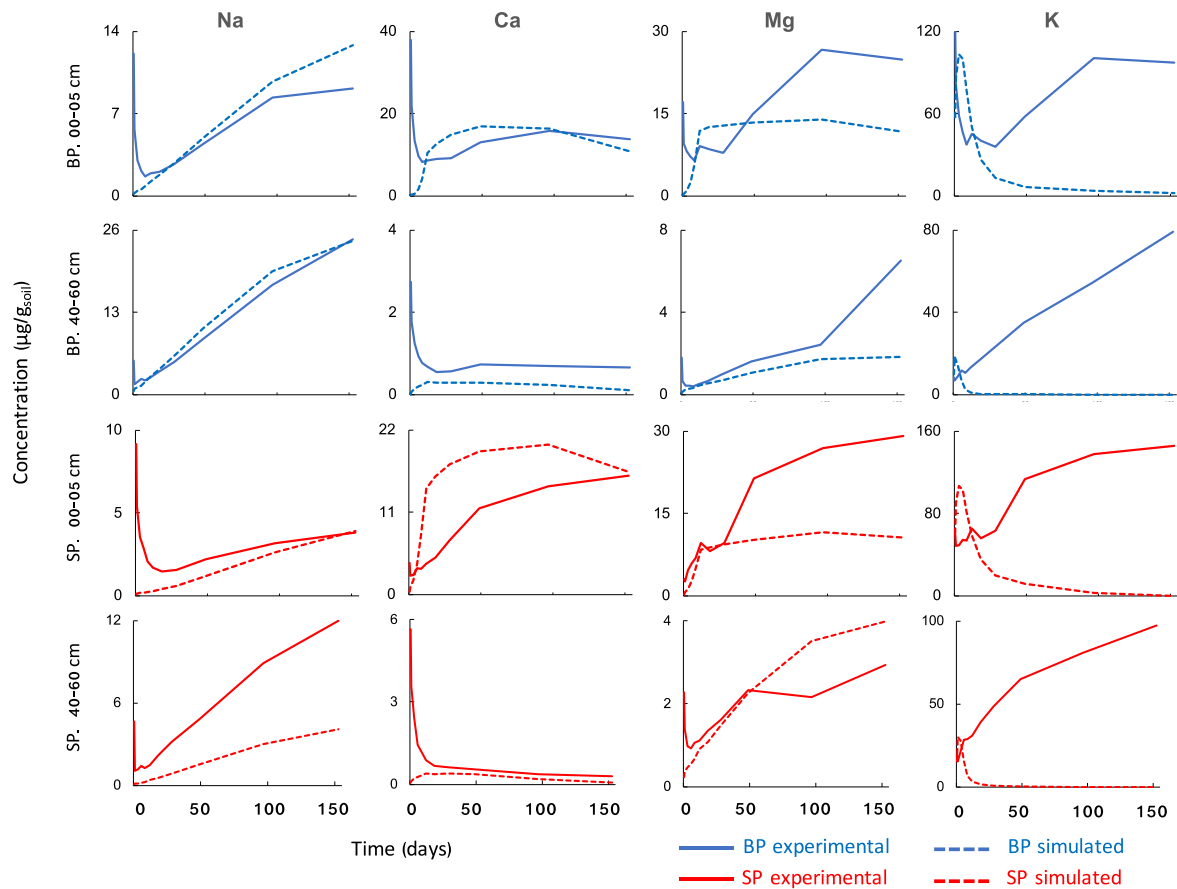
647 0-5 cm corresponds to the level richest in organic matter, where recycling and litter is most
648 important.

649 40-60 cm corresponds to the level of maximum root density, therefore where the root uptake is
650 the most important.

651

<i>Initial settings</i>	<i>Results</i>	<i>Final settings</i>
Smectites represented only by Ca-Montmorillonite alone	Underestimation of Mg concentration in the solution	Smectites represented by Ca-Montmorillonite and Mg-Montmorillonite
Initial conditions of model fixed to zero for cation concentrations and fraction of occupied sites by the cations on exchange complex surface	Underestimation of cation concentrations and Si concentration in the solution	Initial conditions of model fixed to zero for cation concentrations and fraction of occupied sites by the cations on exchange complex surface fixed with experiment
Specific surface of albite fixed to 0.1 m ² /g, as a primary mineral	Underestimation of Na concentration in the solution	Specific surface of albite fixed to 10 m ² /g, as a secondary mineral, according to XRD
No exchange between the solution and exchange complex surface	Ca and K concentrations largely underestimated in the solution	Exchange between the solution and exchange complex surface allowed
No precipitation of secondary phases	Underestimation of Ca and Si concentrations in the solution, equilibrium solution/minerals modified	Precipitation of secondary phases allowed

652 Table 7: Tested hypotheses for model parametrization.



654

655 Fig. 9: Simulated and experimental concentrations for the leaching solutions at two different
 656 depths (0-5 cm and 40-60 cm) and for the two profiles (BP in blue and SP in red) for Na, Ca,
 657 Mg and K.

658

659 5.3.2. Magnesium and Potassium

660 The amounts of K and Mg leached during the experiments rapidly exceeded the initial amount
 661 of exchangeable K and Mg (after 2 to 5 days, except for Mg in the topsoil). These elements
 662 behave quite similarly, and our results suggest that the exchangeable pool is not the sole source
 663 of K and Mg in the system. Several Mg-bearing minerals are present in the soils of the
 664 Strengbach catchment (smectite, biotite, vermiculite and illite), which is also the case for
 665 potassium (orthoclase, muscovite, biotite and smectite). However, other reservoirs such as

666 organic matter could have also contributed to the release of K and Mg during the experiment,
667 especially for the topsoil horizons, which were enriched in organic matter.

668 The WITCH code was thus used to investigate the sources of Mg and K found in the leachate.
669 In the model, these elements can be released through exchange and/or dissolution of K/Mg
670 bearing minerals. Sensitivity tests were performed until the WITCH code enabled satisfactory
671 reproduction of the dynamics of Mg contents in the leachate below 10 cm depth at both sites
672 (Table 7; Fig. 9). Good agreement between the simulated and observed Mg contents was
673 reached when the dissolution of smectite (and to a lesser extent, illite and vermiculite) was
674 considered. These phases supply the exchangeable pools and the leachate with Mg over time.
675 In these horizons, the model also enables to reproduce the differences between sites in terms of
676 Mg contents in the leachate; these differences are attributed to the higher smectite contents at
677 the SP site compared to the BP site (Fig. 5), which confirms that smectite is the main source of
678 Mg in these soil layers. This weathering flux of Mg compensates for the desaturation of the
679 CEC over time in these soil horizons, which is not the case in the 0-10 cm soil layer at the
680 beginning of the experiment. The initial CEC and Mg contents were higher in the topsoil than
681 in the rest of the soil profile at both sites, which may partly explain why the simulated Mg
682 weathering flux was lower than the Mg desaturation flux. Discrepancies between the modeled
683 and experimental Mg contents in the leachate were also observed in the topsoil. We hypothesize
684 that the mineralization of organic matter in the topsoil (not taken into account in the model)
685 may contribute to the supply of the CEC and the leachate over time, which may explain the
686 lower simulated Mg contents compared to the experimental ones.

687 Conversely, the model does not correctly reproduce the dynamics of K contents in the leachate:
688 the experimental K contents in the leachate become rapidly much higher than the simulated
689 contents, and our results suggest that several fluxes/processes are not correctly reproduced by
690 the model. The main input flux of K simulated by the model is the desaturation of the CEC,

691 occurring at the beginning of the experiment, while the simulated weathering flux is particularly
692 low throughout the experiment. We hypothesize that either:

693 (i) The dissolution rate constant and/or the solubility of K-bearing secondary minerals
694 implemented in the WITCH database is/are underestimated. However, this is unlikely because
695 laboratory-derived parameters used in reactive transport models such as WITCH generally
696 overestimate the actual release rates of elements (White and Brantley, 2003; Godd ris et al.,
697 2006; Daval et al., 2011; Wild et al., 2016; Wild et al., 2019);

698 (ii) The model overestimates the precipitation of K-bearing minerals, which is
699 thermodynamically controlled (i.e., instantaneous as soon as the solution is supersaturated);

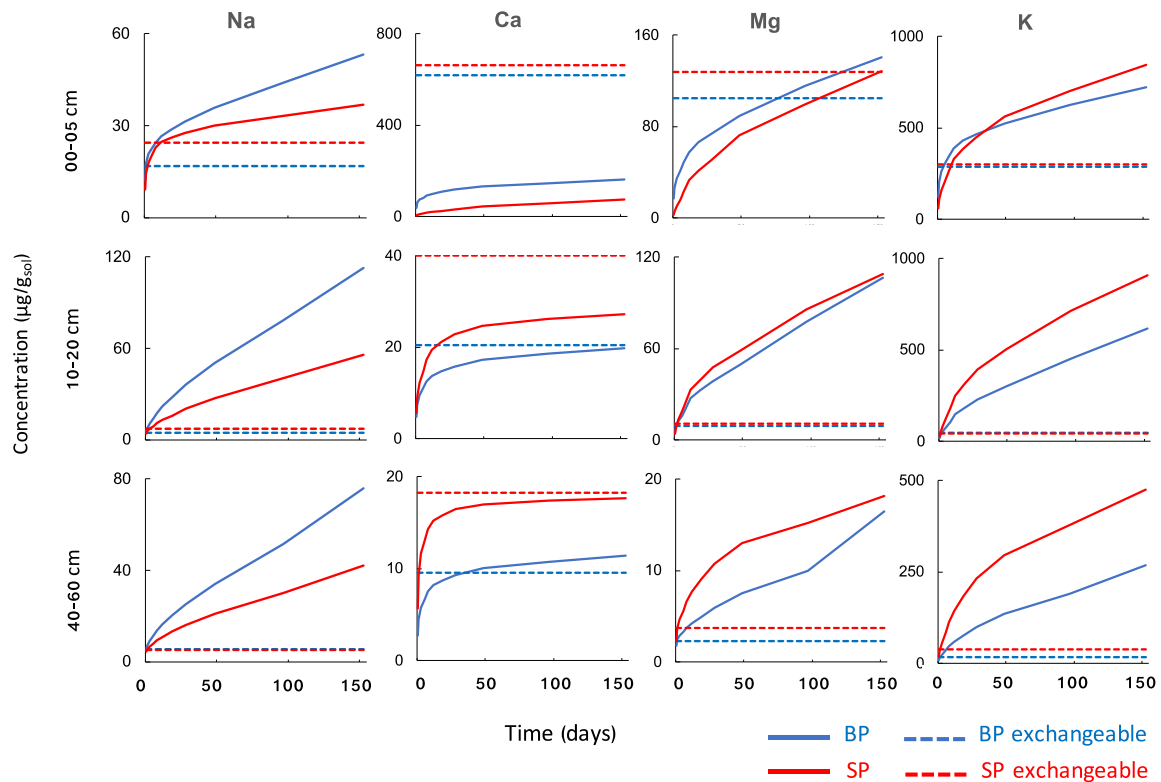
700 (iii) Another source releases K, but is not considered in the model. Organic matter can release
701 K through mineralization, but it is unlikely that this process occurs in the deepest soil layers,
702 which are poor in organic matter.

703 In the end, it is more likely that another source of K, such as interlayer K, was released during
704 the experiment, as suggested by several authors (Rahmatullah and Mengel, 2000; Falk
705  gaard and Krogstad, 2005). In addition, several studies have shown the role played by plant
706 roots in releasing interlayer K in soils (Barr  et al., 2007; Vetterlein et al., 2013; Khormali et
707 al., 2015; Paola et al., 2016). Note that the code is not designed to simulate such a process,
708 which could explain why the simulations fail to reproduce the dynamics of K release over the
709 course of the experiments.

710

711 5.3.3. Calcium

712



713

714 Fig. 10: Cumulative concentrations of Na, Ca, Mg and K from the leached solution at three
 715 representative different depths over the 152 days of experimentation (in µg normalized to 1g of
 716 bulk soil). Blue and red lines represent the BP and SP profiles, respectively. The dashed lines
 717 represent the exchangeable pool in the soils (in µg for 1g of soil). Each concentration is
 718 normalized to 1 g of soil.

719 Unlike other elements, the cumulative concentration of Ca remains below the amount of
 720 exchangeable Ca (Ca-exch), even at the end of the experiments, down to 60 cm depth (Fig. 10).
 721 Below 60 cm depth, the initial stock of exchangeable calcium is reached after 8/12 days (for
 722 BP and SP sites, respectively), whereas for K, Na or Mg, the same threshold is exceeded after
 723 a few hours (Fig. 10).

724 More precisely, over the entire duration of the experiments (152 days), the total amount of
 725 calcium released from the 0-5 cm depth soil was four to ten times lower than the exchangeable
 726 calcium (for SP and BP sites respectively; Fig. 10), while Ca-exch was the most important

727 exchangeable cation in the uppermost horizons (Table 6). Several hypotheses to explain the
728 incomplete mobilization of the exchangeable Ca during leaching experiments are discussed
729 below.

730 A hypothesis could be that the amount of exchangeable calcium is too high to be exchanged or
731 leached during the experiment by the available protons. The total amount of protons available
732 in solution during the whole experiment (11 steps) corresponds to $1.4 \cdot 10^{-4}$ mol (HCl solution at
733 pH=3.5). By considering the sum of cations (Na, K, Mg and Ca), the values obtained are
734 between 0.05 and $0.6 \cdot 10^{-4}$ mol+ in soils below 5 cm depth, underlining the fact that protons are
735 not limiting. Thus, the low Ca release observed during the experiments cannot be explained by
736 a proton-limiting effect.

737 Numerical simulations of experimental Ca release run with WITCH were realized with different
738 scenarios by changing the values of selectivity coefficients associated with the cation adsorption
739 parameter, which represents the exchange between the Ca present on the humic-clay complex
740 and protons in the solution (Fig. 11). These selectivity coefficients are derived from the Gapon
741 convention, and their values are often adjusted to calibrate the models. Regardless of run, the
742 model is not able to simulate the experimental pattern, implying that the release of Ca in solution
743 is controlled not only by simple cationic exchange coupled with dissolution. The model
744 systematically overestimates the Ca released from cation exchange (Fig. 11). The exchangeable
745 Ca might behave differently from other cations such as Mg or K, because of different bonds or
746 exchange sites. Calcium is stabilized in the clay-humic complex via two main mechanisms,
747 involving either weak or strong bonds (Sutton and Sposito, 2006; Kalinichev and Kirkpatrick,
748 2007; Bogatko et al., 2013; Rowley, Grand, and Verrecchia, 2018):

749 1) Inner-sphere complex formation with direct ionic bonds between Ca (having higher affinity
750 than Mg, K or Na) and organic matter (Iskrenova-Tchoukova et al., 2010);(André and

751 Pijarowski, 1977; Baes and Bloom, 1988; Curtin, Selles, and Steppuhn, 1998);(Sentenac and
752 Grignon, 1981).

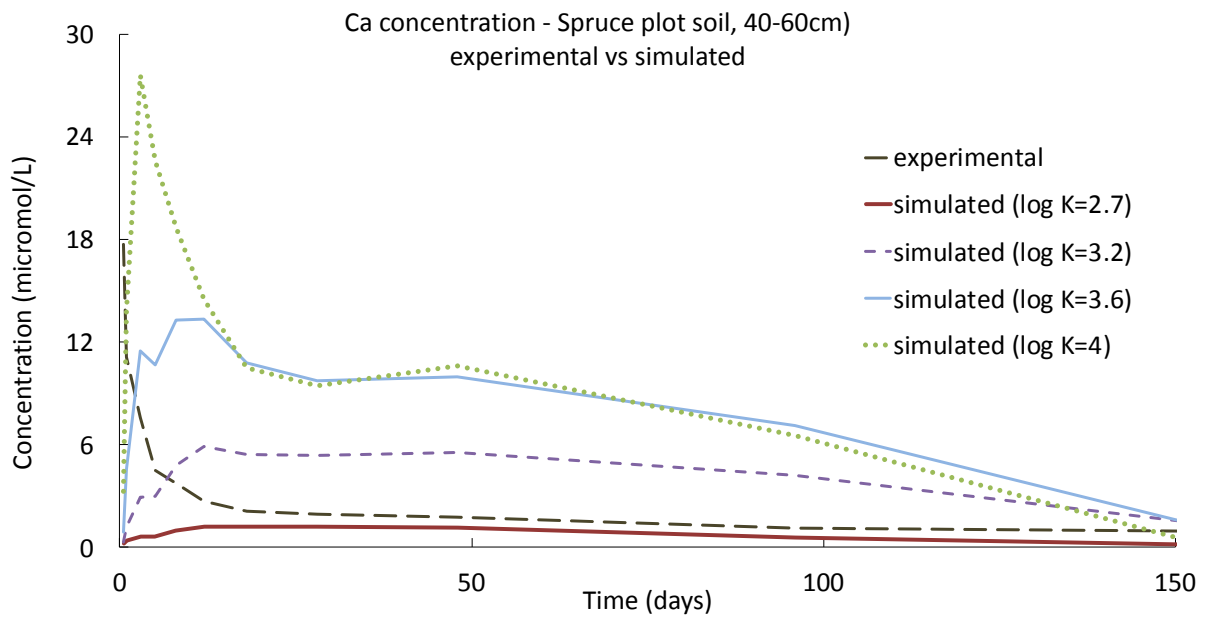
753 2) Outer-sphere complex. Calcium specifically forms a bridge via weak interactions between
754 the different molecules of organic matter and clays, which is well documented (Edwards and
755 Bremner, 1967, Oades, 1988, Clough and Skjemastad, 2000; Feng et al., 2005; Von Lützow et
756 al., 2006; Sutton and Sposito, 2006; Iskrenova-Tchoukova et al., 2010).

757 For all these reasons, Ca-exch is probably less accessible and less mobile during experimental
758 leaching than Na-, K- or Mg-exch because of stronger chemical binding and Ca-chemical
759 bridges occurring among the clay-humic complex.

760 In a practical way, our study highlights that the amount of calcium released in solution during
761 the acid leaching experiment is much lower than the existing exchangeable pool in soil, unlike
762 other cations such as K or Mg. Therefore, we hypothesize that the amount of calcium actually
763 available for plants does not correspond to the amount of Ca-exch determined by classical
764 extraction protocols. Our experiments suggest that the fertility of soils may be overestimated
765 for Ca when considering classical exchangeable Ca.

766 In addition, both BP and SP soil profiles exhibit different behaviors. In the uppermost soil (0-
767 5cm depth), the Ca, but also Mg and K release in solution during experimentation was higher
768 in BP, whereas the Ca, Mg- and K-exch was lower than in SP soil (Fig. 2; 5). This can be due
769 to higher organic matter content in BP, and probably to different reactivities between the two
770 litter types. The biodegradability of decomposed beech litter is significantly higher than that of
771 spruce litter (43% versus 31% after 42 days of incubation; Don and Kalbitz, 2005). This can
772 explain why the quantity of cations released during the experiments was the highest in BP (0-5
773 cm) soil (Fig. 5). Thus, the type of tree and thus of litter can play an important role in the cycling
774 of nutrients and in particular Ca in forest ecosystems, especially in environments with acidic
775 and base-poor soils.

776



777

778 Fig. 11: Evolution of experimental Ca concentrations (leached solution) versus time, compared
779 to simulations run with various values of Ca constants of exchange ($10^{-2.7}$, $10^{-3.2}$, $10^{-3.6}$, 10^{-4}) on
780 SP plot at 40-60 cm. The Ca concentration in the solution increases with the decreasing
781 exchange constant. The calculated concentrations with exchange constants of $10^{-3.2}$, $10^{-3.6}$ and
782 10^{-4} are largely overestimated over time, despite a fast increase at the beginning of the
783 simulation, as in the experimental conditions. This illustration corresponds to the 40-60 cm
784 depth horizon from the spruce plot (SP).

785 5.3.4. Sodium

786 The experiments reveal that the amount of Na leached during the experiment rapidly exceeds
787 the initial amount of exchangeable Na, suggesting the contribution of a other source. The
788 exchangeable Na is low, 10 to 100 times lower than Ca, Mg and K, and it represents less than
789 0.1% of the total Na in bulk soils, for both profiles. Thus, the main source of sodium in the soils
790 is albite ($\text{NaAlSi}_3\text{O}_8$), which represents on average 27% of the crystalline phases at the HP site
791 and 10% at the SP site (Fig. 3, Sup mat.). The differences may be explained by the geological
792 history of the catchment: strongly hydrothermalized granite on the northern slope (SP

793 localisation) having depleted in albite compared to the non-hydrothermalized granite (BP
794 localisation) found on the other slope (El Gh'mari, 1995 ; Fichter et al., 1998a).

795 The WITCH code enables satisfactory reproduction of the dynamics revealed experimentally
796 for Na contents in the leachate over time for samples from both sites (Fig. 9). In the simulation,
797 the contribution of exchangeable Na is negligible and the dissolved Na is mainly due to albite
798 dissolution. Moreover, the release rate of Na from albite is not influenced by secondary
799 processes such as precipitation or complexation with organic matter (Chou and Wollast, 1985;
800 Knauss and Wolery, 1986; Chen and Brantley, 1997). Thus, a simple description of albite
801 hydrolysis remains sufficient to account for the release rate of Na, and the differences between
802 SP and BP soil experiments related to the albite content in soils.

803 As mentioned above, the specific surface area of albite was increased by two orders of
804 magnitude compared to other primary minerals (from 0.1 m²/g to 10 m²/g). This adjustment
805 complies with the surface area estimated from SEM observations and is consistent with the fact
806 that albite in the soils was already partially weathered resulting in a higher specific surface area
807 compared to pristine albite. Discrepancies between modelled and experimental concentrations
808 were observed at the beginning of the experiment, and we hypothesize that this may be due to
809 sodium from interstitial soil water or from the rapid dissolution of a labile Na-source such as
810 salts (not taken into account in the model).

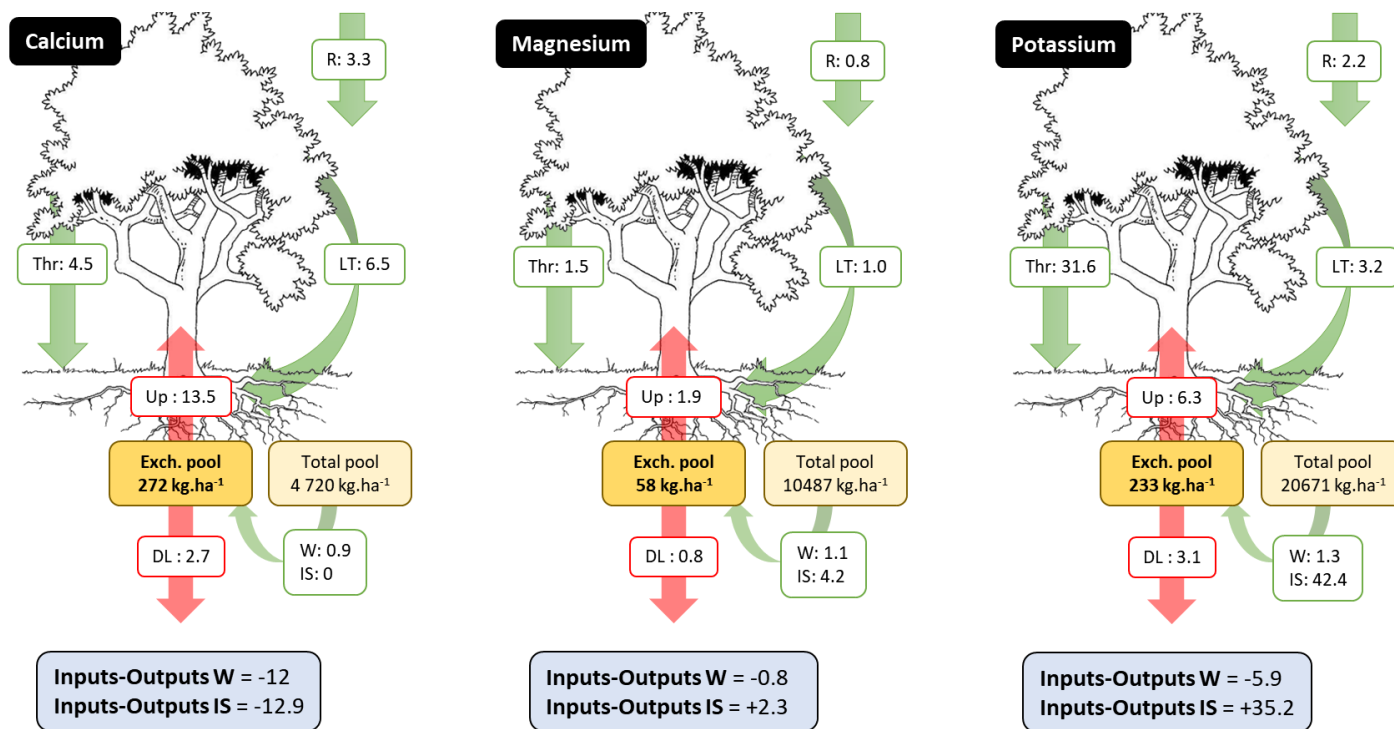
811 Although sodium is not one of the major nutrients for plants (Marschner, 1995), our results
812 demonstrate that it may be used as a proxy for the weathering rates of primary minerals, as
813 suggested by several authors (e.g., Sverdrup and Warfvinge, 1993).

814

815 5.4. Implications for tree nutrition and forest management

816 Plant-available pools are assumed to be stored in the soil as exchangeable cations adsorbed on
817 the cationic exchange complex (van der Heijden et al, 2018). Although the pools of

818 exchangeable sodium, calcium, magnesium and potassium are low at the Strengbach, our results
 819 show that soil intrinsic fluxes of Na, Mg and K (i.e., weathering, mineralisation of OM...) may
 820 supply the exchangeable pools and could thus participate substantially to tree nutrition. Our
 821 results suggest that the situation is more critical for Ca for two major reasons: i) although
 822 reserves are still available in soils (total soil pools 1589 kg.ha⁻¹ and 4720 kg.ha⁻¹ for the SP and
 823 BP sites, respectively), soil intrinsic flux that may supply the pools of exchangeable Ca over
 824 time appears very weak and ii) exchangeable pools of Ca seem only partially available for plants
 825 (see section 5.3.4).
 826



827
 828 Fig. 12: Fluxes and input-output budgets (in kg.ha⁻¹.yr⁻¹) for calcium, magnesium and
 829 potassium at the BP site. IS is the intrinsic flux from soil estimated from our leaching
 830 experiments (corrected for the value of the initial exchangeable pool). W is the weathering flux,
 831 R is the atmospheric wet deposition, Up is the net uptake flux by roots and DL is the deep
 832 leaching (see Beaulieu et al. 2020). See additional explanation in text and Appendix D.
 833 Supplementary material, with the same diagram for the SP site.

834

835 The results of the leaching experiments were extrapolated to the plot scale according to the
836 calculation detailed in Appendix D (Supplementary material), the flux of nutrients (Ca, Mg, K)
837 intrinsic to the 0-80 cm soil profile (IS) was thus calculated for the BP and SP sites on an annual
838 basis (Fig. 12 and Appendix E. Supplementary material). Input-output budgets were then
839 computed (Ranger and Turpault, 1999) at both sites according to two scenarios (Fig. 12 and
840 Appendix E. Supplementary material):

841 • Input-Output **W** = $R + W - U_p - DL$

842 • Input-Output **IS** = $R + IS - U_p - DL$

843 where R is the wet atmospheric deposition flux ($\text{kg}\cdot\text{ha}^{-1}\cdot\text{yr}^{-1}$), W the weathering flux ($\text{kg}\cdot\text{ha}^{-1}\cdot\text{yr}^{-1}$), IS is the intrinsic flux of nutrients from the soil estimated from the leaching experiments
844 ($\text{kg}\cdot\text{ha}^{-1}\cdot\text{yr}^{-1}$), U_p is the net uptake flux by trees ($\text{kg}\cdot\text{ha}^{-1}\cdot\text{yr}^{-1}$) and DL is the drainage losses at the
845 bottom of the soil profile ($\text{kg}\cdot\text{ha}^{-1}\cdot\text{yr}^{-1}$). R, W, U_p and DL fluxes are presented in Beaulieu et al.
846 (2020). The W flux was estimated using a model only considering the release of nutrients from
847 primary mineral dissolution, while the IS flux corresponds to the combination of several
848 nutrient sources in soils (weathering of soil minerals, contribution of non-crystalline secondary
849 minerals, mineralization of organic matter, etc.), corrected for the value of the initial
850 exchangeable available. The conditions during the leaching experiment (pH=3.5, permanent
851 water saturation) were more drastic/aggressive than those in the field, and the actual in situ flux
852 that may supply the pools of exchangeable nutrients is probably lower than the IS flux estimated
853 from the ex situ leaching experiments. Nevertheless, we may hypothesize that this in situ flux
854 lies between the W flux and the IS flux for Ca, Mg and K.

856 Unsurprisingly, the IS flux is null for Ca at the two sites (Fig. 12 and Appendix E.
857 Supplementary material) because the quantities of calcium released during the leaching
858 experiment for the entire soil profile are lower than the initial quantity of Ca adsorbed on the

859 CEC, leading to negative input-output budgets for Ca regardless of the scenarios (Input-Output
860 **W** and Input-Output **IS**). For Mg and K, the IS flux is higher than the W flux and the input-
861 outputs budgets are negative when computing the budget with the W fluxes (input-output **W**),
862 while they are almost balanced for Mg and largely positive for K when computing the budget
863 with the IS fluxes (Fig. 12 and Appendix E. Supplementary material).

864 These results and the relatively high contents of exchangeable Ca in the topsoil at the two sites
865 suggest that tree nutrition for Ca is mainly based on deposition and biological cycling in the
866 Strengbach catchment. This is also true for Mg and K but to a lesser extent since the soil seems
867 to still have the capacity to supply the exchangeable pools and balance the input-output budgets.
868 In base-poor forest ecosystems, atmospheric deposits are a significant source of K, Mg or Ca
869 (Clergue, 2015; Cole, 1986; van der Heijden et al., 2013; Pierret et al., 2019; Turpault,
870 Calvaruso, and Dincher, 2019), and the biological cycling of nutrients (root uptake, litterfall,
871 decomposition) plays an essential role in maintaining nutrients within the plant-soil system
872 (Ranger et Turpault, 1999, Legout et al., 2020). Disturbances of biological cycling through
873 harvesting and biomass exportation at the Strengbach catchment may thus rapidly threaten the
874 sustainability of these ecosystems (Legout et al., 2020) and forest management has to consider
875 this weakness by limiting biomass exportation and avoiding slash removal, unless a nutrient
876 compensation is planned (i.e., liming, fertilization). A recent study also showed that the
877 atmospheric inputs of calcium were reduced by 40% under spruces (from 15 to 9 kg·ha⁻¹ yr⁻¹)
878 and by 70% under beeches (from 6 to 2 kg·ha⁻¹ yr⁻¹) over the period 1986-2012 at the
879 Strengbach, which constitutes an additional pressure on these ecosystems and questions their
880 sustainability (Pierret et al., 2019).

881

882 6. Conclusion

883 The objective of this study was to characterize the sources of nutrient cations (Na, K, Mg and
884 Ca) in the soils of the Strengbach and to assess the potential contribution of these chemically
885 poor soils to tree nutrition. We designed laboratory batch experiments and performed acid
886 leaching to mimic the processes taking place in nature, but simplified, enabling a fine control
887 of key parameters (type of acid, pH, time, etc.). Combining mineralogical, chemical and
888 isotopic analyses with modelling approaches allowed for different test scenarios to assess the
889 capacity of these soils to release nutrient cations over time.

890 The results showed contrasting patterns for Na, K, Mg and Ca. The release of Mg in solution
891 results from a mixing between cationic exchange, mineral dissolution (mainly smectite) and
892 organic matter mineralization (especially in topsoils). The release of K in solution is high and
893 systematically underestimated in our numerical simulations: this result may be attributed either
894 to an unknown source of K (e.g., organic matter, unknown mineral phases or more likely
895 interlayer K) or to an overestimation of the simulated precipitation rate of K-bearing secondary
896 phases. The release of Na in solution is mainly controlled by albite dissolution, with differences
897 between the two sites related to the contrasting geological history of the parent materials. The
898 Sr isotopic approach, used as a proxy to identify the sources of Ca, show that the exchangeable
899 complex supplies nutrients first and rapidly to the solution, followed by the clay compartment
900 and at the very end, the bulk soils, which can control the Sr isotopic signature especially in deep
901 horizons of the spruce plot. However, the release of Ca in solution during the experiment is
902 quite low compared to the Na, Mg and K and results almost exclusively from the progressive
903 desaturation of the CEC. Interestingly, our results also suggest that the exchangeable Ca in soils
904 of the Strengbach catchment is only partially available for plants, due to strong chemical
905 binding with organic matter and/or the occurrence of Ca-chemical bridges between clay and
906 organic matter.

907 In a practical way, this study shows that soil intrinsic fluxes of Na, Mg and K (i.e., weathering,
908 mineralisation of OM etc.) in the Strengbach catchment may replenish the soil exchangeable
909 pools and could thus contribute to tree nutrition in the mid- to the long-term. For Ca, soil
910 intrinsic flux seems nonexistent or extremely low, and tree nutrition must rely on the current
911 bioavailable pool in the short term, and on atmospheric deposition and biological cycling in the
912 long term. This is also true for the other nutrient cations, but to a lesser extent since soil intrinsic
913 fluxes are not null and may thus significantly contribute to tree nutrition. In the topsoil, the
914 exchangeable reservoir contains the largest proportion of total Ca illustrating the low content
915 of Ca in these soils and the important role of biological cycling and organic matter for this
916 nutrient.

917 Sustainable management should consider the fact that exchangeable Ca, conventionally
918 determined, does not necessarily provide an accurate picture of the real availability of Ca and
919 therefore of the fertility of soils, with a risk of overestimation of nutrient reservoirs for trees.
920 These results are particularly important in soils with naturally low Ca content. In these
921 ecosystems, efficient recycling through biological cycling is of paramount importance to
922 maintain nutrients within the plant-soil system. Harvesting and biomass exportation may
923 rapidly impact the biological cycle and threaten the sustainability of these ecosystems, similar
924 to changing tree species that may influence the nature of the litter, its turnover and the input of
925 nutrients to the soil.

926

927

928

929

930

931

932

933

934 **Appendix A. Supplementary material: Mineral and chemical composition of soils.**

935

	Depth	Kaolinite	Illite	Vermiculite	Smectite	Muscovite	Biotite	Quartz	Orthose	Albite	OM
	<i>cm</i>	%	%	%	%	%	%	%	%	%	%
<i>Beech Plot</i>	0-5	1.4	22.0	1.3	5.2	5.7	0.6	8.3	9.6	6.5	39.4
<i>(BP)</i>	5-10	1.5	10.0	0.0	5.3	8.8	0.8	21.3	27.6	17.5	7.2
	10-20	1.1	7.8	1.3	4.8	10.8	0.7	18.9	25.8	21.4	7.5
	20-40	0.8	6.8	3.7	4.2	15.0	0.6	19.6	21.0	24.0	4.4
	40-60	1.4	6.4	2.5	3.5	20.4	0.6	13.8	23.5	24.0	3.9
	60-80	1.1	4.6	1.2	1.7	20.5	1.1	22.1	19.4	25.5	2.8
<i>Spruce Plot</i>	0-5	1.5	20.1	0.4	8.5	4.7	0.0	16.0	6.6	3.3	39.1
<i>(SP)</i>	5-10	0.5	10.7	0.0	7.7	14.4	0.8	38.9	7.7	5.3	14.0
	10-20	0.2	8.9	0.0	6.1	22.6	0.8	39.4	11.6	6.6	3.7
	20-40	0.2	8.6	1.3	9.3	20.9	0.0	32.9	20.0	4.5	2.2
	40-60	0.2	9.2	1.1	7.3	22.3	0.0	37.8	12.9	7.9	1.3
	60-80	0.1	7.3	1.1	7.5	17.6	0.0	39.0	15.4	11.0	1.0

936

937 Mineral composition of soils from beech and spruce plots, calculated from XRD analyses on

938 bulk soils and clays, and from organic matter content.

939

940

941

942

944 Chemical compositions (expressed in $\mu\text{g/g}$ of soil) for initial and final (after experimentation)
945 bulk soils, compared with the contribution of different reservoirs as clay minerals, initial and
946 final exchangeable pool, organic matter as total cumulated experimental leachate calculated for
947 1 g of soil.

948

949 **Appendix B. Supplementary material. Composition of leaching solutions**

950

951 Mean chemical composition and standard deviation (SD) from the three triplicates of the
952 leaching solution at the eleven time-step of each experiment (see Table 1). Chemical
953 compositions are expressed in $\mu\text{g/g}$ of soil. *Data are provided as the excel file containing all*
954 *tables, the table is too big to be copy directly in this document.*

955

956 **Appendix C. Supplementary material. Stock of Ca, Mg, Na and K**

Plot	Depth	Ca	Mg	Na	K	Plot	Depth	Ca	Mg	Na	K
-	cm	kg·ha ⁻¹	kg·ha ⁻¹	kg·ha ⁻¹	kg·ha ⁻¹	-	cm	kg·ha ⁻¹	kg·ha ⁻¹	kg·ha ⁻¹	kg·ha ⁻¹
Bulk soils						Clays					
Beech Plot (BP)	00-05	362	391	2375	7017	Beech Plot (BP)	00-05	92	278	795	2640
	05-10	284	575	4246	12615		05-10	33	331	347	2270
	10-20	550	1277	8672	26886		10-20	38	519	438	3231
	20-40	1285	3029	21187	64112		20-40	51	1864	316	10803
	40-60	1013	2423	16183	51389		40-60	57	896	761	5190
	60-80	1226	2793	16313	44682		60-80	37	504	414	2613
Spruce Plot (SP)	00-05	170	381	450	4050	Spruce Plot (SP)	00-05	45	290	161	2059
	05-10	70	601	691	6719		05-10	16	293	86	1979
	10-20	156	1178	1395	14740		10-20	14	472	81	2901
	20-40	341	4220	5253	47760		20-40	93	1333	1035	7840
	40-60	423	4494	6065	54937		40-60	50	1812	285	10301
	60-80	429	3604	4886	43982		60-80	38	1321	205	7516
Ini Exch						OM					
Beech Plot (BP)	00-05	199	34	5	92	Beech Plot (BP)	00-05	614	88	32	288
	05-10	20	6	2	23		05-10	112	16	6	53
	10-20	13	6	3	30		10-20	234	34	12	110
	20-40	22	8	9	53		20-40	328	47	17	154
	40-60	12	3	7	22		40-60	233	34	12	110
	60-80	6	1	6	13		60-80	150	21	8	70
Spruce Plot (SP)	00-05	142	27	5	65	Spruce Plot (SP)	00-05	1422	37	8	117
	05-10	30	6	2	18		05-10	509	13	3	42
	10-20	17	5	3	19		10-20	269	7	2	22
	20-40	39	7	6	46		20-40	446	12	2	37
	40-60	24	5	7	49		40-60	290	7	2	24
	60-80	15	3	4	41		60-80	176	5	1	14
Final Exch											
Beech Plot (BP)	00-05	143	20	4	32						
	05-10	12	3	7	41						
	10-20	10	5	12	70						
	20-40	13	8	18	147						
	40-60	7	3	9	75						
	60-80	6	2	12	69						
Spruce Plot (SP)	00-05	122	23	1	30						
	05-10	24	7	3	37						
	10-20	8	9	3	85						
	20-40	17	17	9	225						
	40-60	11	22	11	255						
	60-80	11	18	8	262						

957

958 Evaluation of the stock of Ca, Mg, Na and K in bulk soil, and in the different reservoirs: initial
959 and final exchangeable cations, clays, and organic matter in each soil layer (expressed in
960 kg/hectare). This calculation considers the proportion of these different reservoirs inside the
961 bulk soils.

962

963

964 **Appendix D. Supplementary material: Evaluation and calculation of stocks available and**
965 **leaching flux in Strengbach soils. Fluxes and input-output budgets**

966 - Calculation of the total stock and the exchangeable stock expressed in kg/ha:

967 Element inventories are evaluated in the total soil and in the exchangeable phase based on the
968 concentrations previously measured for each horizon studied. These inventories are expressed
969 in $\text{kg}\cdot\text{ha}^{-1}$.

970 The leaching experiments were carried out with the fraction of the soil $f < 2 \text{ mm}$, thus this
971 fraction is used for the calculations:

$$m_{total\ horizon} \times f_{<2mm} = m_{f<2mm} \quad (6-1)$$

972

973 Each horizon has a defined surface area S of 2 m^2 and a thickness e (5,10 or 20 cm), which give
974 the mass per unit of volume:

$$\rho_{f<2mm} = \frac{m_{f<2mm}}{V_{horizon}} = \frac{m_{f<2mm}}{S \times e} \quad (6-2)$$

975 This density is then used to determine the stocks available on a full hectare ($10,000 \text{ m}^2$). A
976 horizon with a thickness e and with a surface area of 1 ha is considered. The stock for each
977 chemical element i (expressed in $\text{kg}\cdot\text{ha}^{-1}$) was calculated with the elemental concentration C_i .

$$Stock_{i_{f<2mm}} = C_{i_{f<2mm}} \times 10000 \times e \times \rho_{f<2mm} \quad (6-3)$$

978

979 The stocks were calculated for the bulk soil and for the exchangeable pool from the
980 concentration in bulk soil and exchangeable fraction respectively.

981 This calculation is performed for each element and for each horizon of the two plots. To
982 simplify certain calculations, the total stock in the entire profile is also used, which is expressed
983 as the sum of the stocks of each horizon:

$$Stock_{total} = \sum Stock_i \quad (6-4)$$

984

985 - Calculation of total leached concentration expressed in kg/ha:

986 The same equation is used to calculate the total amount A of element leached during the
987 experiment for one ha:

$$A_{leaching}(kg \cdot ha^{-1}) = C_{cumulative\ leaching}(kg \cdot kg_{soil}^{-1}) \times 10000 \times e \times \rho_{f<2mm} \quad (6-5)$$

988

989 With $C_{cumulative\ leaching}$ the cumulative concentration leached during the 11 steps of the 152 days
990 of experimentation.

991

992 - Calculation of the leaching flux:

993 The leaching flux is calculated from the results of the leaching experiments, for each plot. The
994 leaching experiments were carried out with 5 grams of soil. The time of experiment should be
995 converted in corresponding in-situ field time in order to evaluate the leaching flux for each
996 element in $kg \cdot ha^{-1} \cdot yr^{-1}$. The idea is to convert the water/material ratio in quantity or duration of
997 rainfall in the site. The mean annual rainfall at the Strengbach catchment is 1400 mm (Pierret
998 et al., 2018). The interception by vegetation is on average 300 mm/yr (Pierret et al., 2019). Thus
999 the annual water flow infiltrating the soil is 1100 mm (1100 $L \cdot m^{-2}$ per year).

1000 During the experiments, a $V_{experimental}$ volume of 440 mL of solution and a $m_{experimental}$ mass of
1001 5 g were used. Thus, for a pit of mass m , the amount of rainfall, noted $V_{equivalent}$ required to
1002 leach in the same proportions is:

$$V_{equivalent}(L \cdot m^{-2}) = m_{f<2mm}(kg) \times \frac{V_{experimental}(L)}{m_{experimental}(kg)} \times \frac{1}{S(m^2)} \quad (6-6)$$

1003 The equivalent time ($t_{equivalent}$ in year) corresponding to the experimental condition i.e. 152 days
1004 (Table 1) is then:

$$t_{equivalent} = \frac{V_{equivalent}}{V_{rain}} \quad (6-7)$$

1005

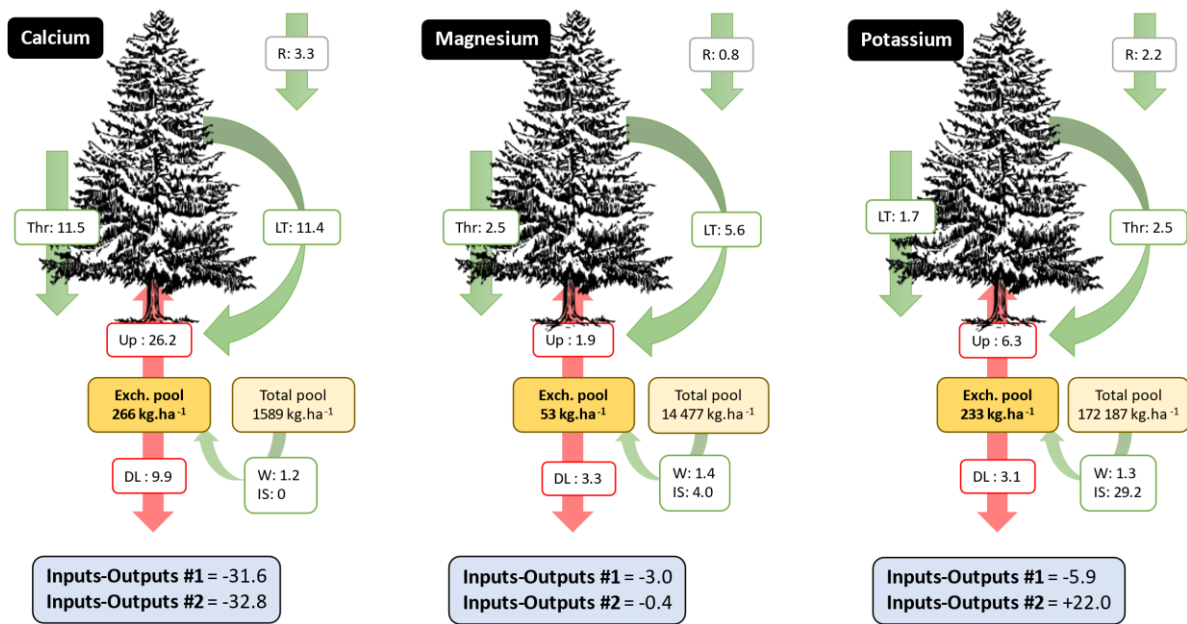
1006 The result obtained give 42 years of rain for experiment with soils from the beech plot and 35
 1007 years with soils from the spruce plot. This equivalent time allows to calculate the equivalent
 1008 annual leaching flow according to:

$$flux_{leaching}(kg \cdot ha^{-1} \cdot yr^{-1}) = IS = \frac{A_{leaching} - Stock_{exchangeable}}{t_{leaching}} \quad (6-8)$$

1009

1010 If the leaching flux is lower than the initial exchangeable pool, then IS is equal to 0 (see figures)

1011



1012

1013 Fluxes and input-output budgets (in kg.ha⁻¹.yr⁻¹) for calcium, magnesium and potassium at the
 1014 SP site. IS is intrinsic flux from soil estimated from our leaching experiments (corrected for the
 1015 value of the initial exchangeable pool). W is the weathering flux, R is the atmospheric wet
 1016 deposition, Up is the net uptake flux by roots and DL is the deep leaching (see Beaulieu et al.
 1017 2020).

1018

1019 CRediT author statement

1020 **Matthias Oursin**: Methodology, validation, Investigation, Formal analysis, writing – original
1021 draft. **Marie-Claire Pierret**: Conceptualization, validation, Methodology, Investigation,
1022 visualization, Project administration, writing – review & editing, Supervision, Funding
1023 acquisition, Resources. **Emilie Beaulieu**: Software, Formal analysis, Data curation,
1024 Methodology, Writing – review & editing, Supervision. **Damien Daval**: Formal analysis,
1025 Methodology, software, Writing – review & editing. **Arnaud Legout**: Conceptualization,
1026 Methodology, Writing – review & editing, Supervision, Formal analysis, Resources,
1027 Supervision.

1028 Funding

1029 ANR HYDROCRIZSTO ANR-15-CE01-0010-02 provided the funding for this study.

1030 Acknowledgments

1031 We thank OHGE (<http://ohge.unistra.fr/> and Solenn Cotel, Daniel Viville and Sylvain
1032 Benarioumlil) for providing all hydro-meteorological data used in this study. We also thank
1033 Colin Fourtet, Bernd Zeller and Serge Didier for their generous support during the sampling
1034 fieldwork. Thank to Amélie Aubert, Colin Fourtet, René Boutin and Thierry Peronne for
1035 technical assistance. The Observatoire Hydro-Géochimique de l'Environnement OHGE is
1036 financially supported by INSU-CNRS and is part of the OZCAR French Critical Zone
1037 Observatory Network (<https://www.ozcar-ri.org/fr>).

1038 This is an EOST - ITES contribution.

1039

1040 Bibliography

- 1041 André, J.P., Pijarowski, L., 1977. Cation exchange properties of sphagnum peat: exchange
1042 between two cations and protons. *Journal of Soil Science* **28** (4), 573–84.
1043 <https://doi.org/10.1111/j.1365-2389.1977.tb02265.x>.
- 1044 Aubert, D., 2001. Contribution de l'altération et des apports atmosphériques aux transferts de
1045 matières en milieu silicaté : traçage par le strontium et les terres rares . Cas du bassin
1046 versant du Strengbach (Vosges, France). Ph. D. Thesis, Strasbourg University, Strasbourg.
- 1047 Aubert, D., Probst, A., Stille, P., Viville, D., 2002. Evidence of hydrological control of Sr
1048 behavior in stream water (Strengbach catchment, Vosges mountains, France). *Applied*
1049 *Geochemistry* **17** (3), 285–300. [https://doi.org/10.1016/S0883-2927\(01\)00080-4](https://doi.org/10.1016/S0883-2927(01)00080-4).
- 1050 Augusto, L., Bonnaud, P., Ranger, J., 1998. Impact of tree species on forest soil acidification.
1051 *Forest Ecology and Management* **105** (1–3), 67–78. [https://doi.org/10.1016/S0378-](https://doi.org/10.1016/S0378-1127(97)00270-3)
1052 [1127\(97\)00270-3](https://doi.org/10.1016/S0378-1127(97)00270-3).
- 1053 Augusto, L., Ranger, J., Binkley, D., Rothe, A., 2002. Impact of several common tree species
1054 of European temperate forests on soil fertility. *Annals of Forest Science* **59** (3), 233–53.
1055 <https://doi.org/10.1051/forest:2002020>.
- 1056 Baes, A., U., Bloom, P., R., 1988. Exchange of alkaline earth cations in soil organic matter.
1057 *Soil Science* **146** (1).
- 1058 Bailey, S., W, Hornbeck, J., W., Driscoll, C., T., Gaudette, H., E., 1996. Calcium inputs and
1059 transport in a base-poor forest ecosystem as interpreted by Sr isotopes. *Water Resources*
1060 *Research* **32** (3), 707–19.
- 1061 Baize, D., 2000. Guide des analyses en pédologie. INRA, Paris.
- 1062 Barré, P., Velde, B., Catel, N., Abbadie, L., 2007. Soil-plant potassium transfer: impact of plant
1063 activity on clay minerals as seen X-ray diffraction. *Plant Soil* **292**, 137-146.
- 1064 Beaulieu, E., Goddérès, Y., Donnadiou, Y., Labat, D., Roelandt, C., 2012. High sensitivity of

1065 the continental-weathering carbon dioxide sink to future climate change. *Nature Climate*
1066 *Change* **2** (5), 346–49. <https://doi.org/10.1038/nclimate1419>.

1067 Beaulieu, E., Pieret, M.-C., Legout, A., Chabaux, F., Godd ris, Y., Viville, D., Herrmann, A.,
1068 2020. Response of forested catchment over the last 25 years to past acid deposition
1069 assessed by biogeochemical cycle modeling (Strengbach, France). *Ecological Modelling*
1070 **430**, 109-124.

1071 Bedel, L., Poszwa, A., Van Der Heijden, G., Legout, A., Aquilina, L., & Ranger, J. (2016).
1072 Unexpected calcium sources in deep soil layers in low-fertility forest soils identified by
1073 strontium isotopes (Lorraine plateau, eastern France). *Geoderma* **264**, 103-116.

1074 B langer, N., Holmden, C., Courchesne, F., C t , B., Hendershot, W., H., 2012. Constraining
1075 soil mineral weathering $^{87}\text{Sr}/^{86}\text{Sr}$ for calcium apportionment studies of a deciduous forest
1076 growing on soils developed from granitoid igneous rocks. *Geoderma* **185–186**, 84–96.
1077 <https://doi.org/10.1016/j.geoderma.2012.03.024>.

1078 Berger, T., W., K llensperger, G., Wimmer, R., 2004. Plant-soil feedback in Spruce (*Picea*
1079 *Abies*) and mixed Spruce-Beech (*Fagus Sylvatica*) stands as indicated by
1080 dendrochemistry. *Plant and Soil* **264** (1–2), 69–83.
1081 <https://doi.org/10.1023/B:PLSO.0000047714.43253.25>.

1082 Blotevogel, S., Schreck, E., Audry, S., Saldi, G., D., Viers, J., Courjault-Rad , P., Darrozes, J.,
1083 Orgogozo, L., Oliva, P., 2019. Contribution of soil elemental contents and Cu and Sr
1084 isotope ratios to the understanding of pedogenetic processes and mechanisms involved in
1085 the soil-to-grape transfer (Soave Vineyard, Italy). *Geoderma* **343**, 72–85.
1086 <https://doi.org/10.1016/j.geoderma.2019.02.015>.

1087 Blum, J., D., Klaue, A., Nezat, C., A., Driscoll, C., T., Johnson, C., E., Siccama, T., G., Eagar,
1088 C., Fahey, T., J., Likens, G., E., 2002. Mycorrhizal weathering of apatite as an important
1089 calcium source in base-poor forest ecosystems. *Nature* **417** (6890), 729–31.

- 1090 <https://doi.org/10.1038/nature00793>.
- 1091 Bogatko, S., Cauët, E., Bylaska, E., Schenter, G., Fulton, J., Weare, J., 2013. The aqueous Ca^{2+}
1092 system, in comparison with Zn^{2+} , Fe^{3+} , and Al^{3+} : an ab initio molecular dynamics study.
1093 *Chemistry – A European Journal* **19** (9), 3047–60.
1094 <https://doi.org/10.1002/chem.201202821>.
- 1095 Bolan, N., S., Adriano, D., C., Curtin, D., 2003. Soil acidification and liming interactions with
1096 nutrient and heavy metal transformation and bioavailability. *Advances in Agronomy* **78**,
1097 215–72. [https://doi.org/10.1016/S0065-2113\(02\)78006-1](https://doi.org/10.1016/S0065-2113(02)78006-1).
- 1098 Bonhomme, M., 1967. Ages radiométriques de quelques granites des Vosges moyennes.
1099 *Bulletin Du Service de La Carte Géologique d'Alsace et de Lorraine* **20** (1), 101–5.
1100 <https://doi.org/10.3406/sgeol.1967.2311>.
- 1101 Brazier, J.-M., 2018. Rôle des phases minérales des sols en tant que réservoirs de nutriments :
1102 approche expérimentale (abiotique), en milieu naturel et multi-isotopique (isotopes
1103 $\text{s}^{87}\text{Sr}/\text{s}^{86}\text{Sr}$). Ph. D., THesis. Strasbourg University, Strasbourg.
- 1104 Bullen, T., D., Bailey, S., W., 2005. Identifying calcium sources at an acid deposition-impacted
1105 spruce forest: a strontium isotope, alkaline earth element multi-tracer approach.
1106 *Biogeochemistry* **74** (1), 63–99. <https://doi.org/10.1007/s10533-004-2619-z>.
- 1107 Calace, N., Fiorentini, F., Petronio, B., M., Pietroletti, M., 2001. Effects of acid rain on soil
1108 humic compounds. *Talanta* **54** (5), 837–46. [https://doi.org/10.1016/S0039-9140\(01\)00334-4](https://doi.org/10.1016/S0039-9140(01)00334-4).
- 1109
- 1110 Cape, J., N., 1993. Direct damage to vegetation caused by acid rain and polluted cloud:
1111 definition of critical levels for forest trees. *Environmental Pollution* **82** (2), 167–80.
- 1112 Capo, R., C., Stewart, B., W., Chadwick, O., A., 1998. Strontium isotopes as tracers of earth
1113 surface processes: theory and methods. *Geoderma* **82**, 197–225.
- 1114 Carignan, J., Hild, P., Mevelle, G., Morel, J., Yeghicheyan, D., 2001. Routine analyses of trace

1115 elements in geological samples using flow injection and low pressure on-line liquid
1116 chromatography coupled to ICP-MS: a study of geochemical. *The Journal of*
1117 *Geostandards and Geoanalysis* **25**, 187–98.

1118 Chen, Y., Brantley, S., L., 1997. Temperature- and pH-dependence of albite dissolution rate at
1119 acid pH. *Chemical Geology* **135** (3–4), 275–90. [https://doi.org/10.1016/S0009-](https://doi.org/10.1016/S0009-2541(96)00126-X)
1120 [2541\(96\)00126-X](https://doi.org/10.1016/S0009-2541(96)00126-X).

1121 Chou, L., Wollast, R., 1985. Steady-state kinetics and dissolution mechanisms of albite.
1122 *American Journal of Science* **285** (10), 963–93. <https://doi.org/10.2475/ajs.285.10.963>.

1123 Chum, H., L., Overend, R., P., 2001. Biomass and renewable fuels. *Fuel Processing Technology*
1124 **71** (1–3): 187–95. [https://doi.org/10.1016/S0378-3820\(01\)00146-1](https://doi.org/10.1016/S0378-3820(01)00146-1).

1125 Ciesielski, H., Sterckeman, T., Santerne, M., Willery, J., P., 1997a. Determination of cation
1126 exchange capacity and exchangeable cations in soils by means of cobalt hexamine
1127 trichloride. Effects of experimental conditions. *Agronomie* **17** (33): 1–7.
1128 <https://doi.org/10.1051/agro:19970101>.

1129 Ciesielski, H., Sterckeman, T., Santerne, M., Willery, J., P., 1997b. A comparison between
1130 three methods for the determination of cation exchange capacity and exchangeable cations
1131 in soils. *Agronomie, EDP Series* **17**: 9–16.

1132 Clough, A., Skjemstad, J.O., 2000. Physical and chemical protection of soil organic carbon in
1133 three agricultural soils with different contents of calcium carbonate. *Aust. J. Soil Res.* **38**,
1134 1005–1016.

1135 Cohen, W., B., Yang, Z., Stehman, S., V., Schroeder, T., A., Bell, D., M., Masek, J., G., Huang,
1136 C., Meigs., G., W., 2016. Forest disturbance across the conterminous United States from
1137 1985-2012: The emerging dominance of forest decline. *Forest Ecology and Management*
1138 **360**: 242–52. <https://doi.org/10.1016/j.foreco.2015.10.042>.

1139 Cole, D., W., 1986. Nutrient cycling in world forests. In *Forest site and productivity* (ed. S.P.

1140 Gessel), pp. 103-15. Martinus Nijhoff, Netherlands., 103–15. <https://doi.org/10.1007/978->
1141 [94-009-4380-3_9](https://doi.org/10.1007/978-94-009-4380-3_9).

1142 Cosby, B., J., Ferrier, R., C., Jenkins, A., Wright, R., F., 2001. Modelling the effects of acid
1143 deposition: refinements, adjustments and inclusion of nitrogen dynamics in the MAGIC
1144 Model. *Hydrology and Earth System Sciences* **5** (3), 499–518.
1145 <https://doi.org/10.5194/hess-5-499-2001>.

1146 Curtin, D., Selles, F., Steppuhn, H., 1998. Estimating calcium-magnesium selectivity in
1147 smectitic soils from organic matter and texture. *Soil Science Society of America Journal*
1148 **62**, 1280–85. <https://doi.org/10.2136/sssaj1998.03615995006200050019x>.

1149 Dambrine, E., Probst, A., Viville, D., Biron, P., Belgrand, M., C., Paces, T., Novak, M., Buzek,
1150 F., Cerny, J., Groscheova, H., 2000. Spatial variability and long-term trends in mass
1151 balance of N and S in central european forested catchments. In *Carbon and Nitrogen*
1152 *Cycling in European Forest Ecosystems*, ed. Ernst-Detlef Schulze, 405–18. Berlin,
1153 Heidelberg: Springer Berlin Heidelberg. https://doi.org/10.1007/978-3-642-57219-7_19.

1154 Dambrine, E., Le Goaster, S., Ranger, J., 1991. Croissance et nutrition minérale d'un
1155 peuplement d'épicéa sur sol pauvre. II: Prélèvement racinaire et translocation d'éléments
1156 minéraux au cours de la croissance. *Acta Oecologica* **12** (6), 791–808.

1157 Dambrine, E., Pollier, B., Poszwa, A., Ranger, J., Probst, A., Viville, D., Biron, P., Granier, A.,
1158 1998. Evidence of current soil acidification in spruce stands in the Vosges mountains,
1159 North-Eastern France. *Water, Air, and Soil Pollution* **105** (1): 43–52.
1160 <https://doi.org/10.1023/A:1005030331423>.

1161 Daval, D., Sissmann, O., Menguy, N., Saldi, G. D., Guyot, F., Martinez, I., Corvisier, J., Garcai,
1162 B., Machouk, I., Knauss, K. G., Hellmann, R., 2011. Influence of amorphous silica layer
1163 formation on the dissolution rate of olivine at 90°C and elevated pCO₂). *Chemical*
1164 *Geology* **284**, 193-209.

1165 DeHayes, D., H., Schaberg, P., G., Hawley, G., J., Strimbeck G., R., 1999. Acid rain impacts
1166 on calcium nutrition and forest health. *BioScience* **49** (10), 789–800.
1167 <https://doi.org/10.2307/1313570>.

1168 Dessert, C., Clergue, C., Rousteau, A., Crispi, O., & Benedetti, M. F., 2020. Atmospheric
1169 contribution to cations cycling in highly weathered catchment, Guadeloupe (Lesser
1170 Antilles). *Chemical Geology*, *531*, 119354.

1171 De Vries, W., Dobbertin, M., H., Solberg, S., Van Dobben, H.,F., and Schaub, M., 2014.
1172 Impacts of acid deposition, ozone exposure and weather conditions on forest ecosystems
1173 in Europe: an overview. *Plant and soil* **380**, 1-45.

1174 Don, A., Kalbitz, K., 2005. Amounts and degradability of dissolved organic carbon from foliar
1175 litter at different decomposition stages. *Soil Biology and Biochemistry* **37**(12), 2171-2179.

1176 Durka, W., Schulze, E.-D., Gebauer, G., Voerkeliust, S., 1994. Effects of forest decline on
1177 uptake and leaching of deposited nitrate determined from 15N and 18O measurements.
1178 *Nature* **372** (6508), 765–67. <https://doi.org/10.1038/372765a0>.

1179 Edwards, A.P., Bremner, J.M., 1967. Microaggregates in soils. *Soil Science* **18**(1), 64-73.
1180 <https://doi.org/10.1111/j.1365-2389.1967.tb01488.x>

1181 El Gh'Mari, A., 1995. Etude minéralogique, pétrophysique et géochimique de la dynamique
1182 d'altération d'un granite soumis aux dépôts atmosphériques acides (bassin versant du
1183 Strengbach, Vosges, France): mécanismes, bilans et modélisations. Ph. D., Thesis.
1184 Université Louis Pasteur de Strasbourg, Strasbourg, 199 pp.

1185 Ellabban, O., Abu-Rub, H., Blaabjerg, F., 2014. Renewable energy resources: current status,
1186 future prospects and their enabling technology. *Renewable and Sustainable Energy*
1187 *Reviews* **39**, 748–64. <https://doi.org/10.1016/j.rser.2014.07.113>.

1188 Falk Øgaard, A., Krogstad, T., 2005. Release of interlayerpotassium in Norwegian grassland
1189 soils. *Journal of Plant Nutrition and Soil Science* **168**, 80-88.
1190 <https://doi.org/10.1002/jpln.200421454>.

1191 Feng, X., Simpson, A., J., Simpson, M., J., 2005. Chemical and mineralogical controls on humic
1192 acid sorption to clay mineral surfaces. *Organic Geochemistry* **36** (11), 1553–66.
1193 <https://doi.org/10.1016/j.orggeochem.2005.06.008>.

1194 Fichter, J., Dambrine, E., Turpault, M., P., Ranger, J., 1998a. Base cation supply in spruce and
1195 beech ecosystems of the Strengbach catchment (Vosges mountains, NE France). *Water,*
1196 *Air, and Soil Pollution* **104**(1-2), 125-148.

1197 Fichter, J., Turpault, M., P., Dambrine, E., Ranger, J., 1998b. Mineral evolution of acid forest
1198 soils in the Strengbach catchment (Vosges mountains, NE France). *Geoderma* **82**(4), 315-
1199 340. [https://doi.org/10.1016/S0016-7061\(97\)00107-9](https://doi.org/10.1016/S0016-7061(97)00107-9)

1200 Fichter, J., Turpault, M., P., Dambrine, E., Ranger, J., 1998. Localization of base cations in
1201 particle size fractions of acid forest soils (Vosges mountains, N-E France). *Geoderma* **82**
1202 (4), 295–314. [https://doi.org/10.1016/S0016-7061\(97\)00106-7](https://doi.org/10.1016/S0016-7061(97)00106-7).

1203 Gaillardet, J., Braud, I., Hankard, S., Anquetin, S., Bour, O., et al., 2018. OZCAR: The French
1204 Network of Critical Zone Observatories. *Vadoze Zone Journal, Soil science society of*
1205 *America - Geological society of America.*, **17**(1), 1-24. 10.2136/vzj2018.04.0067. insu-
1206 01944414.

1207 Gangloff, S., Stille, P., Schmitt, A.-D., Chabaux, F., 2014. Impact of bacterial activity on Sr
1208 and Ca isotopic compositions ($^{87}\text{Sr}/^{86}\text{Sr}$ and $\Delta^{44}/^{40}\text{Ca}$) in soil solutions (the
1209 StrengbachCZO).” *Procedia Earth and Planetary Science* **10**, 109–13.
1210 <https://doi.org/10.1016/j.proeps.2014.08.038>.

1211 Gangloff, S., Stille, P., Pierret, M.-C., Weber, T., Chabaux, F., 2014. Characterization and
1212 evolution of dissolved organic matter in acidic forest soil and its impact on the mobility of
1213 major and trace elements (case of the Strengbach watershed). *Geochimica et*
1214 *Cosmochimica Acta* **130**: 21–41. <https://doi.org/10.1016/j.gca.2013.12.033>.

1215 Giehl, R., F., von Wirén, N., 2014. Root nutrient foraging. *Plant Physiology* **166**, 509–517.

1216 Godd ris, Y., Franois, L., M., Probst, A., Schott, J., Moncoulon, D., Labat, D., Viville, D.,
1217 2006. Modelling weathering processes at the catchment scale: the WITCH numerical
1218 model. *Geochimica et Cosmochimica Acta* **70** (5), 1128–47.
1219 <https://doi.org/10.1016/j.gca.2005.11.018>.

1220 Godd ris, Y., Williams, J., Z., Schott, J., Pollard, D., Brantley, S., L., 2010. Time evolution of
1221 the mineralogical composition of Mississippi valley loess over the last 10kyr: climate and
1222 geochemical modeling. *Geochimica et Cosmochimica Acta* **74** (22), 6357–74.
1223 <https://doi.org/10.1016/j.gca.2010.08.023>.

1224 Graustein, W., C., 1989. $^{87}\text{Sr}/^{86}\text{Sr}$ ratios measure the sources and flow of strontium in
1225 terrestrial ecosystems. In *Stable Isotopes in Ecological Research*, 491–512. Springer.

1226 Guerold, F., Boudot, J.-P., Jacquemin, G., Vein, D., Merlet, D., Rouiller, J., 2000.
1227 Macroinvertebrate community loss as a result of headwater stream acidification in the
1228 Vosges mountains (NE France). *Biodiversity and Conservation* **9**, 767–83.
1229 <https://doi.org/10.1023/A:1008994122865>.

1230 Hansson, K., Laclau, J. P., Saint-Andr , L., Mareschal, L., van der Heijden, G., Nys, C.,
1231 Nicolas, M., Ranger, J., Legout, A., 2020. Chemical fertility of forest ecosystems. Part 1:
1232 Common soil chemical analyses were poor predictors of stand productivity across a wide
1233 range of acidic forest soils. *Forest Ecology and Management* **461**, 117843.

1234 Hayes, N., R., Buss, H., L., Moore, O., W., Kr m, P., Pancost, R., D., 2020. Controls on granitic
1235 weathering fronts in contrasting climates. *Chemical Geology* **535**, 119450.
1236 <https://doi.org/10.1016/j.chemgeo.2019.119450>.

1237 Horwitz, E., P., Dietz, M., L., Fisher, D., E., 1991. Separation and preconcentration of strontium
1238 from biological, environmental, and nuclear waste samples by extraction chromatography
1239 using a crown ether. *Analytical Chemistry* **63** (5), 522–25.
1240 <https://doi.org/10.1021/ac00005a027>.

- 1241 Iskrenova-Tchoukova, E., Kalinichev, A., G., Kirkpatrick, R. J., 2010. Metal cation
1242 complexation with natural organic matter in aqueous solutions: molecular dynamics
1243 simulations and potentials of mean force. *Langmuir* **26** (20), 15909–19.
1244 <https://doi.org/10.1021/la102535n>.
- 1245 Jandl, R., Alewell, C., Prietzel, J., 2004. Calcium loss in Central European forest soils. *Soil*
1246 *Science Society of America Journal* **68** (2), 588–95.
- 1247 Jobbágy, E.G., Jackson, R.B., 2001. The distribution of soil nutrients with depth: Global
1248 patterns and the imprint of plants. *Biogeochemistry* **53**, 51-77.
- 1249 Jonard, M., Andfe, F., Dambrine, E., Ponette, Q., Ulrich, E., 2009. Temporal trends in the foliar
1250 nutritional status of the french, Walloon and Luxembourg broad-leaved plots of forest
1251 monitoring. *Annals of Forest Science* **66** (4). <https://doi.org/10.1051/forest/2009025>.
- 1252 Jonard, M., Legout, A., Nicolas, M., Dambrine, E., Nys, C., Ulrich, E., van der Perre, R.,
1253 Ponette, Q., 2012. Deterioration of Norway spruce vitality despite a sharp decline in acid
1254 deposition: a long-term integrated perspective. *Global Change Biology* **18** (2), 711–25.
1255 <https://doi.org/10.1111/j.1365-2486.2011.02550.x>.
- 1256 Kalinichev, A., G., Kirkpatrick, R., J., 2007. Molecular dynamics simulation of cationic
1257 complexation with natural organic matter. *European Journal of Soil Science* **58** (4), 909–
1258 17. <https://doi.org/10.1111/j.1365-2389.2007.00929.x>.
- 1259 Kennedy, M., J., Hedin, L., O., Derry, L., A., 2002. “Decoupling of unpolluted temperate forests
1260 from rock nutrient sources revealed by natural ⁸⁷Sr/⁸⁶Sr and ⁸⁴Sr tracer addition.
1261 *Proceedings of the National Academy of Sciences of the United States of America* **99** (15),
1262 9639–44. <https://doi.org/10.1073/pnas.152045499>.
- 1263 Khokhar, M., F., Frankenberg, C., Van Roozendaal, M., Beirle, S., Köhl, S., Richter, A., Platt,
1264 U., Wagner, T., 2005. Satellite observations of atmospheric SO₂ from volcanic eruptions
1265 during the time-period of 1996-2002. *Advances in Space Research* **36** (5): 879–87.

- 1266 <https://doi.org/10.1016/j.asr.2005.04.114>.
- 1267 Khormali, F., Rezaei, F., Rahimzadeh, N., Hosseinifard, S. J., Dordipour, E. 2015. Rhizosphere-
1268 induced weathering of minerals in loess-derived soils of Golestan Province, Iran.
1269 *Geoderma Regional* **5**, 34-43.
- 1270 Klimont, Z., Smith, S., J., Cofala, J., 2013. The last decade of global anthropogenic sulfur
1271 dioxide: 2000-2011 Emissions.” *Environmental Research Letters* **8** (1).
1272 <https://doi.org/10.1088/1748-9326/8/1/014003>.
- 1273 Knauss, K., G., Wolery, T., J., 1986. Dependence of albite dissolution kinetics on pH and time
1274 at 25°C and 70°C. *Geochimica et Cosmochimica Acta* **50** (11), 2481–97.
1275 [https://doi.org/10.1016/0016-7037\(86\)90031-1](https://doi.org/10.1016/0016-7037(86)90031-1).
- 1276 Kopáček, J., Veselý, J., 2005. Sulfur and nitrogen emissions in the Czech Republic and
1277 Slovakia from 1850 till 2000. *Atmospheric Environment* **39** (12), 2179–88.
1278 <https://doi.org/10.1016/j.atmosenv.2005.01.002>.
- 1279 Landmann, G., 1995. “Forest decline and air pollution effects in the french mountains: a
1280 synthesis. In *Forest Decline and Atmospheric Deposition Effects in the French Mountains*,
1281 ed. Guy Landmann, Maurice Bonneau, and Michèle Kaennel, 407–52. Berlin, Heidelberg:
1282 Springer Berlin Heidelberg.
- 1283 Larque, P., Weber, F., 1978. Techniques de préparation des minéraux argileux en vue de
1284 l’analyse par diffraction des rayons-X. *Notes Techniques de l’Institut de Géologie*,
1285 *Université de Strasbourg*, 1–33.
- 1286 Lefèvre, Y., 1988. Les sols du bassin d’Aubure (Haut-Rhin) : caractérisation et facteurs de
1287 répartition.” *Annales Des Sciences Forestières* **45** (4), 417–22.
1288 <https://doi.org/10.1051/forest:19880409>.

1289 le Goaster, S., Dambrine, E., Ranger, J., 1991. Croissance et nutrition minérale d'un peuplement
1290 d'épicéa sur sol pauvre. I: evolution de la biomasse et dynamique d'incorporation
1291 d'éléments minéraux. *Acta Oecologica* **12** (6), 771–89.

1292 Legout, A., van der Heijden, G., Jaffrain, J., Boudot, J.-P., Ranger, J., 2016. Tree species effects
1293 on solution chemistry and major element fluxes: a case study in the Morvan (Breuil,
1294 France). *Forest Ecology and Management* **378**, 244–58.
1295 <https://doi.org/10.1016/j.foreco.2016.07.003>.

1296 Legout, A., Hansson, K., van der Heijden, G., Laclau, J. P., Mareschal, L., Nys, C., Nicolas,
1297 M., Sant-André, L., Ranger, J., 2020. Chemical fertility of forest ecosystems. Part 2:
1298 Towards redefining the concept by untangling the role of the different components of
1299 biogeochemical cycling. *Forest Ecology and Management* **461**, 117844.

1300 Li, Y., Sun, J., Tian, D., Wang, J., Ha, D., Qu, Y., Jing, G., Niu, S., 2018. Soil acid cations
1301 induced reduction in soil respiration under nitrogen enrichment and soil acidification.
1302 *Science of the Total Environment* **615**, 1535–46.
1303 <https://doi.org/10.1016/j.scitotenv.2017.09.131>.

1304 Likens, G., E., Driscoll, C., T., Buso, D., C., 1996. Long-term effects of acid rain: response and
1305 recovery of a forest ecosystem. *Science*, **272**(5259), 244-246.

1306 Lu, Z., Streets, D., G., Zhang, Q., Wang, S., Carmichael, G., R., Cheng, Y., F., Wei, C., Chin,
1307 M., Diehl, T., Tan., Q., 2010. Sulfur dioxide emissions in China and sulfur trends in East
1308 Asia since 2000. *Atmospheric Chemistry and Physics* **10** (13), 6311–31.
1309 <https://doi.org/10.5194/acp-10-6311-2010>.

1310 Lucas, R., W., Klaminder, J., Futter, M., N., Bishop, K., H., Egnell, G., Laudon, H., Högberg,
1311 P., 2011. A meta-analysis of the effects of nitrogen additions on base cations: implications
1312 for plants, soils, and streams. *Forest Ecology and Management* **262** (2), 95–104.
1313 <https://doi.org/10.1016/j.foreco.2011.03.018>.

1314 Ludwig, B., Khanna, P., K., Hölscher, D., Anurugsa, B., 1999. Modelling changes in cations
1315 in the topsoil of an amazonian acrisol in response to additions of wood ash. *European*
1316 *Journal of Soil Science* **50** (4), 717–26. <https://doi.org/10.1046/j.1365-2389.1999.00268.x>.

1317 Mareschal, L., Ranger, J., Turpault, M., P., 2009. Stoichiometry of a dissolution reaction of a
1318 trioctahedral vermiculite at pH 2.7. *Geochimica et Cosmochimica Acta* **73**, 307-319.

1319 Marschner, H., 1995. Mineral nutrition of higher plants. In: Marschner, H. (Ed.), Mineral
1320 Nutrition of Higher Plants (Second Edition). Academic Press, London, pp. v-vi.

1321 McMorrow, J., Abdul Talip, M., 2001. Decline of forest area in Sabah, Malaysia: relationship
1322 to state policies, land code and land capability. *Global Environmental Change* **11** (3), 217–
1323 30. [https://doi.org/10.1016/S0959-3780\(00\)00059-5](https://doi.org/10.1016/S0959-3780(00)00059-5).

1324 Meek, K., Derry, L., Sparks, J., Cathles, L., 2016. $^{87}\text{Sr}/^{86}\text{Sr}$, Ca/Sr, and Ge/Si ratios as tracers
1325 of solute sources and biogeochemical cycling at a temperate forested shale catchment,
1326 Central Pennsylvania, USA. *Chemical Geology* **445**, 84–102.
1327 <https://doi.org/10.1016/j.chemgeo.2016.04.026>.

1328 Mehne-Jakobs, B., 1995. The influence of magnesium deficiency on carbohydrate
1329 concentrations in Norway Spruce (*Picea Abies*) needles. *Tree Physiology* **15** (9), 577–84.
1330 <https://doi.org/10.1093/treephys/15.9.577>.

1331 Miller, E., K., Blum, J., D., Friedland, A., J., 1993. Determination of soil exchangeable-cation
1332 loss and weathering rates using Sr isotopes. *Nature* **362** (6419), 438–41.
1333 <https://doi.org/10.1038/362438a0>.

1334 Novak, M., Holmden, C., Farkaš, J., Kram, P., Hruska, J., Curik, J., ... & Fottova, D. (2020).
1335 Calcium and strontium isotope dynamics in three polluted forest ecosystems of the Czech
1336 Republic, Central Europe. *Chemical Geology* **536**, 119472.

1337 Paces, T., 1985. Sources of acidification in Central Europe estimated from elemental budgets
1338 in small basins. *Nature* **315** (6014), 31–36. <https://doi.org/10.1038/315031a0>.

- 1339 Pang, X., Trubins, R., Lekavicius, V., Galinis, A., Mozgeris, G., Kulbokas, G., Mörtberg, U.,
1340 2019. Forest bioenergy feedstock in Lithuania – renewable energy goals and the use of
1341 forest resources. *Energy Strategy Reviews* **24**, 244–53.
1342 <https://doi.org/10.1016/j.esr.2019.04.004>.
- 1343 Paola, A., Barré, P., Cozzolino, V., Di Meo, V., Velde, B., 2016. Short term clay mineral release
1344 and re-capture of potassium in a *Zea mays* field experiment. *Geoderma* **264**, 54–60.
- 1345 Pett-Ridge, J., C., Derry, L., A., Barrows, J., K., 2009. Ca/Sr and ⁸⁷Sr/⁸⁶Sr ratios as tracers of
1346 Ca and Sr cycling in the Rio Icacos watershed, Luquillo mountains, Puerto Rico. *Chemical*
1347 *Geology* **267** (1–2), 32–45. <https://doi.org/10.1016/j.chemgeo.2008.11.022>.
- 1348 Philip H., E., Chiarizia, R., Dietz, M., L., 1992. A novel strontium-selective extraction
1349 chromatographic resin*. *Solvent Extraction and Ion Exchange* **10** (2), 313–36.
1350 <https://doi.org/10.1080/07366299208918107>.
- 1351 Pierret, M.-C., Cotel, S., Ackerer, P., Beaulieu, E., Benarioumlil, S., Boucher, M., Boutin, R.,
1352 Chabaux, F., Delay, F., Fournier, C., Friedmann, P., Fritz, B., Gangloff, S., Girard, J.-F.,
1353 Legtchenko, A., Viville, D., Weill, S., Probst, A., 2018. The Strengbach catchment: a
1354 multidisciplinary environmental sentry for 30 years.” *Vadose Zone Journal* **17** (1), 0.
1355 <https://doi.org/10.2136/vzj2018.04.0090>.
- 1356 Pierret, M.-C., Stille, P., Prunier, J., Viville, D., Chabaux, F., 2014. Chemical and U-Sr isotopic
1357 variations in stream and source waters of the Strengbach watershed (Vosges mountains,
1358 France). *Hydrology and Earth System Sciences* **18** (10), 3969–85.
1359 <https://doi.org/10.5194/hess-18-3969-2014>.
- 1360 Pierret, M.-C., Viville, D., Dambrine, E., Cotel, S., Probst, A., 2019. Twenty-five year record
1361 of chemicals in open field precipitation and throughfall from a medium-altitude forest
1362 catchment (Strengbach - NE France): an obvious response to atmospheric pollution trends.
1363 *Atmospheric Environment* **202**, 296–314. <https://doi.org/10.1016/j.atmosenv.2018.12.026>.

1364 Poszwa, A., Dambrine, E., Pollier, B., Atteia, O., 2000. A comparison between Ca and Sr
1365 cycling in forest ecosystems. *Plant and Soil* **225** (1–2), 299–310.
1366 <https://doi.org/10.1023/A:1026570812307>.

1367 Poszwa, A., Ferry, B., Dambrine, E., Pollier, B., Wickman, T., Loubet, M., Bishop, K., 2004.
1368 Variations of bioavailable Sr concentration and $^{87}\text{Sr}/^{86}\text{Sr}$ ratio in boreal forest
1369 ecosystems. *Biogeochemistry* **67** (1), 1–20.
1370 <https://doi.org/10.1023/B:BIOG.0000015162.12857.3e>.

1371 Probst, A., Fritz, B., Stille, P., 1992. Consequence of acid deposition on natural weathering
1372 processes: field studies and modelling. In *Proceedings of the 7th International Symposium*
1373 *on Water-Rock Interaction, –WR-7/Park City/Utah/USA/13–18 July*.

1374 Probst, A., El Gh'mari, A., Aubert, D., Fritz, B., McNutt, R., 2000. Strontium as a tracer of
1375 weathering processes in a silicate catchment polluted by acid atmospheric inputs,
1376 Strengbach, France. *Chemical Geology* **170** (1–4), 203–19. [https://doi.org/10.1016/S0009-](https://doi.org/10.1016/S0009-2541(99)00248-X)
1377 [2541\(99\)00248-X](https://doi.org/10.1016/S0009-2541(99)00248-X).

1378 Probst, A., Party, J., P., Fevrier, C., Dambrine, E., Thomas, A., L., Stussi, J., M., 1999. Evidence
1379 of springwater acidification in the Vosges mountains (North-East of France): influence of
1380 bedrock buffering capacity. *Water, Air, and Soil Pollution* **114** (3), 395–411.
1381 <https://doi.org/10.1023/A:1005156615921>.

1382 Probst, A., Viville, D., Fritz, B., Ambroise, B., Dambrine, E., 1992. Hydrochemical budgets of
1383 a small forested granitic catchment exposed to acid deposition: the Strengbach catchment
1384 case study (Vosges massif, France). *Water, Air, & Soil Pollution* **62** (3–4), 337–47.
1385 <https://doi.org/10.1007/BF00480265>.

1386 Prunier, J., Chabaux, F., Stille, P., Gangloff, S., Pierret, M.-C., Viville, D., Aubert, A., 2015.
1387 Geochemical and isotopic (Sr, U) monitoring of soil solutions from the Strengbach
1388 catchment (Vosges mountains, France): evidence for recent weathering evolution.

1389 *Chemical Geology* **417**, 289–305. <https://doi.org/10.1016/j.chemgeo.2015.10.012>.

1390 Prunier, J., 2008. Etude du fonctionnement d'un écosystème forestier en climat tempéré, par
1391 l'apport de la géochimie élémentaire et isotopique (Sr, U-Th-Ra): Cas du bassin versant du
1392 Strengbach (Vosges, France), Ph. D. Thesis, Strasbourg University, Strasbourg.

1393 Qiu, Q., Wu, J., Liang, G., Liu, J., Chu, G., Zhou, G., Zhang, D., 2015. Effects of simulated acid
1394 rain on soil and soil solution chemistry in a monsoon evergreen broad-leaved forest in
1395 southern China. *Environmental Monitoring and Assessment* **187** (5).
1396 <https://doi.org/10.1007/s10661-015-4492-8>.

1397 Rahmatullah, Mengel K., 2000. Potassium release from mineral structures by H⁺ ion resin.
1398 *Geoderma* **96**, 291-305. [https://doi.org/10.1016/S0016-7061\(00\)00014-8](https://doi.org/10.1016/S0016-7061(00)00014-8).

1399 Ranger, J., Turpault, M.P., 1999. Input-output nutrient budgets as a diagnostic-tool for the
1400 sustainability of forest management. *Forest Ecology and Management* **122**, 7-16.

1401 Reichle, D., E., 1981. *Dynamic Properties of Forest Ecosystems*. Vol. 23. Cambridge
1402 University Press.

1403 Robert, M., Tessier, D., 1974. *Méthode de Préparation Des Argiles Des Sols Pour Des Études*
1404 *Minéralogiques*. *Ann. Agron.* Vol. 25.

1405 Rodhe, H., Grennfelt, P., Wisniewski, J., Ågren, C., Bengtsson, G., Johansson, K., Kauppi, P.,
1406 Kucera, V., Rasmussen, L., Rosseland, B., Schotte, L., Sellden, G., 1995. “Acid Reign
1407 ’95? - Conference Summary Statement.” *Water, Air, & Soil Pollution* **85** (1), 1–14.
1408 <https://doi.org/10.1007/BF00483684>.

1409 Rowley, M., C., Grand, S., Verrecchia, E., P., 2018. Calcium-mediated stabilisation of soil
1410 organic carbon. *Biogeochemistry* **137** (1–2), 27–49. [https://doi.org/10.1007/s10533-017-](https://doi.org/10.1007/s10533-017-0410-1)
1411 [0410-1](https://doi.org/10.1007/s10533-017-0410-1).

1412 Schlesinger, W.H., 1997. *Biogeochemistry: an analysis of global change*. Academic press, San
1413 Diego. 588p

- 1414 Schmitt, A.-D., Gangloff, S., Labolle, F., Chabaux, F., Stille, P., 2017. Calcium biogeochemical
1415 cycle at the beech tree-soil solution interface from the Strengbach CZO (NE France):
1416 insights from stable Ca and radiogenic Sr isotopes. *Geochimica et Cosmochimica Acta*
1417 **213**, 91–109. <https://doi.org/10.1016/j.gca.2017.06.039>.
- 1418 Schulze, E.-D., 1989. Air pollution and forest decline in a Spruce (*Picea Abies*) forest. *Science*
1419 **244** (7), 776. <https://doi.org/10.1126/science.244.4906.776>.
- 1420 Sentenac, H., Grignon, C., 1981. A model for predicting ionic equilibrium concentrations in
1421 cell walls. *Plant Physiology* **68** (2), 415 LP – 419. <https://doi.org/10.1104/pp.68.2.415>.
- 1422 Siefertmann-Harms, D., Boxler-Baldoma, C., Von Wilpert, K., Günther Heumann, H., 2004.
1423 The rapid yellowing of Spruce at a mountain site in the central black forest (Germany).
1424 Combined effects of Mg deficiency and ozone on biochemical, physiological and
1425 structural properties of the chloroplasts. *Journal of Plant Physiology* **161** (4), 423–37.
1426 <https://doi.org/10.1078/0176-1617-01095>.
- 1427 Smith, S., J., Pitchera, H., Wigley, T., M., L., 2001. Global and regional anthropogenic sulfur
1428 dioxide emissions. *Global and Planetary Change* **29** (1–2), 99–119.
1429 [https://doi.org/10.1016/S0921-8181\(00\)00057-6](https://doi.org/10.1016/S0921-8181(00)00057-6).
- 1430 Stoddard, J., L., Jeffries, D., S., Lükewille, A., Clair, T., A., Dillon, P., J., Driscoll, C., T.,
1431 Forsius, M., Johannessen, M., Kahl, J., S., Kellogg, J., H., Kemp, A., Mannio, J., Monteith,
1432 D., T., Murdoch, P., S., Patrick, S., Rebsdorf, A., Skjelkvåle, B., L., Stainton, M., P.,
1433 Traaen, T., van Dam, H., Webster, K., E., Wieting, J., Wilander, A., 1999. Regional trends
1434 in aquatic recovery from acidification in North America and Europe. *Nature* **401** (6753),
1435 575–78. <https://doi.org/10.1038/44114>.
- 1436 Sudalma, S., Purwanto, P., Santoso, L., W., 2015. The effect of SO₂ and NO₂ from
1437 transportation and stationary emissions sources to SO₄²⁻ and NO₃⁻ in rain water in
1438 Semarang. *Procedia Environmental Sciences* **23**, 247–52.

1439 <https://doi.org/10.1016/j.proenv.2015.01.037>.

1440 Sutton, R., Sposito, G., 2006. Molecular simulation of humic substance-Ca-montmorillonite
1441 complexes. *Geochimica et Cosmochimica Acta* **70** (14), 3566–81.
1442 <https://doi.org/10.1016/j.gca.2006.04.032>.

1443 Sverdrup, H., Thelin, G., Robles, M., Stjernquist, I., Sørensen, J., 2006. Assessing nutrient
1444 sustainability of forest production for different tree species considering Ca, Mg, K, N and
1445 P at Björnstorp Estate, Sweden. *Biogeochemistry* **81** (2), 219–38.
1446 <https://doi.org/10.1007/s10533-006-9038-2>.

1447 Sverdrup, H., Warfvinge, P., Blake, L., Goulding, K., 1995. Modelling recent and historic soil
1448 data from the rothamsted experimental station, UK using SAFE. *Agriculture, Ecosystems
1449 and Environment* **53** (2), 161–77. [https://doi.org/10.1016/0167-8809\(94\)00558-V](https://doi.org/10.1016/0167-8809(94)00558-V).

1450 Sverdrup, H., Warfvinge, P., 1993. Calculating field weathering rates using a mechanistic
1451 geochemical model PROFILE. *Applied Biochemistry* **8**, 273-283.

1452 Thimonier, A., Dupouey, J., L., Le Tacon, F., 2000. Recent losses of base cations from soils of
1453 *Fagus Sylvatica* L. stands in Northeastern France. *Ambio* **29** (6), 314–21.
1454 <https://doi.org/10.1579/0044-7447-29.6.314>.

1455 Thiry, M., Carrillo, N., Franke, C., Martineau, N., Thiry, M., Carrillo, N., Franke, C.,
1456 Martineau, N., 2013. Technique de préparation des minéraux argileux en vue de l'analyse
1457 par diffraction des rayons X et introduction à l'interprétation des diagrammes. Rapport
1458 Technique N° RT131010MTHI, Centre de Géosciences, Ecole des Mines de Paris,
1459 Fontainebleau, France, 34 p.

1460 Tian, D., Niu, S., 2015. A global analysis of soil acidification caused by nitrogen addition.
1461 *Environmental Research Letters* **10** (2). <https://doi.org/10.1088/1748-9326/10/2/024019>.

1462 Turpault, M.-P., Calvaruso, C., Dincher, M., 2019. Contribution of carbonates and oxalates to
1463 the calcium cycle in three beech temperate forest ecosystems with contrasting soil calcium

1464 availability. *Biogeochemistry* **4** (v). <https://doi.org/10.1007/s10533-019-00610-4>.

1465 Ulrich, B., 1986. Natural and anthropogenic components of soil acidification. *Zeitschrift Für*
1466 *Pflanzenernährung Und Bodenkunde* **149** (6), 702–17.
1467 <https://doi.org/10.1002/jpln.19861490607>.

1468 van der Heijden, G., Bel, J., Craig, C.A., Midwood, A.J., Mareschal, L., Ranger, J., Dambrine,
1469 E., Legout, A., 2018. Measuring Plant-Available Mg, Ca, and K Pools in the Soil-An
1470 Isotopic Dilution Assay. *ACS Earth Space Chem.* **2**, 292-313.

1471 van der Heijden, G., Legout, A., Pollier, B., Ranger, J., Dambrine, E., 2014. The dynamics of
1472 calcium and magnesium inputs by throughfall in a forest ecosystem on base poor soil are
1473 very slow and conservative: evidence from an isotopic tracing experiment (^{26}Mg and
1474 ^{44}Ca). *Biogeochemistry* **118**, 413–442.

1475 van der Heijden, G., Legout, A., Midwood, A., J., Craig, C.-A., Pollier, B., Ranger, J.,
1476 Dambrine, E., 2013. Mg and Ca root uptake and vertical transfer in soils assessed by an in
1477 situ ecosystem-scale multi-isotopic (^{26}Mg & ^{44}Ca) tracing experiment in a beech stand
1478 (Breuil-Chenue, France). *Plant and Soil* **369** (1–2), 33–45.
1479 <https://doi.org/10.1007/s11104-012-1542-7>.

1480 van der Heijden, G., Legout, A., Nicolas, M., Ulrich, E., Johnson, D., W., Dambrine, E., 2011.
1481 Long-term sustainability of forest ecosystems on sandstone in the Vosges mountains
1482 (France) facing atmospheric deposition and silvicultural change. *Forest Ecology and*
1483 *Management* **261** (3), 730–40. <https://doi.org/10.1016/j.foreco.2010.12.003>.

1484 Verttein, D., Kühn, T., Kaiser, K., Jahn, R., 2013. Illite transformation and potassium release
1485 upon changes in composition of the rhizosphere soil solution. *Plant and Soil* **371** (1-2),
1486 267-279.

1487 Viana, H., Cohen, W., B., Lopes, D., Aranha, J., 2010. Assessment of forest biomass for use as
1488 energy. GIS-based analysis of geographical availability and locations of wood-fired power

1489 plants in Portugal. *Applied Energy* **87** (8), 2551–60.
1490 <https://doi.org/10.1016/j.apenergy.2010.02.007>.

1491 Viville, D., Chabaux, F., Stille, P., Pierret, M.-C., Gangloff, S., 2012. Erosion and weathering
1492 fluxes in granitic basins: the example of the Strengbach catchment (Vosges massif, Eastern
1493 France). *Catena* **92**, 122–29. <https://doi.org/10.1016/j.catena.2011.12.007>.

1494 Viville, D., Biron, P., Granier, A., Dambrine, E., Probst, A., 2013. Interception in a
1495 mountainous declining spruce stand in the Strengbach catchment (Vosges, France).
1496 *Journal of Hydrology* **144** (1-4), 273-282.

1497 von Lützow, M., Kögel-Knabner, I., Ekschmitt, K., Matzner, E., Guggenberger, G., Marschner,
1498 B., Flessa, H., 2006. Stabilization of organic matter in temperate soils: mechanisms and
1499 their relevance under different soil conditions - a review. *European Journal of Soil Science*
1500 **57**(4):426–445.

1501 Wei, H., Liu, W., JZhang, J., Qin, Z., 2017. Effects of simulated acid rain on soil fauna
1502 community composition and their ecological niches. *Environmental Pollution* **220**, 460–68.
1503 <https://doi.org/10.1016/j.envpol.2016.09.088>.

1504 White, A. F., Brantley, S. L., 2003. The effect of time on the weahtering of silicate minerals:
1505 why do weathering rates differ in the laboratory and field? *Chemical Geology* **202**, 479-
1506 506.

1507 Wild, B., Daval, D., Guyot, F., Knauss, K. G., Pollet-Villard, M., Imfeld, G., 2016. pH-
1508 dependent control of feldspar dissolution rate by altered surface layers. *Chemical Geology*
1509 **442**, 148-159.

1510 Wild, B., Daval, D., Beaulieu, E., Pierret, M.-C., Viville, D., Imfeld, G., 2019. *In-situ*
1511 dissolution rates of silicate minerals and associated bacterial communities in the critical
1512 zone (Strengbach catchment, France). *Geochimica et Cosmochimica Acta* **249**, 95-120.

1513 Zetterberg, T., Köhler, S., J., Löfgren, S., 2014. Sensitivity analyses of MAGIC modelled

1514 predictions of future impacts of whole-tree harvest on soil calcium supply and stream acid
1515 neutralizing capacity. *Science of the Total Environment* **494–495**, 187–201.
1516 <https://doi.org/10.1016/j.scitotenv.2014.06.114>.

1517

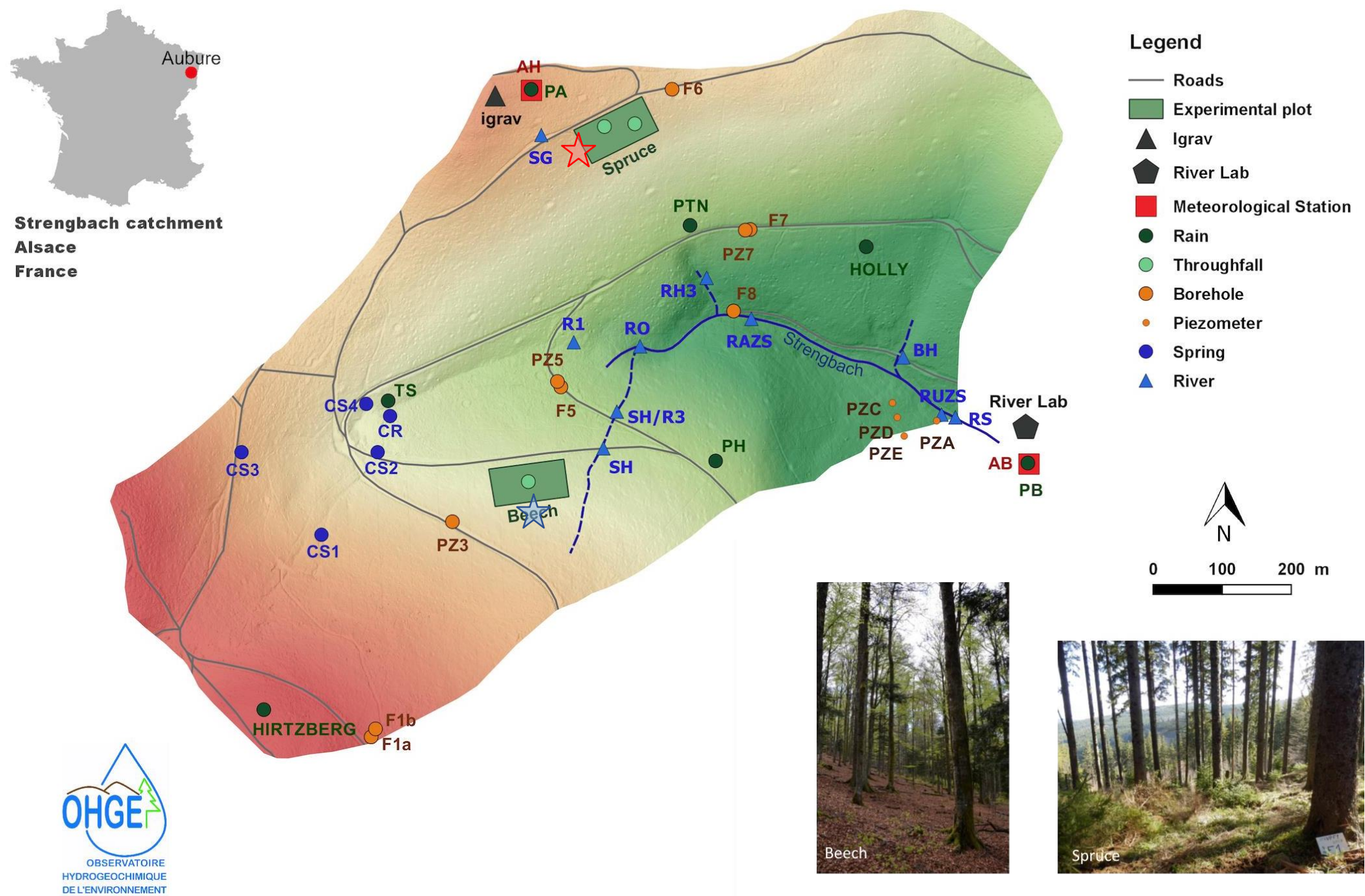


Fig. 1: Strengbach catchment map with different equipment and monitoring stations (see legend). The red star corresponds to the soil pit at the SP site (SP: Spruce plot), and the blue star corresponds to the soil pit at the BP site (BP: beech plot).

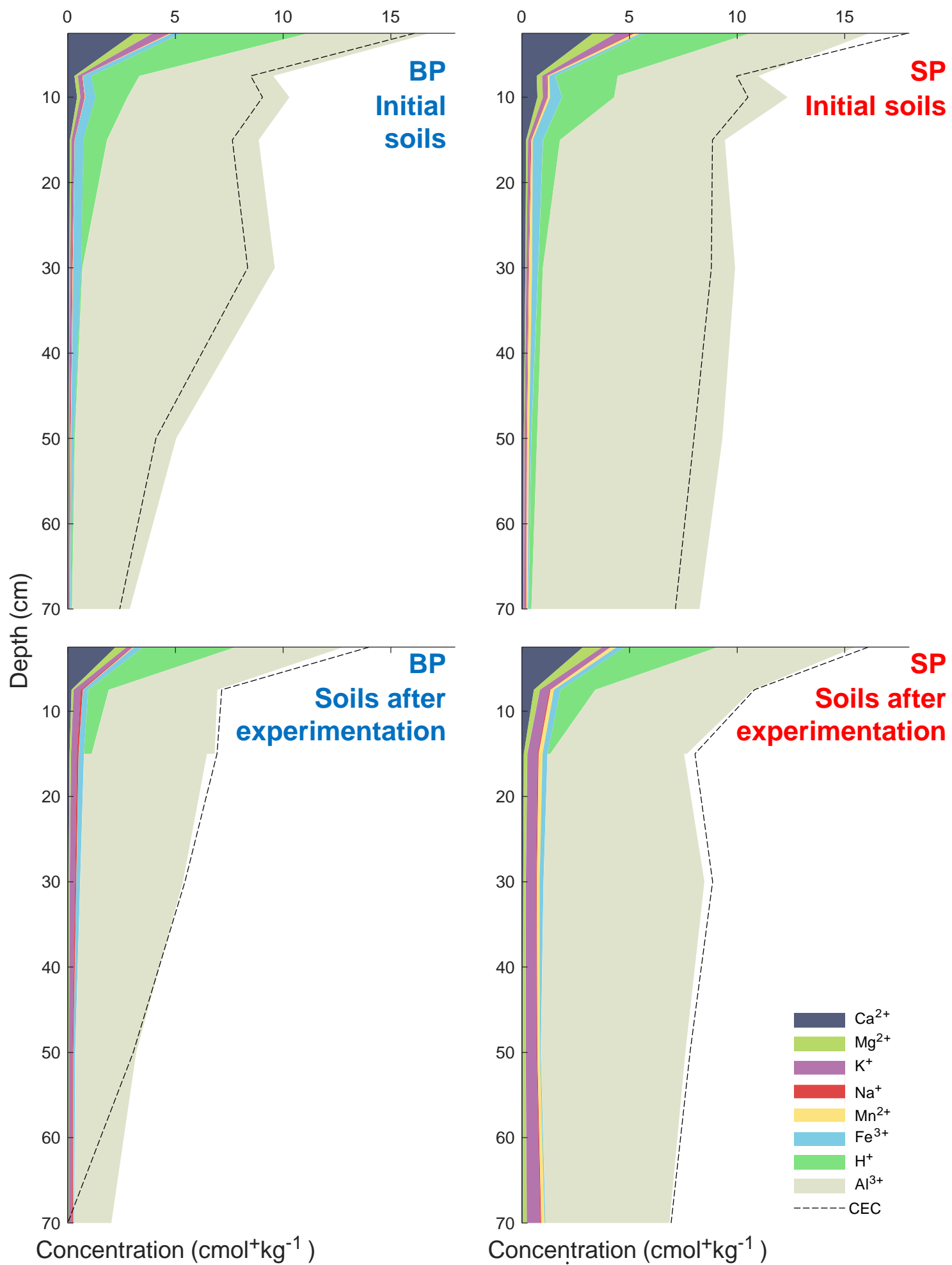


Fig. 2: Composition of the exchangeable phase for both BP (under beech) and SP (under spruce) soils at various depths, in initial soils and in soils after experimentation. Compositions were determined by cobaltihexamine extraction protocol.

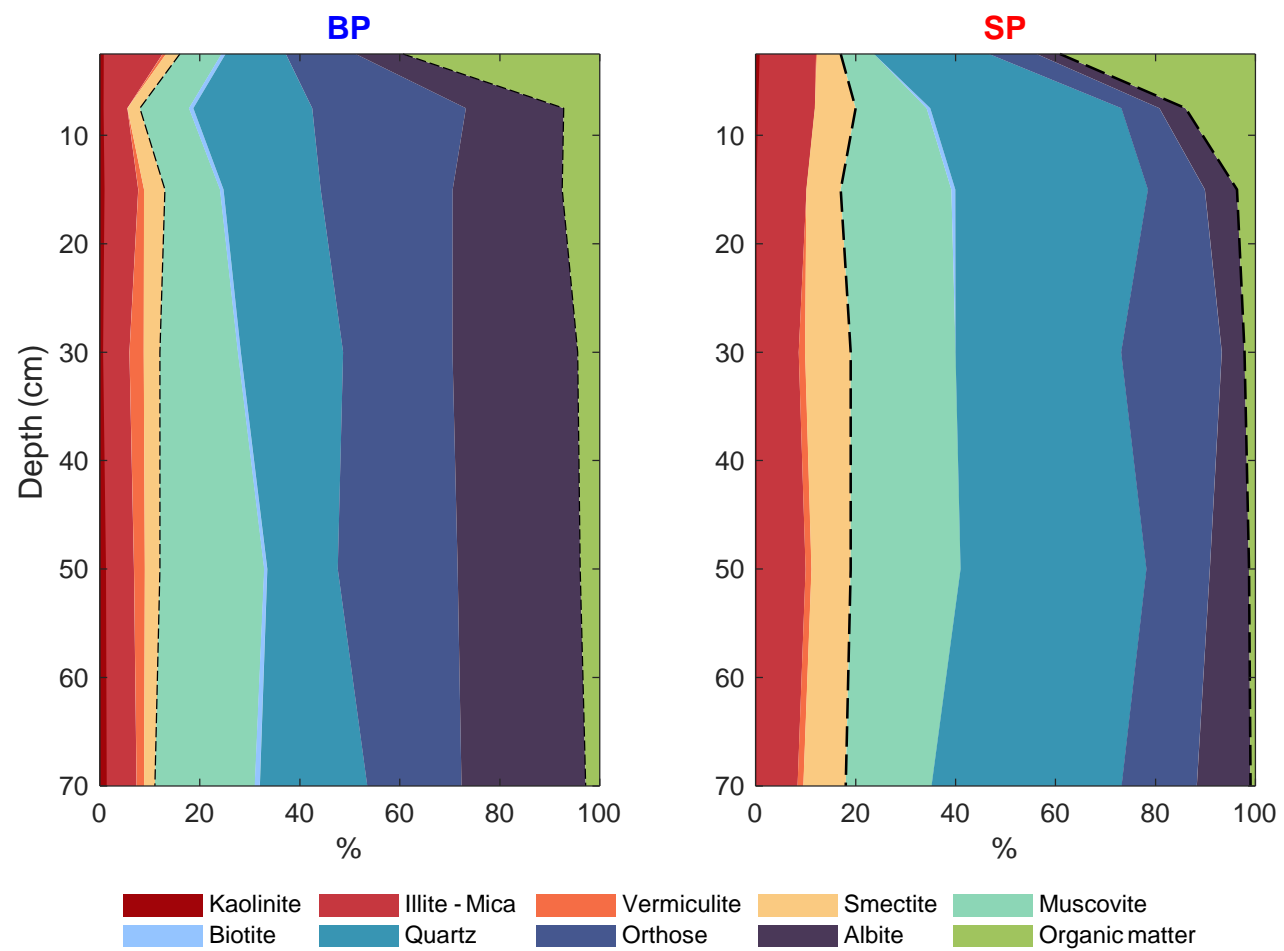


Fig. 3: Mineral composition in % of the soils from BP (left) and SP (right) profiles. Reddish parts correspond to clays, blueish parts correspond to primary minerals and greenish parts to organic matter (data in appendix A - supplementary material).

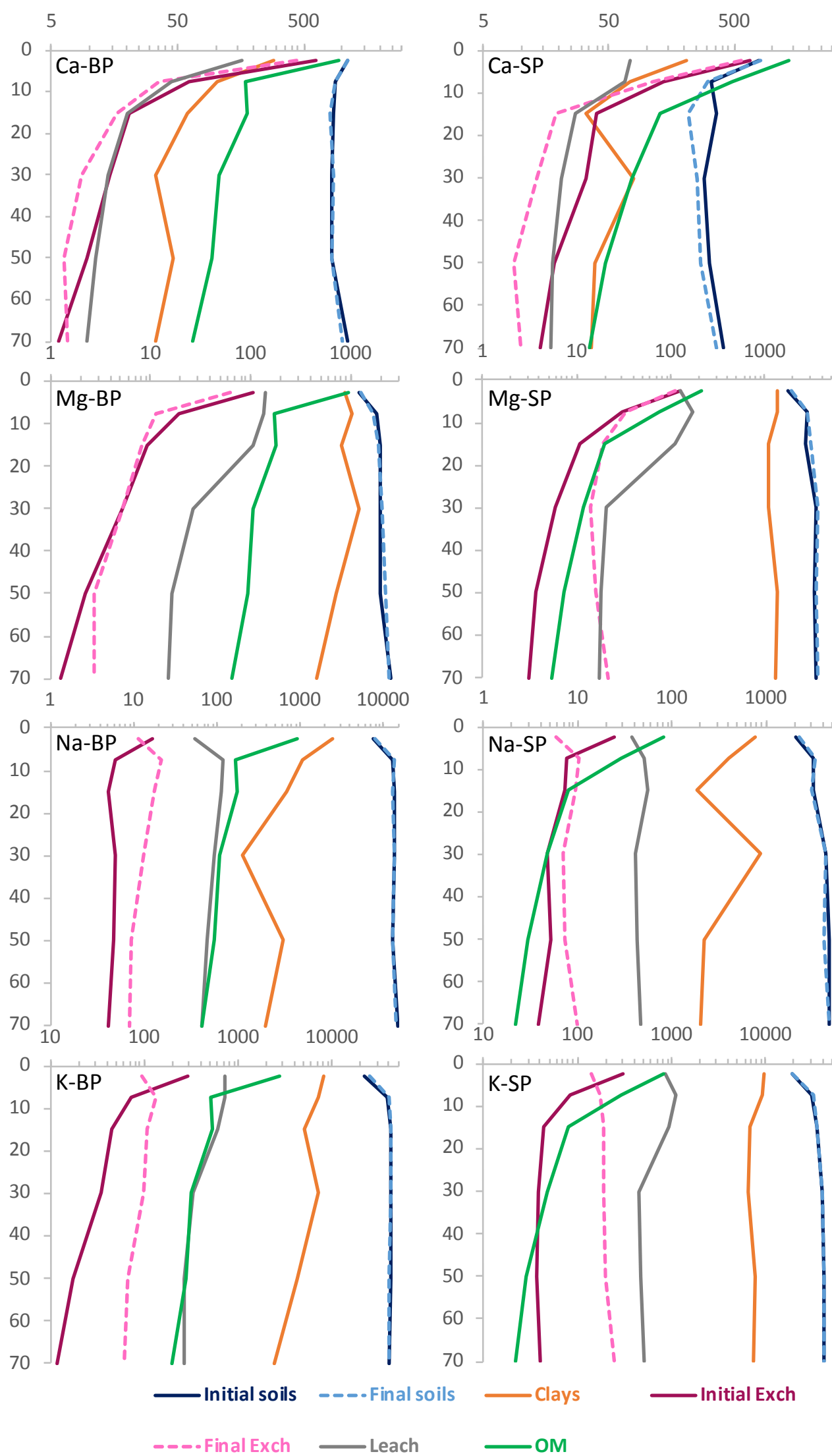


Fig. 4: Variation versus depth of chemical compositions (expressed in $\mu\text{g/g}$ of soil) for initial and final (after experimentation) bulk soils, compare with the contribution of different reservoirs as clay minerals, initial and final exchangeable pool, organic matter as total cumulated experimental leachate calculated for 1 g of soil (see text; Appendix A-Supplementary material) for two sites: BP-Beech Plot and SP-Spruce Plot.

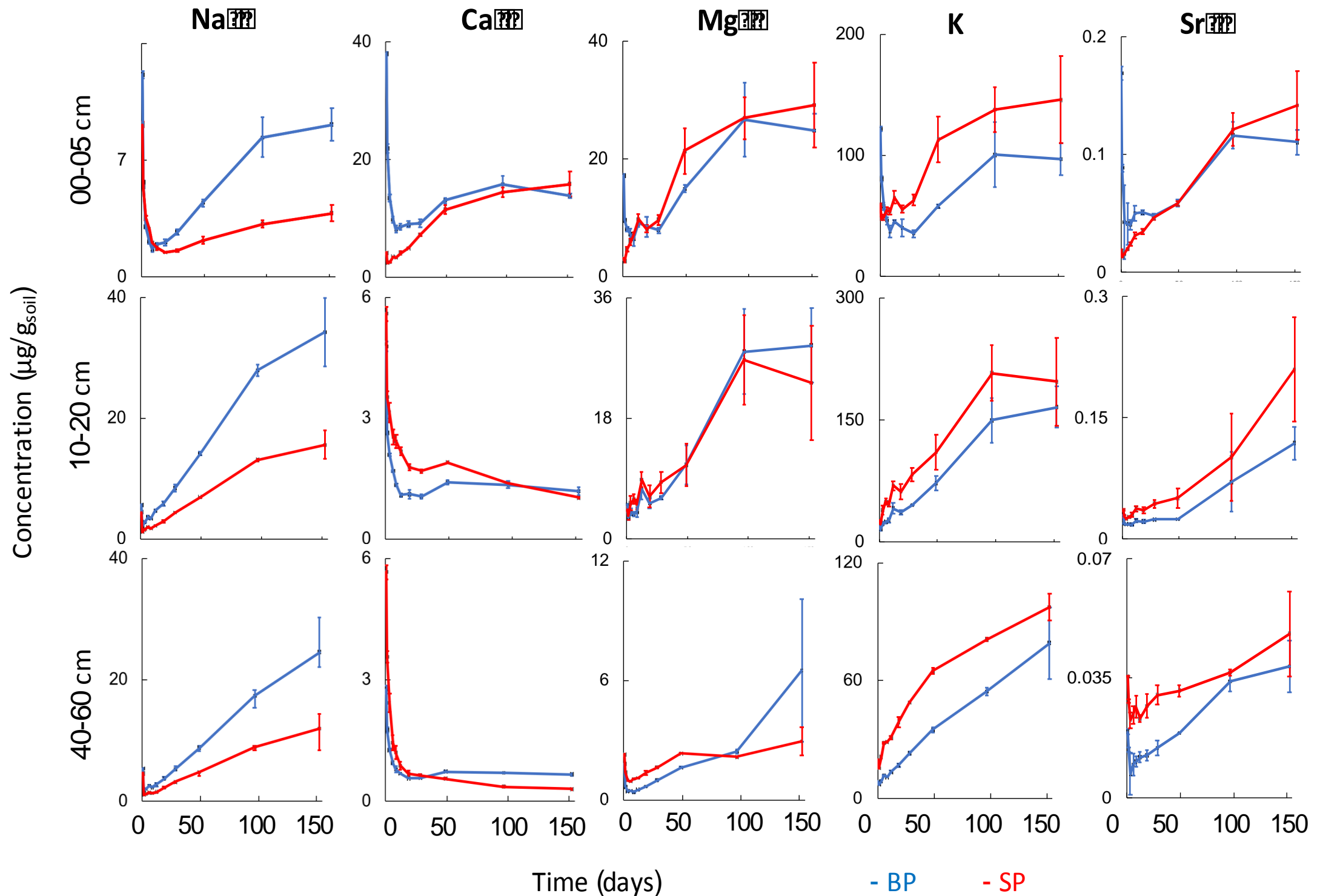


Fig. 5: Na, Ca, Mg, K and Sr concentrations leached over time for experiments conducted with soils from three different depths (00:05; 10-20 cm; 40-60 cm). Concentrations are expressed in μg of element per g of soil. The concentrations for the BP and SP profiles are in blue and red, respectively. The symbols represent the average concentrations from triplicate measurements and the vertical bars indicate the standard deviation.

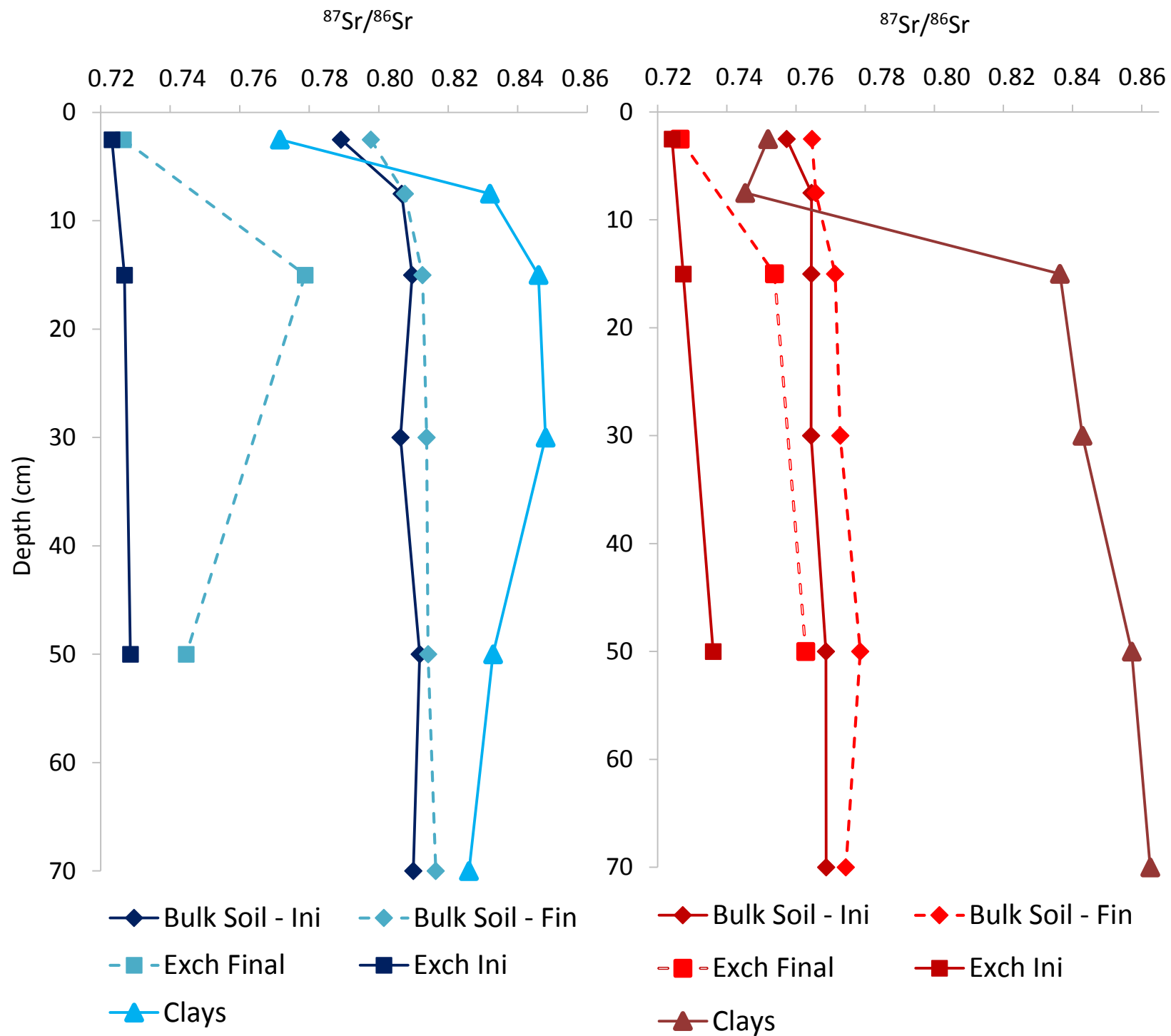


Fig. 6: Evolution versus depth of the isotopic ratio $^{87}\text{Sr}/^{86}\text{Sr}$ of the clays, the bulk soils and the exchangeable fraction (Exch.) before (Ini) and after leaching (Final) in the BP profile (left) and the SP profile (right).

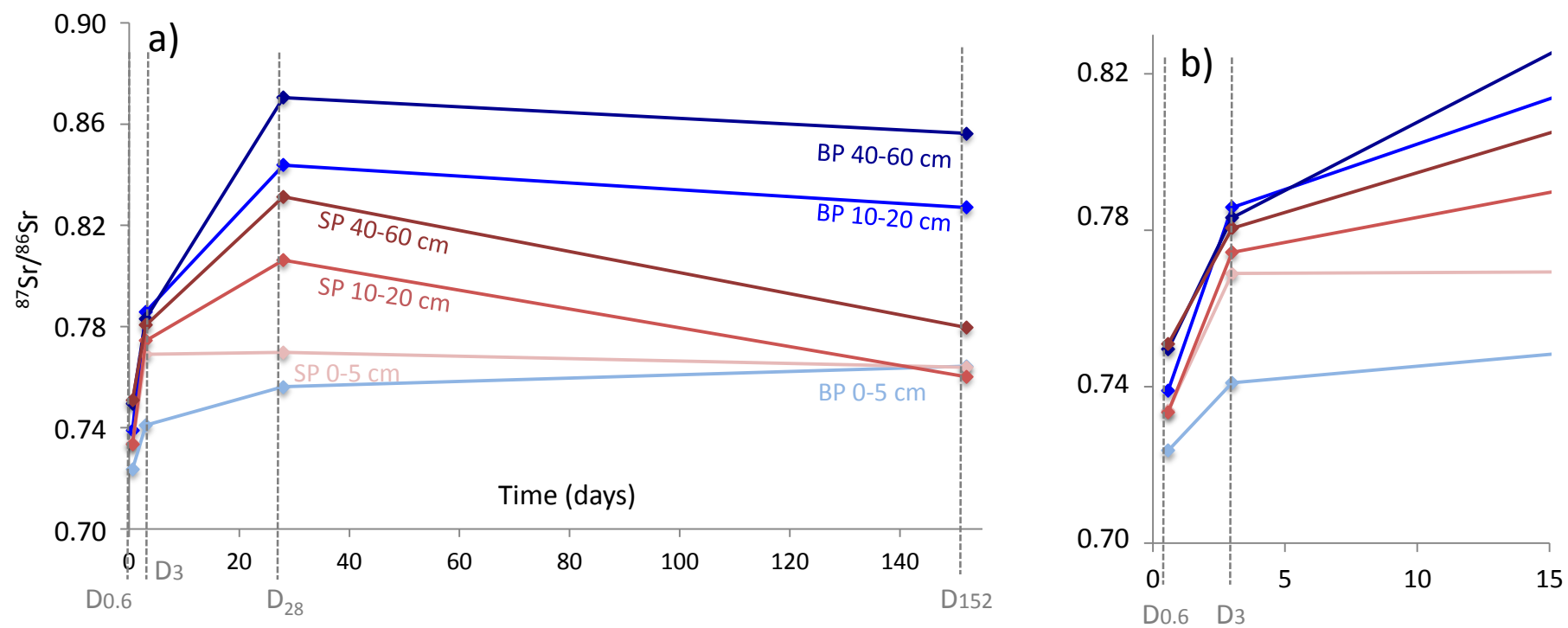


Fig. 7: Variation of the $^{87}\text{Sr}/^{86}\text{Sr}$ isotopic ratios versus time for experimental BP and SP leached solutions a) at 4 steps $D_{0.6}$ (14 h), D_3 (3 days), D_{28} (28 d) and D_{152} (152 d) and b) with a zoom for the first 15 days, for 3 different soil horizons (0-5 cm; 10-20 cm and 40-60 cm)

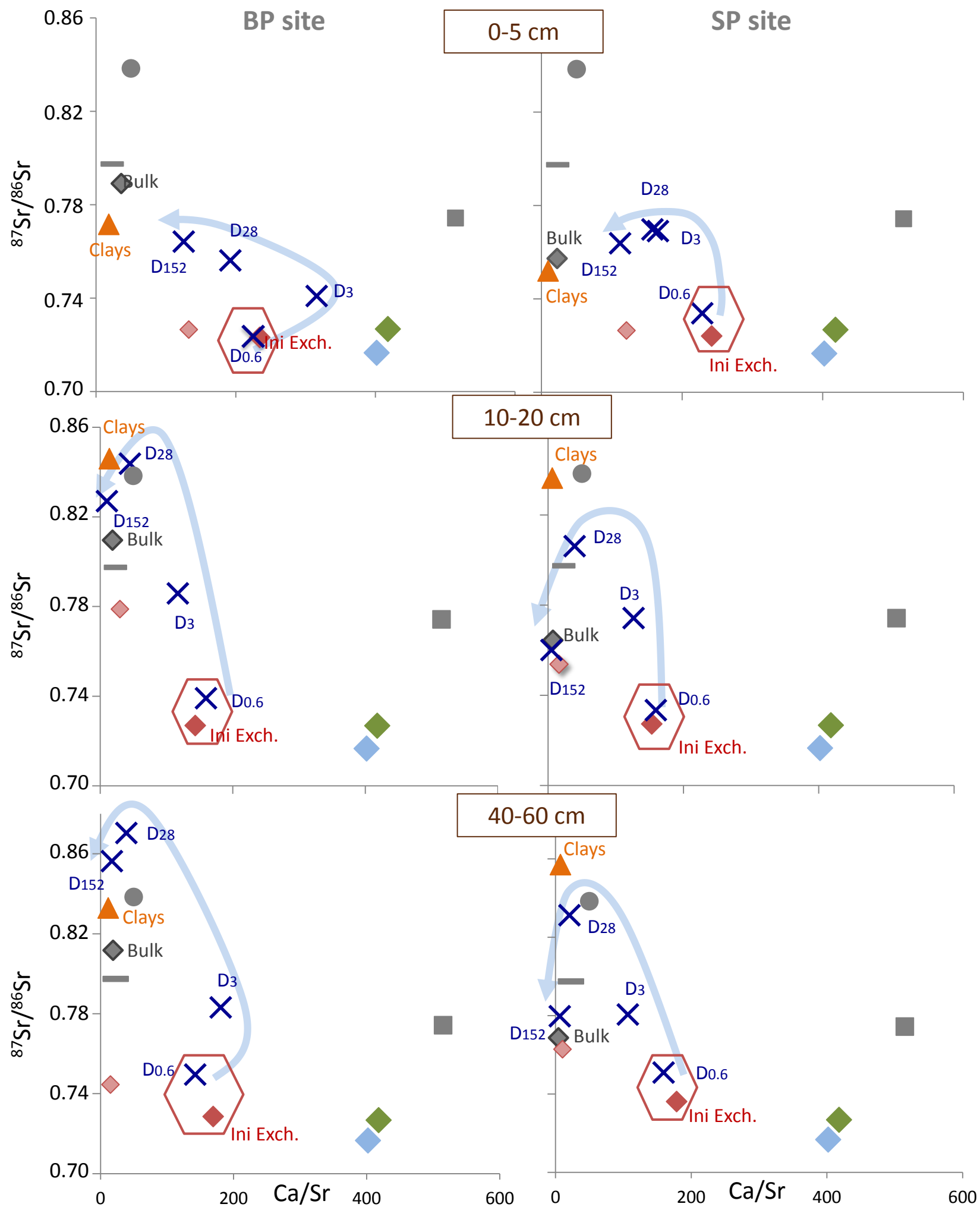


Fig. 8: $^{87}\text{Sr}/^{86}\text{Sr}$ isotopic ratio versus Ca/Sr ratios (mass ratio) for the different end-members (defined in text), and the exchangeable fraction in initial and final soils. The leached solutions obtained during the experiment at four different time steps $D_{0.6}$ (14 h-0.6d), D_3 (3 days), D_{28} (28 d) and D_{152} (152 d) (see Table 1) are represented by the dark blue cross and for soils at three representative horizons (0-5 cm; 10-20 and 40-60 cm). The signatures of bulk soil and clay are specific for each corresponding depth. Granite and primary mineral signatures are from Aubert et al., (2002). BP (under beech) and SP (under spruce) represent the two studied plots.

◆ Bulk Soil

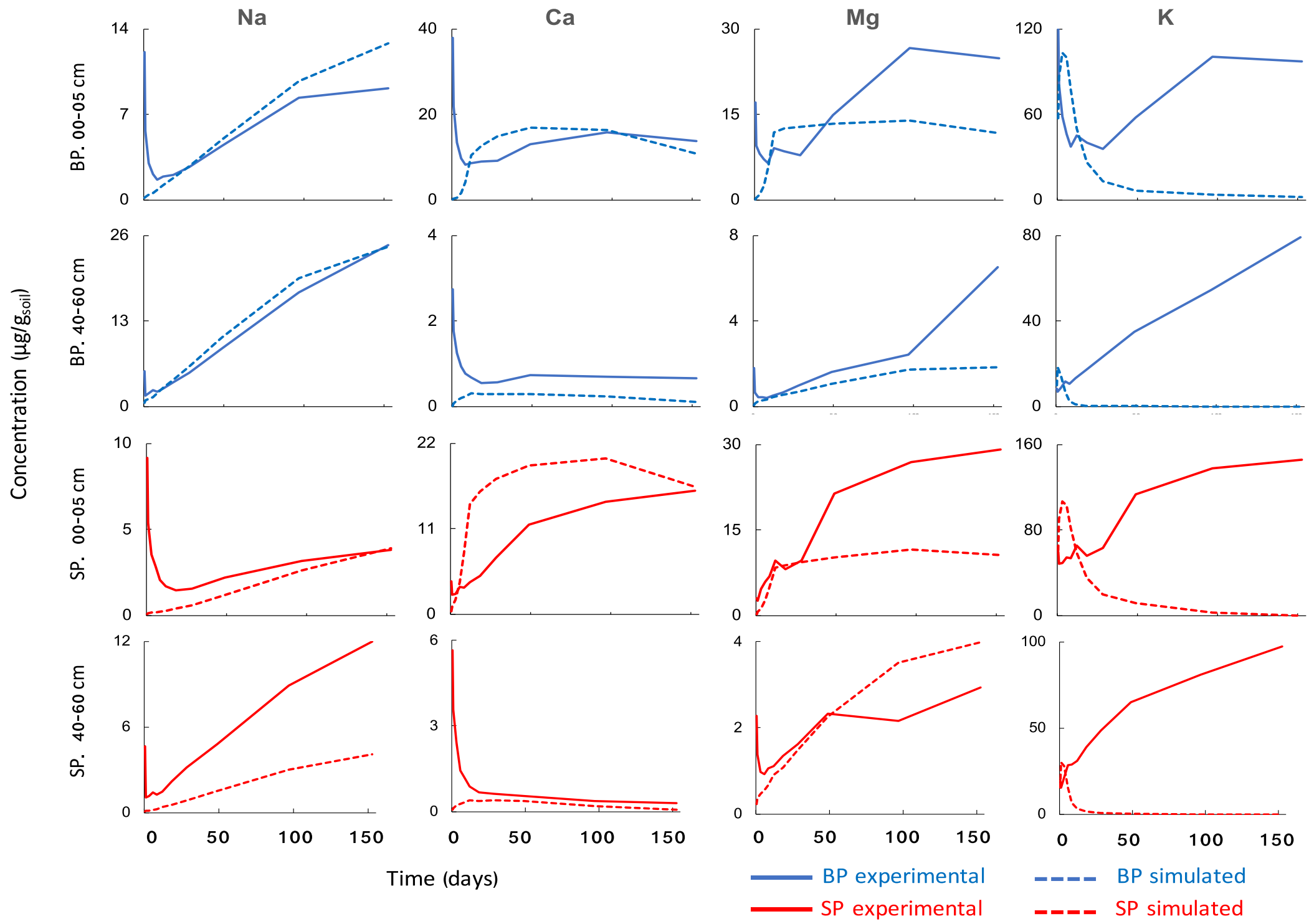


Fig. 9: Simulated and experimental concentrations for two different depths (00-05 cm & 40-60 cm) and for the two profiles (BP in blue and SP in red) for Na, Ca, Mg and K.

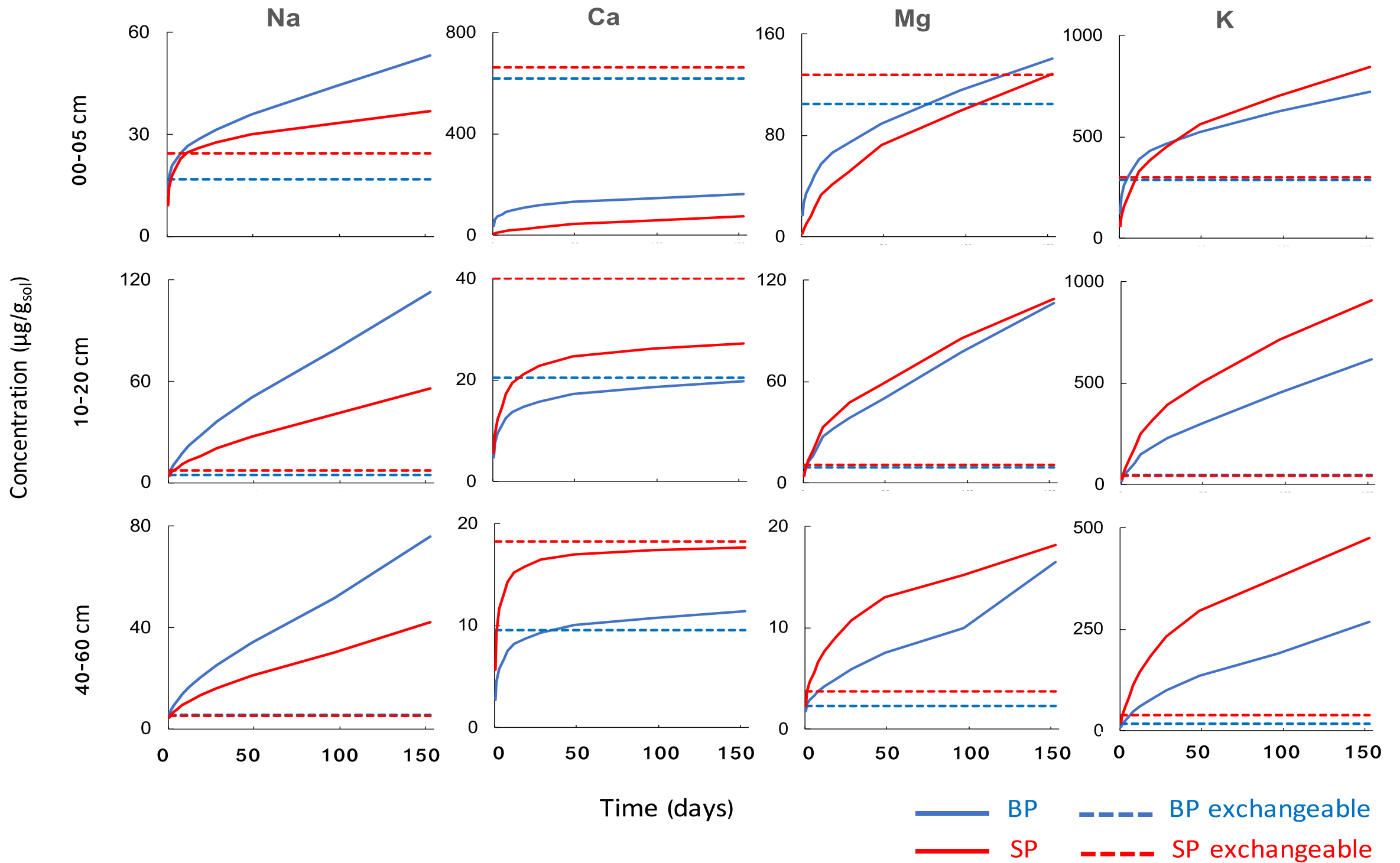


Fig. 10: Cumulative concentrations of Na, Ca, Mg and K from the leached solution over the 152 days of experimentation (in mg normalized to 1g of bulk soil). Blue and red lines represent the BP and SP profiles, respectively. The dashed lines represent the exchangeable pool in the soils (in mg for 1g of soil). Each concentration is normalized to 1 g of soil.

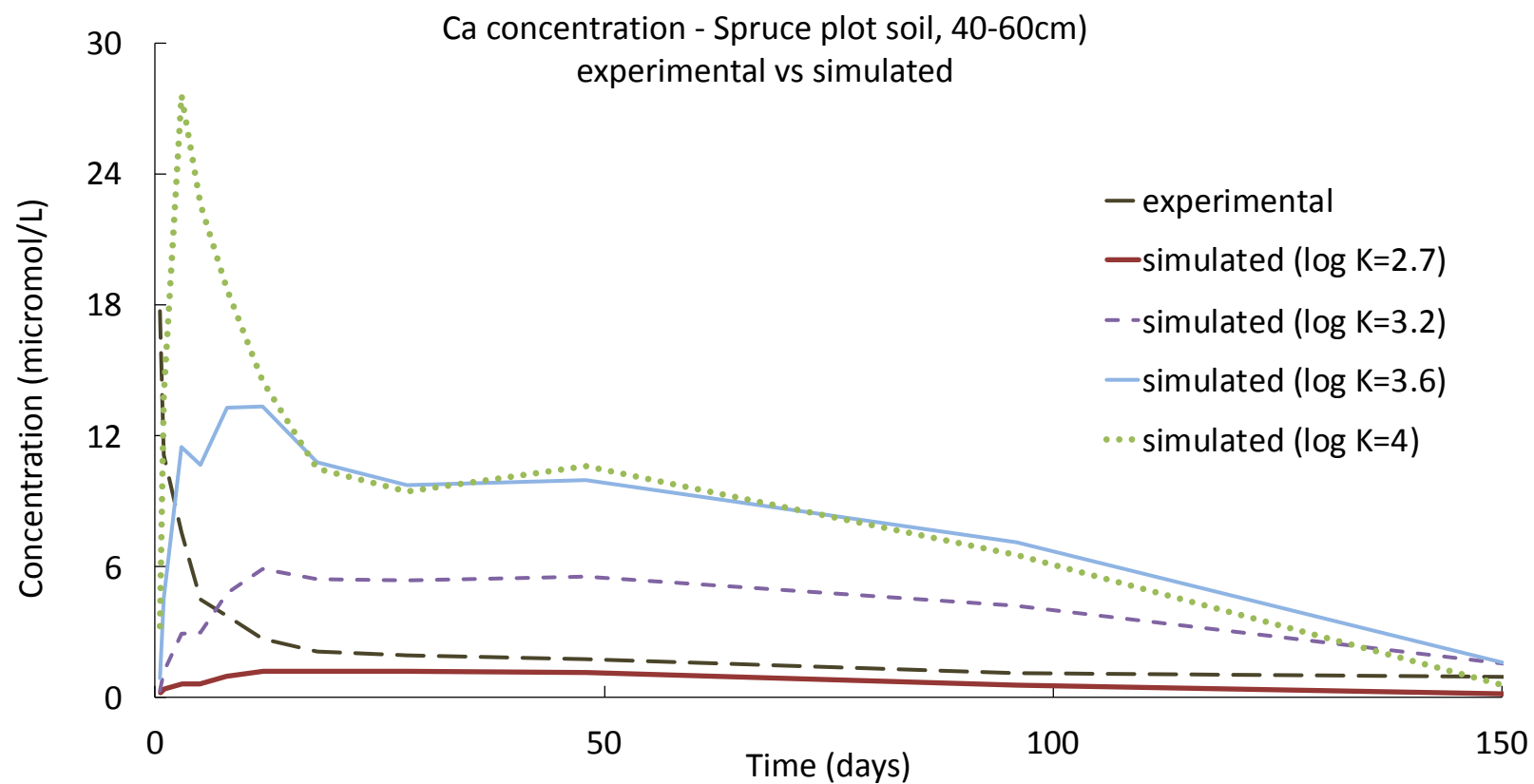


Fig. 11: Evolution of experimental Ca concentrations (leached solution) versus time, compared to simulations run with various values of Ca constants of exchange ($10^{-2.7}$, $10^{-3.2}$, $10^{-3.6}$, 10^{-4}) on SP plot at 40-60 cm. The Ca concentration in the solution increases with the decreasing exchange constant. The calculated concentrations with exchange constants of $10^{-3.2}$, $10^{-3.6}$ and 10^{-4} are largely overestimated over time, despite a fast increase at the beginning of the simulation, as in the experimental conditions. This illustration corresponds to the 40-60 cm depth horizon from the spruce plot (SP).

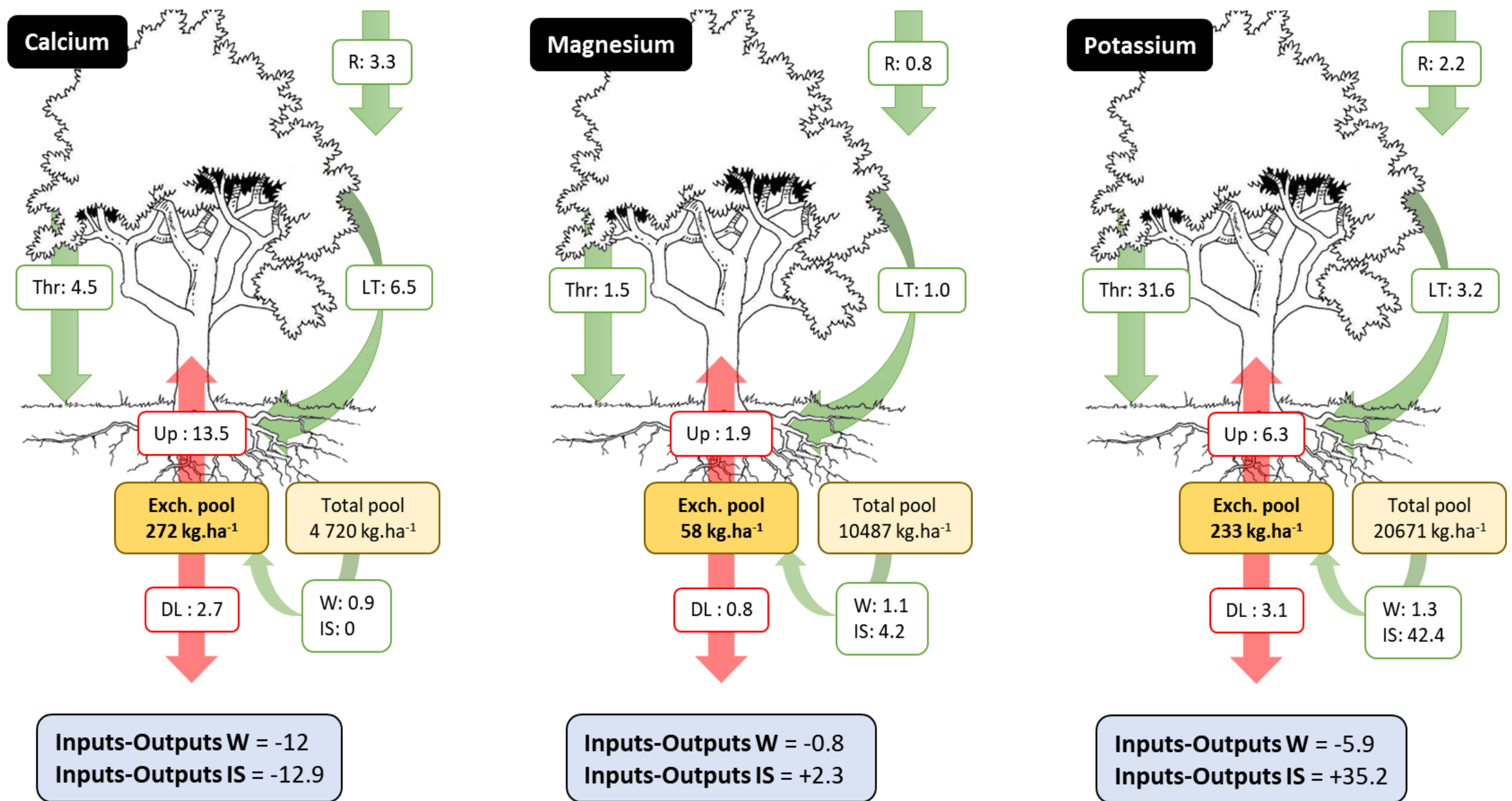
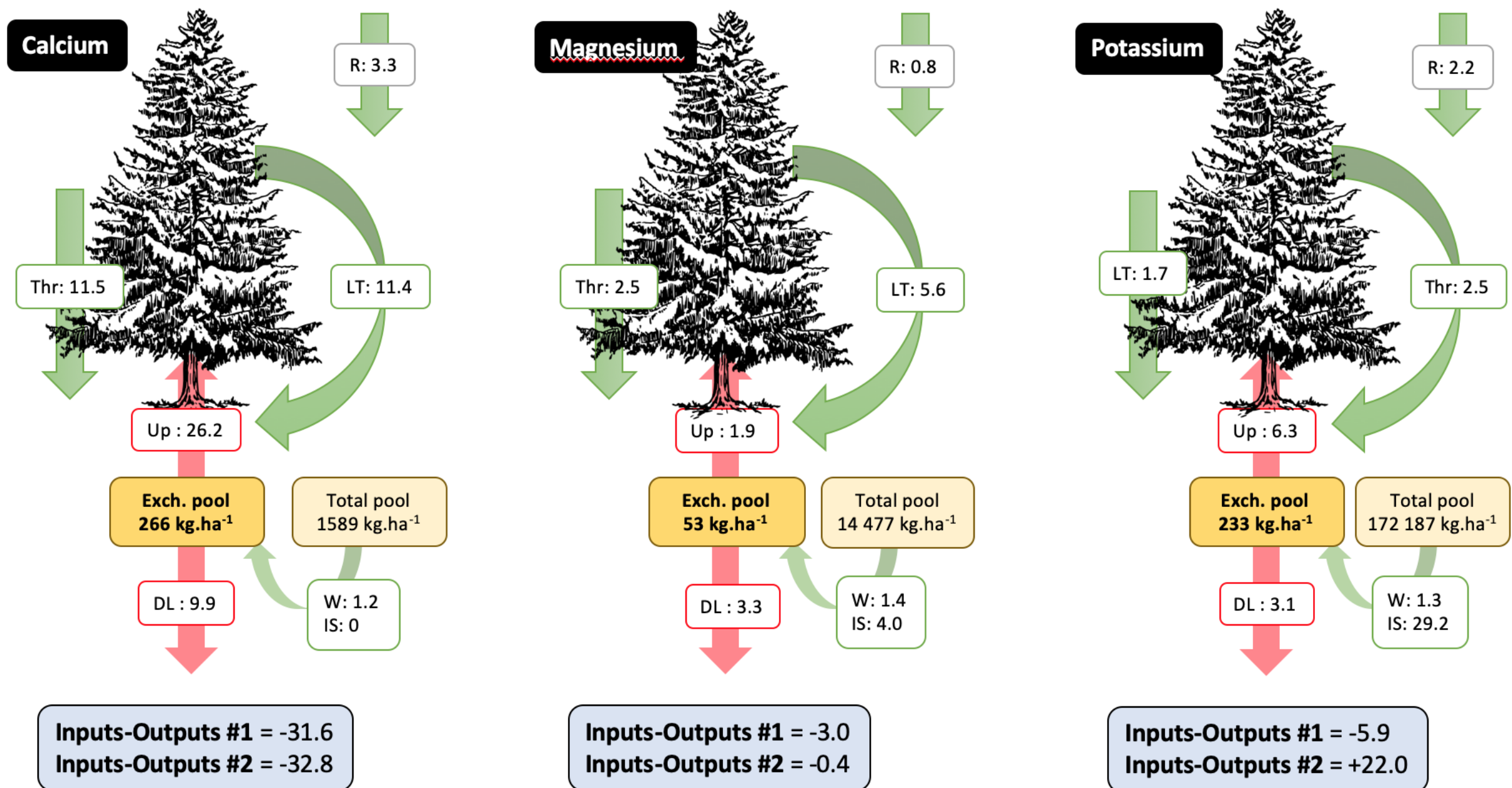


Fig. 12: Fluxes and input-output budgets (in kg.ha⁻¹.yr⁻¹) for calcium, magnesium and potassium at the BP site. IS is the intrinsic flux from soil estimated from our leaching experiments (corrected for the value of the initial exchangeable pool). W is the weathering flux, R is the atmospheric wet deposition, Up is the net uptake flux by roots and DL is the deep leaching (see Beaulieu et al. 2020). See additional explanation in text and Appendix D. Supplementary material, with the same diagram for the SP site.



Appendix E. Supplementary material: Fluxes and input-output budgets (in kg.ha⁻¹.yr⁻¹) for calcium, magnesium and potassium at the SP site. IS is the input from soil estimated from our leaching experiments (corrected for the value of the initial exchangeable pool). W is the weathering flux, R is the atmospheric wet deposition, Up is the net uptake flux by roots and DL is the deep leaching (see Beaulieu et al. 2020).

Name of step	T1	T2	T3	T4	T5	T6	T7
Δt	14 h	10 h	2 d	2d	3 d	4 d	6 d
Duration	14 h	1 d	3 d	5 d	8 d	12 d	18 d

Table 1

Table 1: Time between each step (between T_i and T_{i-1}) and total duration for each iteration of t

T8	T9	T10	T11
10 d	20 d	48 d	56 d
28 d	48 d	96 d	152 d

the batch experiments

	Si	Al	Mg	Ca
	µg/g	µg/g	µg/g	µg/g
BP OL	12200	1231	549	3945
BP OF-OH	55672	8402	772	2409
SP OL	11312	773	549	5618
SP OF-OH	15800	2006	537	3473

Table 2: Composition of the two litter layers for spruce (SP) and beech (BP) pl remains, and OF-OH contains degraded materials and humic components.

Na	K	Sr	⁸⁷Sr/⁸⁶Sr	err (2σ)
μg/g	μg/g	μg/g		
356	2515	11	0.753399	0.000003
2411	7164	19	0.729347	0.000004
<d.l.	1212	11	0.730029	0.000003
215	2133	12	0.724282	0.000003

lots in μg/g. OL corresponds to the horizon of recognizable

	<i>Depth</i>	<i>C</i>	<i>pH_{H2O}</i>	<i>Clay</i>	<i>Silt</i>	<i>Sand</i>	<i>CEC</i>
	<i>cm</i>	<i>%</i>		<i>%</i>	<i>%</i>	<i>%</i>	
Beech Plot (BP)	<i>Initial values</i>						
	0-5	22.9	3.52	29.9	25.1	45	16.1
	5-10	4.2	3.56	16.8	22.7	60.5	8.49
	10-20	4.4	3.69	15	19.7	65.3	7.64
	20-40	2.6	4.12	15.5	20.5	64	8.35
	40-60	2.3	4.45	13.8	23.1	63.1	4.09
Spruce Plot (SP)	60-80	1.6	4.59	8.6	26.7	64.7	2.41
	0-5	22.8	3.85	30.4	20.9	48.7	17.9
	5-10	8.1	3.54	18.9	17.3	63.8	9.97
	10-20	2.2	3.79	15.2	13.4	71.4	8.85
	20-40	1.3	4.04	19.5	19	61.5	8.8
	40-60	0.8	4.17	17.8	16.5	65.7	7.99
	60-80	0.6	4.33	16	16.1	67.9	7.13

CEC

BP	0-5	14.00
BP	5-10	7.15
BP	10-20	6.93
BP	20-40	5.44
BP	40-60	3.04
BP	60-80	<1.5
SP	0-5	16.1
SP	5-10	10.8
SP	10-20	8.04
SP	20-40	8.86
SP	40-60	7.81
SP	60-80	6.93

BP	0-5	-13
BP	5-10	-16
BP	10-20	-9
BP	20-40	-35
BP	40-60	-26
BP	60-80	-
SP	0-5	-10
SP	5-10	8
SP	10-20	-9

SP	20-40	1
SP	40-60	-2
SP	60-80	-3

Table 3: Soil description (particles smaller than 2 mm diameter) from the beech and spruce plots at the exchange capacity, determined with cobaltihexamine. Data from the initial soils before leaching and after leaching. The variation corresponds to the ratio between the exchangeable element X normalized by the CEC of the soil: $(\text{ExchXf}/\text{CECf}) - (\text{ExchXi}/\text{CECi}) / (\text{ExchXf}/\text{CECf}) \times 100$.

Ca_{exch}	Mg_{exch}	K_{exch}	Na_{exch}	Al_{exch}	H_{exch}
<i>cmol/kg</i>					
3.09	0.86	0.73	0.07	5.62	5.87
0.31	0.16	0.19	0.03	6.21	2.24
0.1	0.08	0.12	0.02	7.04	1.1
0.07	0.04	0.09	0.03	8.93	<0.05
0.05	0.02	0.05	0.03	4.7	<0.05
0.03	0.01	0.03	0.02	2.68	<0.05
3.31	1.05	0.77	0.11	5.52	4.88
0.69	0.25	0.22	0.03	6.53	2.89
0.2	0.09	0.11	0.04	7.66	0.79
0.16	0.05	0.1	0.02	8.93	0.21
0.09	0.03	0.1	0.02	8.61	0.27
0.07	0.03	0.1	0.02	7.81	0.13
Ca_{exch}	Mg_{exch}	K_{exch}	Na_{exch}	Al_{exch}	H_{exch}
<i>cmol/kg</i>					
After experimentation					
2.22	0.51	0.25	0.05	5.00	4.3
0.18	0.09	0.34	0.1	5.04	0.96
0.08	0.07	0.28	0.08	5.71	0.36
0.04	0.04	0.25	0.06	4.77	<0.05
0.03	0.02	0.17	0.04	2.83	<0.05
0.03	0.02	0.16	0.04	1.72	<0.05
2.84	0.9	0.36	0.03	6.36	4.32
0.56	0.28	0.45	0.04	7.31	1.62
0.09	0.16	0.49	0.04	6.34	0.13
0.07	0.12	0.49	0.03	7.47	<0.05
0.04	0.13	0.52	0.03	6.71	<0.05
0.05	0.18	0.64	0.04	5.75	<0.05
Variation (%)					
-17	-32	-61	-18	2	-16
-31	-33	112	296	-4	-49
-12	-4	157	341	-11	-64
-12	53	326	207	-18	-
-19	35	357	79	-19	-
-	-	-	-	-	-
-5	-5	-48	-70	28	-2
-25	3	89	23	3	-48
-50	96	390	10	-9	-82

-57	138	387	49	-17	-
-55	343	432	53	-20	-
-27	517	558	106	-24	-

e Strengbach catchment. CEC: Cation
fter the end of the experimentation.
f the final and initial soils:

	Depth	Kaolinite	Illite	Vermiculite	Smectite
	<i>cm</i>	%	%	%	%
Beech Plot	<i>0-5</i>	1.4	22.0	1.3	5.2
(BP)	<i>5-10</i>	1.5	10.0	0.0	5.3
	<i>10-20</i>	1.1	7.8	1.3	4.8
	<i>20-40</i>	0.8	6.8	3.7	4.2
	<i>40-60</i>	1.4	6.4	2.5	3.5
	<i>60-80</i>	1.1	4.6	1.2	1.7
Spruce Plot	<i>0-5</i>	1.5	20.1	0.4	8.5
(SP)	<i>5-10</i>	0.5	10.7	0.0	7.7
	<i>10-20</i>	0.2	8.9	0.0	6.1
	<i>20-40</i>	0.2	8.6	1.3	9.3
	<i>40-60</i>	0.2	9.2	1.1	7.3
	<i>60-80</i>	0.1	7.3	1.1	7.5

Table 4: Mineral composition of soils from beech and spruce plots, calculated from XRD :

Muscovite	Biotite	Quartz	Orthose	Albite	OM
%	%	%	%	%	%
5.7	0.6	8.3	9.6	6.5	39.4
8.8	0.8	21.3	27.6	17.5	7.2
10.8	0.7	18.9	25.8	21.4	7.5
15.0	0.6	19.6	21.0	24.0	4.4
20.4	0.6	13.8	23.5	24.0	3.9
20.5	1.1	22.1	19.4	25.5	2.8
4.7	0.0	16.0	6.6	3.3	39.1
14.4	0.8	38.9	7.7	5.3	14.0
22.6	0.8	39.4	11.6	6.6	3.7
20.9	0.0	32.9	20.0	4.5	2.2
22.3	0.0	37.8	12.9	7.9	1.3
17.6	0.0	39.0	15.4	11.0	1.0

analyses on bulk soils and clays, and from organic matter content (see text).

	<i>Depth</i>	<i>Si</i>	<i>Al</i>	<i>Na</i>
	<i>cm</i>	<i>mg/g</i>	<i>mg/g</i>	<i>mg/g</i>
Bulk soil				
Beech Plot	0-5	167.48	21.76	7.4
(BP)	5-10	290.94	36.94	13.23
	10-20	297.9	39.13	13.52
	20-40	303.32	40.62	13.79
	40-60	303.65	40.63	13.13
	60-80	295.84	44.96	14.83
Spruce Plot	0-5	182.3	20.09	2.1
(SP)	5-10	292.95	33.35	3.23
	10-20	332.91	33.93	3.26
	20-40	310.43	43.29	4.4
	40-60	314.68	43.31	4.61
	60-80	315.43	44.02	4.73
Clays				
Beech Plot	0-5	56.47	11.01	2.48
(BP)	5-10	40.68	11.35	1.08
	10-20	28.66	8.67	0.68
	20-40	32.29	10.83	0.21
	40-60	24.59	8.6	0.62
	60-80	14.43	5.51	0.38
Spruce Plot	0-5	52.24	12.95	0.75
(SP)	5-10	43.27	12.58	0.4
	10-20	30.23	9.76	0.19
	20-40	37.62	12.07	0.87
	40-60	36.39	12.16	0.22
	60-80	33.45	11.26	0.2

Table 5: Chemical and Sr isotopic composition of bulk soils and clays from the be

<i>K</i>	<i>Mg</i>	<i>Ca</i>	<i>Sr</i>	$^{87}\text{Sr}/^{86}\text{Sr}$	err (2 σ)
<i>mg/g</i>	<i>mg/g</i>	<i>mg/g</i>	$\mu\text{g/g}$		
21.87	1.22	1.13	31.34	0.789114	0.000014
39.32	1.79	0.89	45.51	0.806601	0.000016
41.91	1.99	0.86	46.7	0.809622	0.000012
41.73	1.97	0.84	48.29	0.806266	0.000012
41.7	1.97	0.82	43.67	0.811786	0.00001
40.62	2.54	1.11	43.12	0.809955	0.000026
18.9	1.78	0.79	35.4	0.757335	0.000014
31.36	2.8	0.33	53.87	0.764484	0.000012
34.4	2.75	0.36	51.24	0.764455	0.00001
40	3.53	0.29	76.23	0.764404	0.000014
41.8	3.42	0.32	72.43	0.768632	0.000016
42.54	3.49	0.41	73.8	0.768716	0.000012
8.23	0.87	0.29	15.7	0.771566	0.000004
7.08	1.03	0.1	7.17	0.83199	0.000003
5.04	0.81	0.06	4.26	0.845975	0.000004
7.03	1.21	0.03	4.99	0.848006	0.000006
4.21	0.73	0.05	3.94	0.8329	0.000004
2.38	0.46	0.03	2.24	0.825962	0.000004
9.61	1.35	0.21	21.94	0.751935	0.000004
9.24	1.37	0.07	12.68	0.745304	0.000007
6.77	1.1	0.03	5.02	0.836336	0.000003
6.57	1.12	0.08	5.9	0.84285	0.000003
7.84	1.38	0.04	5.22	0.857096	0.000003
7.27	1.28	0.04	4.84	0.862445	0.000003

ech and spruce plots at the Strengbach catchment.

Plot	Depth	Ca		Mg	
		kg·ha ⁻¹	%	kg·ha ⁻¹	%
-	cm				
Beech Plot (BP)	00-05	199	54.83	34	8.61
	05-10	20	7.01	6	1.09
	10-20	13	2.38	6	0.47
	20-40	22	1.72	8	0.27
	40-60	12	1.16	3	0.12
	60-80	6	0.52	1	0.05
	<i>Total</i>		272		58
Spruce Plot (SP)	00-05	142	83.61	27	7.17
	05-10	30	42.18	6	1.08
	10-20	17	11.00	5	0.40
	20-40	39	11.50	7	0.17
	40-60	24	5.66	5	0.11
	60-80	15	3.40	3	0.09
	<i>Total</i>		267		53

Table 6: Evaluation of the stock of exchangeable cation par soil layer (expressed in kg/hecta Na, and K (expressed in %). The total corresponds to the sum over the whole soil profile.

Na		K	
kg·ha ⁻¹	%	kg·ha ⁻¹	%
5	0.23	92	1.31
2	0.05	23	0.19
3	0.04	30	0.11
9	0.04	53	0.08
7	0.04	22	0.04
6	0.03	13	0.03
32		233	
5	1.17	65	1.59
2	0.24	18	0.27
3	0.22	19	0.13
6	0.11	46	0.10
7	0.11	49	0.09
4	0.08	41	0.09
27		238	

ire) and proportion of exchangeable pool in the bulk soils for Ca, Mg,

	<i>Depth</i>	<i>Si</i>	<i>Al</i>	<i>Na</i>
	$\mu\text{g/g}$	$\mu\text{g/g}$	$\mu\text{g/g}$	$\mu\text{g/g}$
Bulk soil	<i>initial</i>			
Beech Plot (BP)	0-5	167484.2	21760.4	7403.8
	5-10	290935.4	36936.8	13234.8
	10-20	297900.2	39125.3	13516.7
	20-40	303322.6	40615.2	13791.2
	40-60	303649.8	40628.4	13131.0
	60-80	295843.5	44960.4	14829.8
Spruce Plot (SP)	0-5	182302.0	20087.9	2099.5
	5-10	292945.4	33353.8	3227.1
	10-20	332911.6	33925.4	3256.8
	20-40	310427.7	43293.2	4399.2
	40-60	314681.4	43306.4	4614.4
	60-80	315429.3	44015.7	4725.7
Clays				
Beech Plot (BP)	0-5	56465.0	11010.9	2477.7
	5-10	40678.6	11351.4	1081.8
	10-20	28663.5	8674.4	682.1
	20-40	32285.2	10833.9	205.8
	40-60	24590.0	8604.9	617.3
	60-80	14431.8	5515.0	376.4
Spruce Plot (SP)	0-5	52236.7	12950.4	753.3
	5-10	43272.1	12578.7	399.6
	10-20	30225.1	9755.4	189.4
	20-40	37618.0	12071.4	866.5
	40-60	36385.3	12162.2	216.6
	60-80	33453.8	11263.9	198.2
Exch Initial		<i>Si</i>	<i>Al</i>	<i>Na</i>
Beech Plot (BP)	0-5	12.4	505.45	16.81
	5-10	6.6	558.52	6.16
	10-20	5.4	633.17	4.9
	20-40	14.00	803.15	6.16
	40-60	17.8	422.71	5.77
	60-80	25.00	241.04	5.03
Spruce Plot (SP)	0-5	13.6	496.46	24.6
	5-10	7.6	587.3	7.77
	10-20	2.8	688.93	7.26
	20-40	8.4	803.15	4.69

	40-60	9.2	774.37	5.13
	60-80	10.2	702.42	3.91
Exch Final				
Beech Plot (BP)	0-5	5.82	449.69	11.36
	5-10	3.98	453.29	22.00
	10-20	4.66	513.55	17.86
	20-40	5.98	429.01	13.27
	40-60	9.38	254.53	9.26
	60-80	11.18	154.69	9.08
Spruce Plot (SP)	0-5	6.36	572.01	5.89
	5-10	4.58	657.45	10.12
	10-20	4.54	570.21	9.47
	20-40	6.6	671.84	6.87
	40-60	8.56	603.49	7.22
	60-80	10.3	517.15	9.68
Bulk soil Final				
Beech Plot (BP)	0-5	180619.3	23888.0	7774.7
	5-10	301873.5	36952.7	13442.5
	10-20	305379.3	38934.8	13049.4
	20-40	309679.8	41276.7	13405.5
	40-60	302855.1	41917.1	12849.1
	60-80	300424.4	43817.2	14221.5
Spruce Plot (SP)	0-5	190716.0	21850.4	2255.3
	5-10	290234.2	34195.3	3368.1
	10-20	323375.8	35931.3	3115.8
	20-40	303883.5	44148.0	4236.0
	40-60	308651.4	43703.4	4109.9
	60-80	307295.8	44457.6	4658.9
Cumul Leach				
Beech Plot (BP)	0-5	2734.9	1318.61	53.42
	5-10	3802.07	1882.27	118.32
	10-20	3097.11	1571.13	112.29
	20-40	970.15	431.98	91.77
	40-60	582.85	315.81	75.95
	60-80	491.69	305.42	66.36
Spruce Plot (SP)	0-5	3393.17	1647.26	36.92
	5-10	4627.06	2444.36	50.04
	10-20	3406.41	1640.92	56.59
	20-40	769.93	184.3	41.67
	40-60	749.09	148.82	41.95
	60-80	796.28	146.34	46.77
Organic matter				
Beech Plot	0-5	21673.19	3270.9	938.6

<i>(BP)</i>	5-10	3975.0	599.9	172.15
	10-20	4164.28	628.47	180.34
	20-40	2460.71	371.37	106.57
	40-60	2176.78	328.52	94.27
	60-80	1514.28	228.53	65.58
<i>Spruce Plot</i>	0-5	6123.89	777.49	83.37
<i>(SP)</i>	5-10	2175.59	276.21	29.62
	10-20	590.9	75.02	8.04
	20-40	349.17	44.33	4.75
	40-60	214.87	27.28	2.93
	60-80	161.15	20.46	2.19

Appendix A. Supplementary material

Chemical compositions (expressed in $\mu\text{g/g}$ of soil) for initial and final (after experimentation) bulk soils, cation exchangeable pool, organic matter as total cumulated experimental leachate calculated for 1 g of soil

<i>K</i>	<i>Mg</i>	<i>Ca</i>	<i>Sr</i>	$^{87}\text{Sr}/^{86}\text{Sr}$	err (2σ)
μg/g	μg/g	μg/g	μg/g		
21874.5	1218.1	1129.2	31.3	0.789114	0.000014
39324.3	1791.0	886.2	45.5	0.806601	0.000016
41906.0	.0	857.6	46.7	0.809622	0.000012
41731.7	1971.9	836.2	48.3	0.806266	0.000012
41698.5	1965.9	821.9	43.7	0.811786	0.00001
40619.3	2538.8	1114.9	43.1	0.809955	0.000026
18902.5	1779.0	793.3	35.4	0.757335	0.000014
31363.1	2804.1	328.8	53.9	0.764484	0.000012
34401.5	2749.9	364.5	51.2	0.764455	0.00001
39996.7	3533.8	285.9	76.2	0.764404	0.000014
41798.1	3419.2	321.6	72.4	0.768632	0.000016
42537.0	3485.6	414.5	73.8	0.768716	0.000012
8228.3	867.3	286.4	15.7	0.771566	0.000004
7076.5	1032.4	103.3	7.2	0.83199	0.000003
5035.7	809.6	59.0	4.3	0.845975	0.000004
7032.0	1213.3	33.2	5.0	0.848006	0.000006
4211.3	727.3	46.4	3.9	0.8329	0.000004
2375.2	457.9	33.2	2.2	0.825962	0.000004
9612.6	1354.8	210.7	21.9	0.751935	0.000004
9236.6	1367.7	72.9	12.7	0.745304	0.000007
6771.0	1100.9	32.6	5.0	0.836336	0.000003
6565.8	1116.0	78.0	5.9	0.84285	0.000003
7837.6	1378.3	38.2	5.2	0.857096	0.000003
7269.5	1277.5	36.6	4.8	0.862445	0.000003
<i>K</i>	<i>Mg</i>	<i>Ca</i>	<i>Sr</i>	$^{87}\text{Sr}/^{86}\text{Sr}$	err (2σ)
286.59	104.88	619.21	2.64	0.723266	0.000004
73.11	19.57	62.12	0.29	nd	nd
46.14	9.31	20.44	0.14	0.726888	0.000003
34.41	5.27	14.35	0.09	nd	nd
17.83	2.27	9.56	0.06	0.728579	0.000002
12.04	1.26	5.77	0.08	nd	nd
301.45	127.6	663.29	2.74	0.724128	0.0000069
84.84	30.26	138.67	0.57	nd	nd
44.18	10.89	40.08	0.26	0.72737087	0.00002
38.2	6.03	32.86	0.12	nd	nd

37.42	3.71	18.22	0.1	0.736045	0.00002
39.49	3.17	14.11	0.09	nd	nd
95.79	62.46	444.87	3.35	0.726558	0.00002
130.98	11.39	35.27	0.77		
108.3	8.12	16.63	0.56	0.778818	0.00004
98.53	5.27	8.82	0.49		
66.47	2.78	6.39	0.43	0.7446	0.00002
60.6	2.78	6.67	0.35		
141.54	109.62	569.11	4.71	0.726483	0.000003
176.72	33.66	112.22	1.62		
191.58	19.32	18.64	1.16	0.753777	0.00002
190.41	14.22	13.15	0.79		
201.36	16.28	8.62	0.84	0.762804	0.00004
248.27	21.27	10.04	0.97		
25078.9	1266.4	1107.8	29.6	0.797721	0.000012
40652.5	1670.4	886.2	42.8	0.807514	0.000012
41308.3	1917.7	814.8	44.0	0.812608	0.000008
41789.8	2086.5	850.5	44.8	0.81377	0.000014
40445.0	2195.1	829.0	41.6	0.814216	0.000008
40395.2	2382.0	1000.6	42.7	0.816388	0.000012
19575.0	1917.7	807.6	33.6	0.764611	0.000038
32093.6	2846.4	307.3	54.6	0.765714	0.00001
35098.8	3015.2	214.4	51.5	0.771332	0.000004
40420.1	3678.6	250.1	65.0	0.772802	0.00001
41922.6	3576.0	271.6	59.1	0.778583	0.000026
42296.2	3612.2	364.5	66.8	0.774415	0.00001
721.6	139.91	161.08	0.8	0.764283	0.00002
727.25	133.31	45.38	0.48	nd	nd
612.38	105.63	19.75	0.37	0.826984	0.00004
326.99	26.18	14.26	0.23	nd	nd
267.1	16.38	11.41	0.19	0.85638	0.00003
268.29	15.22	9.46	0.21	nd	nd
843.55	128.01	74.26	0.52	0.763848	0.00004
1099.15	167.92	66.02	0.68	nd	nd
918.21	110.49	27.02	0.62	0.760167	0.00002
441.7	20.91	20.75	0.34	nd	nd
475.91	18.21	17.63	0.34	0.779635	0.00004
509.44	17.74	17.33	0.36	nd	nd
2789.02	300.5	937.63	7.51		

511.52	55.11	171.97	1.38		
535.88	57.74	180.16	1.44		
316.66	34.12	106.46	0.85		
280.12	30.18	94.17	0.75		
194.87	21.0	65.51	0.52		
826.94	208.02	1346.29	3.57		
293.78	73.9	478.29	1.27		
79.79	20.07	129.91	0.34		
47.15	11.86	76.76	0.2		
29.02	7.3	47.24	0.13		
21.76	5.47	35.43	0.09		

mpared with the contribution of different reservoirs as clay minerals, initial and final

site	Depth	time		Mg	Ca	Na	K
-	cm	-	-	µg/gsol	µg/gsol	µg/gsol	µg/gsol
BP	00-05 cm	T1	mean	17.18	37.97	12.12	122.17
BP	00-05 cm	T1	SD	0.2	0.3	0.2	1.9
BP	05-10 cm	T1	mean	7.82	11.54	6.10	27.42
BP	05-10 cm	T1	SD	0.1	0.1	0.1	0.3
BP	10-20 cm	T1	mean	5.16	4.78	5.63	18.98
BP	10-20 cm	T1	SD	0.1	0.1	0.1	0.6
BP	20-40 cm	T1	mean	2.58	3.19	4.20	10.41
BP	20-40 cm	T1	SD	0.1	0.1	0.1	0.4
BP	40-60 cm	T1	mean	1.81	2.74	5.36	8.60
BP	40-60 cm	T1	SD	0.1	0.1	0.1	0.1
BP	60-80 cm	T1	mean	0.95	2.27	4.65	6.34
BP	60-80 cm	T1	SD	0.1	0.1	0.1	0.1
BP	00-05 cm	T2	mean	9.59	21.89	5.67	80.80
BP	00-05 cm	T2	SD	0.2	0.6	0.1	2.1
BP	05-10 cm	T2	mean	4.45	5.72	2.03	20.08
BP	05-10 cm	T2	SD	0.3	0.1	0.1	1.3
BP	10-20 cm	T2	mean	3.21	2.63	1.97	15.52
BP	10-20 cm	T2	SD	0.3	0.1	0.1	1.4
BP	20-40 cm	T2	mean	1.33	2.24	1.66	8.90
BP	20-40 cm	T2	SD	0.1	0.1	0.1	0.4
BP	40-60 cm	T2	mean	0.65	1.76	1.73	7.07
BP	40-60 cm	T2	SD	0.1	0.1	0.1	0.1
BP	60-80 cm	T2	mean	0.30	1.35	1.46	5.34
BP	60-80 cm	T2	SD	0.1	0.1	0.1	0.1
BP	00-05 cm	T3	mean	8.09	13.48	3.01	58.24
BP	00-05 cm	T3	SD	0.4	0.6	0.1	2.9
BP	05-10 cm	T3	mean	5.38	4.74	2.81	26.28
BP	05-10 cm	T3	SD	0.2	0.1	0.1	1.1
BP	10-20 cm	T3	mean	3.97	2.08	2.83	21.93
BP	10-20 cm	T3	SD	0.5	0.1	0.1	2.1
BP	20-40 cm	T3	mean	0.84	1.64	2.38	11.17
BP	20-40 cm	T3	SD	0.1	0.1	0.1	0.6
BP	40-60 cm	T3	mean	0.43	1.25	1.99	8.720
BP	40-60 cm	T3	SD	0.1	0.1	0.1	0.5
BP	60-80 cm	T3	mean	0.31	0.96	1.67	8.750
BP	60-80 cm	T3	SD	0.1	0.1	0.1	0.2
BP	00-05 cm	T4	mean	7.22	9.82	2.11	46.21
BP	00-05 cm	T4	SD	0.8	0.5	0.1	3.1
BP	05-10 cm	T4	mean	5.82	3.89	3.68	32.12
BP	05-10 cm	T4	SD	0.5	0.1	0.1	2.5

BP	10-20 cm	T4	mean	3.70	1.68	3.60	24.34
BP	10-20 cm	T4	SD	0.3	0.1	0.1	1.4
BP	20-40 cm	T4	mean	0.70	1.22	3.12	14.20
BP	20-40 cm	T4	SD	0.1	0.1	0.1	0.7
BP	40-60 cm	T4	mean	0.44	0.94	2.47	11.71
BP	40-60 cm	T4	SD	0.1	0.1	0.2	0.4
BP	60-80 cm	T4	mean	0.39	0.74	2.10	10.72
BP	60-80 cm	T4	SD	0.1	0.1	0.1	0.3
BP	00-05 cm	T5	mean	6.42	8.21	1.67	37.37
BP	00-05 cm	T5	SD	1.1	0.5	0.1	4.6
BP	05-10 cm	T5	mean	5.56	3.23	3.53	32.01
BP	05-10 cm	T5	SD	0.5	0.1	0.2	2.2
BP	10-20 cm	T5	mean	3.96	1.33	3.41	26.12
BP	10-20 cm	T5	SD	0.7	0.1	0.1	2.6
BP	20-40 cm	T5	mean	0.55	0.98	2.85	13.90
BP	20-40 cm	T5	SD	0.1	0.1	0.1	0.3
BP	40-60 cm	T5	mean	0.38	0.78	2.26	10.74
BP	40-60 cm	T5	SD	0.1	0.1	0.1	0.2
BP	60-80 cm	T5	mean	0.34	0.53	1.79	9.86
BP	60-80 cm	T5	SD	0.1	0.1	0.1	0.7
BP	00-05 cm	T6	mean	9.10	8.63	1.94	45.30
BP	00-05 cm	T6	SD	0.5	0.5	0.1	1.0
BP	05-10 cm	T6	mean	10.01	2.69	4.89	51.85
BP	05-10 cm	T6	SD	1.5	0.1	0.2	7.2
BP	10-20 cm	T6	mean	7.36	1.09	4.70	41.04
BP	10-20 cm	T6	SD	1.5	0.1	0.3	6.5
BP	20-40 cm	T6	mean	0.66	0.96	3.40	17.51
BP	20-40 cm	T6	SD	0.1	0.1	0.2	0.7
BP	40-60 cm	T6	mean	0.51	0.67	2.74	13.40
BP	40-60 cm	T6	SD	0.1	0.1	0.2	0.6
BP	60-80 cm	T6	mean	0.49	0.5	2.27	12.71
BP	60-80 cm	T6	SD	0.1	0.1	0.1	0.9
BP	00-05 cm	T7	mean	8.48	9.00	2.07	40.19
BP	00-05 cm	T7	SD	1.6	0.5	0.1	7.1
BP	05-10 cm	T7	mean	7.19	2.60	5.89	43.46
BP	05-10 cm	T7	SD	1.0	0.2	0.3	3.2
BP	10-20 cm	T7	mean	5.29	1.11	5.87	36.27
BP	10-20 cm	T7	SD	0.7	0.1	0.1	2.8
BP	20-40 cm	T7	mean	0.72	0.79	4.61	20.46
BP	20-40 cm	T7	SD	0.1	0.1	0.2	1.0
BP	40-60 cm	T7	mean	0.67	0.55	3.68	16.93
BP	40-60 cm	T7	SD	0.1	0.1	0.3	0.8
BP	60-80 cm	T7	mean	0.67	0.45	3.1	16.88

BP	60-80 cm	T7	SD	0.1	0.1	0.1	0.7
BP	00-05 cm	T8	mean	7.90	9.21	2.69	35.68
BP	00-05 cm	T8	SD	0.4	0.7	0.1	2.9
BP	05-10 cm	T8	mean	8.44	2.33	8.44	53.48
BP	05-10 cm	T8	SD	1.2	0.1	0.2	4.0
BP	10-20 cm	T8	mean	6.07	1.05	8.43	44.88
BP	10-20 cm	T8	SD	0.2	0.1	0.1	0.9
BP	20-40 cm	T8	mean	0.99	0.73	6.40	25.58
BP	20-40 cm	T8	SD	0.1	0.1	0.3	0.7
BP	40-60 cm	T8	mean	0.98	0.56	5.19	22.92
BP	40-60 cm	T8	SD	0.1	0.1	0.5	0.9
BP	60-80 cm	T8	mean	0.97	0.50	4.29	22.21
BP	60-80 cm	T8	SD	0.1	0.1	0.2	1.5
BP	00-05 cm	T9	mean	14.94	13.08	4.45	58.10
BP	00-05 cm	T9	SD	0.5	0.4	0.2	1.5
BP	05-10 cm	T9	mean	17.94	3.18	15.04	97.72
BP	05-10 cm	T9	SD	5.2	0.1	0.5	19.9
BP	10-20 cm	T9	mean	11.02	1.41	14.09	72.14
BP	10-20 cm	T9	SD	2.9	0.1	0.6	8.8
BP	20-40 cm	T9	mean	1.66	0.99	10.54	38.59
BP	20-40 cm	T9	SD	0.1	0.1	0.2	0.1
BP	40-60 cm	T9	mean	1.62	0.72	8.80	34.89
BP	40-60 cm	T9	SD	0.1	0.1	0.2	1.3
BP	60-80 cm	T9	mean	1.73	0.70	7.32	36.05
BP	60-80 cm	T9	SD	0.1	0.1	0.6	2.2
BP	00-05 cm	T10	mean	26.68	15.84	8.36	100.53
BP	00-05 cm	T10	SD	6.2	1.3	1.1	26.7
BP	05-10 cm	T10	mean	33.3	3.07	29.79	176.16
BP	05-10 cm	T10	SD	7.4	0.2	1.1	27.1
BP	10-20 cm	T10	mean	27.93	1.34	27.87	149.29
BP	10-20 cm	T10	SD	6.3	0.1	1.8	27.4
BP	20-40 cm	T10	mean	2.48	0.73	21.02	56.04
BP	20-40 cm	T10	SD	0.1	0.1	2.0	2.3
BP	40-60 cm	T10	mean	2.43	0.69	17.30	54.46
BP	40-60 cm	T10	SD	0.1	0.1	0.9	1.8
BP	60-80 cm	T10	mean	2.80	0.77	13.58	55.39
BP	60-80 cm	T10	SD	0.1	0.1	1.3	3.6
BP	00-05 cm	T11	mean	24.80	13.86	9.14	97.05
BP	00-05 cm	T11	SD	2.8	0.4	0.9	12.9
BP	05-10 cm	T11	mean	26.97	2.38	36.19	165.58
BP	05-10 cm	T11	SD	6.2	0.2	4.0	31.7
BP	10-20 cm	T11	mean	28.87	1.18	34.18	165.54
BP	10-20 cm	T11	SD	5.5	0.1	2.4	25.1

BP	20-40 cm	T11	mean	13.25	0.73	31.32	107.76
BP	20-40 cm	T11	SD	6.1	0.1	0.7	25.2
BP	40-60 cm	T11	mean	6.49	0.66	24.55	79.19
BP	40-60 cm	T11	SD	3.5	0.1	5.6	18.2
BP	60-80 cm	T11	mean	5.56	0.60	23.62	80.52
BP	60-80 cm	T11	SD	3.6	0.1	1.5	11.7

Appendix B. Supplementary material

Mean chemical composition and standard deviation (SD) of the leaching solution from each triplicate (see Table 1).

Chemical compositions are expressed in $\mu\text{g/g}$ of soil

Sr	site	Depth	time		Mg	Ca	Na	K
µg/gsol	-	cm	-	-	µg/gsol	µg/gsol	µg/gsol	µg/gsol
0.168	SP	00-05 cm	T1	mean	3.08	4.20	9.13	59.30
0.005	SP	00-05 cm	T1	SD	0.1	0.1	0.1	1.3
0.055	SP	05-10 cm	T1	mean	6.97	12.39	7.16	40.56
0.001	SP	05-10 cm	T1	SD	0.5	0.5	0.1	2.4
0.029	SP	10-20 cm	T1	mean	4.35	5.59	4.43	25.05
0.001	SP	10-20 cm	T1	SD	0.2	0.1	0.3	1.3
0.018	SP	20-40 cm	T1	mean	2.64	5.87	4.91	16.5
0.001	SP	20-40 cm	T1	SD	0.1	0.1	0.1	0.2
0.019	SP	40-60 cm	T1	mean	2.28	5.66	4.65	19.49
0.001	SP	40-60 cm	T1	SD	0.1	0.1	0.1	0.4
0.017	SP	60-80 cm	T1	mean	1.98	5.93	3.90	22.74
0.001	SP	60-80 cm	T1	SD	0.1	0.2	0.1	0.2
0.088	SP	00-05 cm	T2	mean	2.67	2.51	5.38	48.23
0.002	SP	00-05 cm	T2	SD	0.2	0.1	0.1	1.6
0.028	SP	05-10 cm	T2	mean	4.56	6.51	2.11	29.52
0.001	SP	05-10 cm	T2	SD	0.1	0.1	0.1	1.2
0.018	SP	10-20 cm	T2	mean	3.43	3.52	1.21	21.96
0.001	SP	10-20 cm	T2	SD	0.5	0.1	0.1	3.5
0.014	SP	20-40 cm	T2	mean	1.65	3.77	1.16	13.57
0.001	SP	20-40 cm	T2	SD	0.1	0.1	0.1	0.4
0.014	SP	40-60 cm	T2	mean	1.37	3.56	1.07	15.40
0.001	SP	40-60 cm	T2	SD	0.1	0.1	0.1	0.1
0.011	SP	60-80 cm	T2	mean	1.25	3.64	0.92	16.42
0.001	SP	60-80 cm	T2	SD	0.1	0.1	0.1	0.4
0.042	SP	00-05 cm	T3	mean	4.67	2.61	3.54	49.20
0.031	SP	00-05 cm	T3	SD	0.3	0.1	0.1	2.2
0.028	SP	05-10 cm	T3	mean	7.45	5.69	1.45	45.41
0.001	SP	05-10 cm	T3	SD	0.6	0.1	0.1	3.7
0.017	SP	10-20 cm	T3	mean	5.31	3.13	1.54	38.79
0.001	SP	10-20 cm	T3	SD	1.0	0.1	0.1	5.6
0.012	SP	20-40 cm	T3	mean	1.31	2.88	1.25	19.39
0.001	SP	20-40 cm	T3	SD	0.1	0.1	0.1	0.5
0.006	SP	40-60 cm	T3	mean	0.97	2.42	1.13	21.18
0.006	SP	40-60 cm	T3	SD	0.1	0.2	0.1	0.6
0.009	SP	60-80 cm	T3	mean	0.91	2.17	1.20	24.47
0.001	SP	60-80 cm	T3	SD	0.1	0.1	0.1	0.1
0.041	SP	00-05 cm	T4	mean	5.99	3.56	2.86	54.49
0.017	SP	00-05 cm	T4	SD	0.5	0.1	0.1	2.8
0.026	SP	05-10 cm	T4	mean	8.61	5.06	1.57	55.30
0.001	SP	05-10 cm	T4	SD	0.9	0.1	0.1	4.6

0.017	SP	10-20 cm	T4	mean	5.93	2.53	1.96	49.58
0.001	SP	10-20 cm	T4	SD	0.6	0.1	0.1	4.1
0.011	SP	20-40 cm	T4	mean	1.18	1.83	1.49	26.34
0.001	SP	20-40 cm	T4	SD	0.1	0.1	0.1	0.9
0.009	SP	40-60 cm	T4	mean	0.92	1.44	1.39	28.37
0.003	SP	40-60 cm	T4	SD	0.1	0.1	0.1	0.3
0.009	SP	60-80 cm	T4	mean	0.95	1.26	1.58	32.49
0.001	SP	60-80 cm	T4	SD	0.1	0.1	0.1	0.6
0.040	SP	00-05 cm	T5	mean	6.95	3.39	2.08	53.77
0.003	SP	00-05 cm	T5	SD	0.5	0.1	0.1	2.8
0.024	SP	05-10 cm	T5	mean	9.09	4.63	1.48	57.65
0.001	SP	05-10 cm	T5	SD	0.7	0.1	0.1	3.6
0.017	SP	10-20 cm	T5	mean	5.10	2.42	1.76	46.60
0.001	SP	10-20 cm	T5	SD	0.7	0.1	0.1	3.4
0.010	SP	20-40 cm	T5	mean	1.16	1.71	1.27	26.53
0.001	SP	20-40 cm	T5	SD	0.1	0.1	0.1	0.7
0.010	SP	40-60 cm	T5	mean	1.05	1.20	1.27	28.79
0.001	SP	40-60 cm	T5	SD	0.1	0.1	0.1	0.5
0.008	SP	60-80 cm	T5	mean	1.08	0.98	1.35	31.19
0.001	SP	60-80 cm	T5	SD	0.1	0.1	0.1	0.5
0.050	SP	00-05 cm	T6	mean	9.72	4.16	1.72	65.41
0.006	SP	00-05 cm	T6	SD	0.9	0.2	0.1	5.3
0.033	SP	05-10 cm	T6	mean	13.75	4.44	1.83	84.14
0.003	SP	05-10 cm	T6	SD	1.4	0.1	0.1	8.4
0.022	SP	10-20 cm	T6	mean	8.83	2.16	2.20	69.09
0.002	SP	10-20 cm	T6	SD	1.0	0.1	0.1	5.5
0.013	SP	20-40 cm	T6	mean	1.21	1.29	1.47	28.97
0.001	SP	20-40 cm	T6	SD	0.1	0.1	0.1	0.8
0.011	SP	40-60 cm	T6	mean	1.10	0.86	1.48	31.01
0.001	SP	40-60 cm	T6	SD	0.1	0.1	0.1	0.8
0.009	SP	60-80 cm	T6	mean	1.16	0.71	1.61	34.22
0.001	SP	60-80 cm	T6	SD	0.1	0.1	0.1	0.5
0.050	SP	00-05 cm	T7	mean	8.15	4.96	1.48	55.79
0.002	SP	00-05 cm	T7	SD	0.5	0.1	0.1	2.6
0.026	SP	05-10 cm	T7	mean	10.15	4.29	2.15	68.99
0.001	SP	05-10 cm	T7	SD	1.5	0.2	0.1	8.2
0.021	SP	10-20 cm	T7	mean	6.33	1.77	2.88	61.28
0.001	SP	10-20 cm	T7	SD	1.6	0.1	0.1	9.2
0.013	SP	20-40 cm	T7	mean	1.39	0.85	2.22	37.06
0.001	SP	20-40 cm	T7	SD	0.2	0.2	0.1	1.7
0.012	SP	40-60 cm	T7	mean	1.35	0.66	2.17	38.83
0.001	SP	40-60 cm	T7	SD	0.1	0.1	0.1	2.5
0.010	SP	60-80 cm	T7	mean	1.30	0.69	2.28	38.47

0.001	SP	60-80 cm	T7	SD	0.1	0.2	0.2	5.9
0.047	SP	00-05 cm	T8	mean	9.71	7.28	1.57	63.24
0.001	SP	00-05 cm	T8	SD	0.8	0.2	0.1	4.6
0.028	SP	05-10 cm	T8	mean	11.55	4.55	3.17	84.14
0.001	SP	05-10 cm	T8	SD	1.4	0.2	0.1	6.5
0.023	SP	10-20 cm	T8	mean	8.41	1.69	4.36	82.63
0.001	SP	10-20 cm	T8	SD	1.5	0.1	0.1	8.0
0.014	SP	20-40 cm	T8	mean	1.57	0.85	3.15	44.80
0.001	SP	20-40 cm	T8	SD	0.1	0.1	0.1	1.3
0.014	SP	40-60 cm	T8	mean	1.62	0.62	3.14	48.74
0.002	SP	40-60 cm	T8	SD	0.1	0.1	0.1	0.4
0.014	SP	60-80 cm	T8	mean	1.73	0.57	3.62	53.33
0.001	SP	60-80 cm	T8	SD	0.1	0.1	0.1	0.6
0.058	SP	00-05 cm	T9	mean	21.35	11.49	2.18	113.3
0.002	SP	00-05 cm	T9	SD	3.8	0.7	0.2	18.8
0.031	SP	05-10 cm	T9	mean	24.23	6.00	6.26	155.63
0.004	SP	05-10 cm	T9	SD	3.2	0.2	1.7	16.5
0.024	SP	10-20 cm	T9	mean	11.01	1.89	6.94	109.82
0.001	SP	10-20 cm	T9	SD	3.1	0.1	0.6	21.1
0.020	SP	20-40 cm	T9	mean	2.03	0.83	4.55	58.15
0.001	SP	20-40 cm	T9	SD	0.1	0.1	0.2	2.7
0.018	SP	40-60 cm	T9	mean	2.32	0.55	4.82	64.81
0.001	SP	40-60 cm	T9	SD	0.1	0.1	0.1	1.5
0.020	SP	60-80 cm	T9	mean	2.45	0.60	5.34	69.86
0.001	SP	60-80 cm	T9	SD	0.1	0.1	0.2	2.1
0.116	SP	00-05 cm	T10	mean	26.9	14.44	3.18	137.70
0.011	SP	00-05 cm	T10	SD	3.6	0.8	0.2	18.6
0.087	SP	05-10 cm	T10	mean	34.9	6.54	9.71	226.92
0.016	SP	05-10 cm	T10	SD	4.4	0.2	0.8	22.1
0.070	SP	10-20 cm	T10	mean	26.67	1.37	13.12	207.52
0.037	SP	10-20 cm	T10	SD	6.6	0.2	0.4	34.0
0.031	SP	20-40 cm	T10	mean	2.59	0.51	8.36	75.76
0.002	SP	20-40 cm	T10	SD	0.3	0.1	0.6	3.8
0.034	SP	40-60 cm	T10	mean	2.15	0.35	8.90	80.90
0.002	SP	40-60 cm	T10	SD	0.1	0.1	0.2	0.9
0.062	SP	60-80 cm	T10	mean	1.78	0.35	10.05	83.02
0.041	SP	60-80 cm	T10	SD	0.1	0.1	0.9	2.1
0.110	SP	00-05 cm	T11	mean	29.13	15.87	3.83	146.00
0.010	SP	00-05 cm	T11	SD	7.1	2.1	0.4	36.00
0.108	SP	05-10 cm	T11	mean	35.11	5.73	12.77	244.32
0.022	SP	05-10 cm	T11	SD	3.6	0.3	1.2	20.1
0.118	SP	10-20 cm	T11	mean	23.28	1.02	15.57	196.72
0.020	SP	10-20 cm	T11	SD	8.5	0.1	3.6	54.3

0.067	SP	20-40 cm	T11	mean	4.11	0.37	11.91	95.59
0.025	SP	20-40 cm	T11	SD	1.1	0.1	0.7	7.0
0.038	SP	40-60 cm	T11	mean	2.94	0.29	11.96	97.44
0.007	SP	40-60 cm	T11	SD	0.7	0.1	2.3	6.7
0.029	SP	60-80 cm	T11	mean	3.11	0.36	14.83	104.74
0.010	SP	60-80 cm	T11	SD	0.5	0.1	1.5	2.4

ch experiment at the eleven time steps from the three

Sr
µg/gsol

0.018
0.001
0.058
0.004
0.035
0.001
0.037
0.001
0.035
0.001
0.034
0.001
0.013
0.001
0.035
0.001
0.027
0.001
0.026
0.001
0.028
0.001
0.025
0.001
0.015
0.001
0.032
0.001
0.024
0.001
0.021
0.001
0.022
0.002
0.020
0.001
0.019
0.001
0.033
0.001

0.026
0.001
0.022
0.002
0.024
0.002
0.022
0.002
0.024
0.001
0.034
0.001
0.029
0.002
0.024
0.003
0.026
0.003
0.025
0.003
0.031
0.002
0.041
0.002
0.036
0.002
0.023
0.004
0.023
0.001
0.026
0.002
0.034
0.001
0.037
0.004
0.034
0.003
0.025
0.005
0.026
0.003
0.025

0.004
0.046
0.001
0.043
0.004
0.043
0.004
0.029
0.006
0.030
0.002
0.029
0.003
0.058
0.001
0.049
0.004
0.050
0.011
0.030
0.003
0.031
0.001
0.033
0.002
0.121
0.013
0.147
0.034
0.100
0.053
0.039
0.001
0.036
0.001
0.044
0.019
0.141
0.029
0.164
0.015
0.209
0.064

0.054

0.009

0.047

0.012

0.065

0.012

Plot	Depth	Ca	Mg	Na	K
-	cm	kg·ha ⁻¹	kg·ha ⁻¹	kg·ha ⁻¹	kg·ha ⁻¹
Bulk soils					
Beech Plot (BP)	00-05	362	391	2375	7017
	05-10	284	575	4246	12615
	10-20	550	1277	8672	26886
	20-40	1285	3029	21187	64112
	40-60	1013	2423	16183	51389
	60-80	1226	2793	16313	44682
	Spruce Plot (SP)	00-05	170	381	450
05-10		70	601	691	6719
10-20		156	1178	1395	14740
20-40		341	4220	5253	47760
40-60		423	4494	6065	54937
60-80		429	3604	4886	43982
Ini Exch					
Beech Plot (BP)	00-05	199	34	5	92
	05-10	20	6	2	23
	10-20	13	6	3	30
	20-40	22	8	9	53
	40-60	12	3	7	22
	60-80	6	1	6	13
Spruce Plot (SP)	00-05	142	27	5	65
	05-10	30	6	2	18
	10-20	17	5	3	19
	20-40	39	7	6	46
	40-60	24	5	7	49
	60-80	15	3	4	41
Final Exch					
Beech Plot (BP)	00-05	143	20	4	32
	05-10	12	3	7	41
	10-20	10	5	12	70
	20-40	13	8	18	147
	40-60	7	3	9	75
	60-80	6	2	12	69
Spruce Plot (SP)	00-05	122	23	1	30
	05-10	24	7	3	37
	10-20	8	9	3	85

	20-40	17	17	9	225
	40-60	11	22	11	255
	60-80	11	18	8	262
Clays					
Beech Plot (BP)	00-05	92	278	795	2640
	05-10	33	331	347	2270
	10-20	38	519	438	3231
	20-40	51	1864	316	10803
	40-60	57	896	761	5190
	60-80	37	504	414	2613
Spruce Plot (SP)	00-05	45	290	161	2059
	05-10	16	293	86	1979
	10-20	14	472	81	2901
	20-40	93	1333	1035	7840
	40-60	50	1812	285	10301
	60-80	38	1321	205	7516
OM					
Beech Plot (BP)	00-05	614	88	32	288
	05-10	112	16	6	53
	10-20	234	34	12	110
	20-40	328	47	17	154
	40-60	233	34	12	110
	60-80	150	21	8	70
Spruce Plot (SP)	00-05	1422	37	8	117
	05-10	509	13	3	42
	10-20	269	7	2	22
	20-40	446	12	2	37
	40-60	290	7	2	24
	60-80	176	5	1	14

Appendix C. Supplementary material

Evaluation of the stock of Ca, Mg, Na and K in bulk soil and in the different reservoirs: initial and final organic matter in each soil layer (expressed in kg/hectare). This calculation considers the proportion of the bulk soils.

val exchangeable cations, clays, and
in of these different reservoirs inside

site	depth	Duplicate	time		Mg µg/gsol
-	-		-	-	
BP	00-05 cm	#1	T1	value	16.9
BP	00-05 cm	#2	T1	value	17.4
BP	00-05 cm	#3	T1	value	17.3
BP	00-05 cm		T1	mean	17.2
BP	00-05 cm		T1	SD	0.2
BP	05-10 cm	#1	T1	value	7.78
BP	05-10 cm	#2	T1	value	7.85
BP	05-10 cm	#3	T1	value	7.86
BP	00-05 cm		T1	mean	7.83
BP	00-05 cm		T1	SD	0.04
BP	10-20 cm	#1	T1	value	5.3
BP	10-20 cm	#2	T1	value	5.2
BP	10-20 cm	#3	T1	value	5.1
BP	10-20 cm		T1	mean	5.2
BP	10-20 cm		T1	SD	0.1
BP	20-40 cm	#1	T1	value	2.61
BP	20-40 cm	#2	T1	value	2.59
BP	20-40 cm	#3	T1	value	2.55
BP	20-40 cm		T1	mean	2.58
BP	20-40 cm		T1	SD	0.03
BP	40-60 cm	#1	T1	value	1.79
BP	40-60 cm	#2	T1	value	1.86
BP	40-60 cm	#3	T1	value	1.79
BP	40-60 cm		T1	mean	1.81
BP	40-60 cm		T1	SD	0.04
BP	60-80 cm	#1	T1	value	0.92
BP	60-80 cm	#2	T1	value	1.01
BP	60-80 cm	#3	T1	value	0.95
BP	60-80 cm		T1	mean	0.96
BP	60-80 cm		T1	SD	0.05
BP	00-05 cm	#1	T2	value	9.7
BP	00-05 cm	#2	T2	value	9.3
BP	00-05 cm	#3	T2	value	9.8
BP	00-05 cm		T2	mean	9.6
BP	00-05 cm		T2	SD	0.3
BP	05-10 cm	#1	T2	value	4.9
BP	05-10 cm	#2	T2	value	4.4

BP	05-10 cm	#3	T2	value	4.1
BP	05-10 cm		T2	mean	4.5
BP	05-10 cm		T2	SD	0.4
BP	10-20 cm	#1	T2	value	3
BP	10-20 cm	#2	T2	value	3.6
BP	10-20 cm	#3	T2	value	3
BP	10-20 cm		T2	mean	3.2
BP	10-20 cm		T2	SD	0.3
BP	20-40 cm	#1	T2	value	1.32
BP	20-40 cm	#2	T2	value	1.36
BP	20-40 cm	#3	T2	value	1.33
BP	20-40 cm		T2	mean	1.34
BP	20-40 cm		T2	SD	0.02
BP	40-60 cm	#1	T2	value	0.64
BP	40-60 cm	#2	T2	value	0.64
BP	40-60 cm	#3	T2	value	0.67
BP	40-60 cm		T2	mean	0.65
BP	40-60 cm		T2	SD	0.02
BP	60-80 cm	#1	T2	value	0.31
BP	60-80 cm	#2	T2	value	0.31
BP	60-80 cm	#3	T2	value	0.28
BP	60-80 cm		T2	mean	0.3
BP	60-80 cm		T2	SD	0.02
BP	00-05 cm	#1	T3	value	7.8
BP	00-05 cm	#2	T3	value	7.9
BP	00-05 cm	#3	T3	value	8.6
BP	00-05 cm		T3	mean	8.1
BP	00-05 cm		T3	SD	0.5
BP	05-10 cm	#1	T3	value	5.2
BP	05-10 cm	#2	T3	value	5.3
BP	05-10 cm	#3	T3	value	5.6
BP	05-10 cm		T3	mean	5.4
BP	05-10 cm		T3	SD	0.2
BP	10-20 cm	#1	T3	value	4.1
BP	10-20 cm	#2	T3	value	4.4
BP	10-20 cm	#3	T3	value	3.4
BP	10-20 cm		T3	mean	4
BP	10-20 cm		T3	SD	0.5
BP	20-40 cm	#1	T3	value	0.89
BP	20-40 cm	#2	T3	value	0.84
BP	20-40 cm	#3	T3	value	0.8
BP	20-40 cm		T3	mean	0.84
BP	20-40 cm		T3	SD	0.04

BP	40-60 cm	#1	T3	value	0.42
BP	40-60 cm	#2	T3	value	0.43
BP	40-60 cm	#3	T3	value	0.45
BP	40-60 cm		T3	mean	0.43
BP	40-60 cm		T3	SD	0.02
BP	60-80 cm	#1	T3	value	0.306
BP	60-80 cm	#2	T3	value	0.314
BP	60-80 cm	#3	T3	value	0.321
BP	60-80 cm		T3	mean	0.314
BP	60-80 cm		T3	SD	0.007
BP	00-05 cm	#1	T4	value	8.2
BP	00-05 cm	#2	T4	value	6.6
BP	00-05 cm	#3	T4	value	6.8
BP	00-05 cm		T4	mean	7.2
BP	00-05 cm		T4	SD	0.9
BP	05-10 cm	#1	T4	value	6.1
BP	05-10 cm	#2	T4	value	5.2
BP	05-10 cm	#3	T4	value	6.1
BP	05-10 cm		T4	mean	5.8
BP	05-10 cm		T4	SD	0.5
BP	10-20 cm	#1	T4	value	3.7
BP	10-20 cm	#2	T4	value	3.4
BP	10-20 cm	#3	T4	value	4
BP	10-20 cm		T4	mean	3.7
BP	10-20 cm		T4	SD	0.3
BP	20-40 cm	#1	T4	value	0.694
BP	20-40 cm	#2	T4	value	0.704
BP	20-40 cm	#3	T4	value	0.707
BP	10-20 cm		T4	mean	0.702
BP	10-20 cm		T4	SD	0.007
BP	40-60 cm	#1	T4	value	0.42
BP	40-60 cm	#2	T4	value	0.45
BP	40-60 cm	#3	T4	value	0.47
BP	40-60 cm		T4	mean	0.45
BP	40-60 cm		T4	SD	0.03
BP	60-80 cm	#1	T4	value	0.38
BP	60-80 cm	#2	T4	value	0.4
BP	60-80 cm	#3	T4	value	0.4
BP	60-80 cm		T4	mean	0.4
BP	60-80 cm		T4	SD	0.01
BP	00-05 cm	#1	T5	value	6
BP	00-05 cm	#2	T5	value	5
BP	00-05 cm	#3	T5	value	8

BP	00-05 cm		T5	mean	6
BP	00-05 cm		T5	SD	1
BP	05-10 cm	#1	T5	value	5.3
BP	05-10 cm	#2	T5	value	5.2
BP	05-10 cm	#3	T5	value	6.2
BP	05-10 cm		T5	mean	5.6
BP	05-10 cm		T5	SD	0.6
BP	10-20 cm	#1	T5	value	3.9
BP	10-20 cm	#2	T5	value	4.8
BP	10-20 cm	#3	T5	value	3.3
BP	10-20 cm		T5	mean	4
BP	10-20 cm		T5	SD	0.7
BP	20-40 cm	#1	T5	value	0.58
BP	20-40 cm	#2	T5	value	0.53
BP	20-40 cm	#3	T5	value	0.57
BP	20-40 cm		T5	mean	0.56
BP	20-40 cm		T5	SD	0.02
BP	40-60 cm	#1	T5	value	0.39
BP	40-60 cm	#2	T5	value	0.38
BP	40-60 cm	#3	T5	value	0.4
BP	40-60 cm		T5	mean	0.39
BP	40-60 cm		T5	SD	0.01
BP	60-80 cm	#1	T5	value	0.34
BP	60-80 cm	#2	T5	value	0.34
BP	60-80 cm	#3	T5	value	0.37
BP	60-80 cm		T5	mean	0.35
BP	60-80 cm		T5	SD	0.02
BP	00-05 cm	#1	T6	value	9.4
BP	00-05 cm	#2	T6	value	8.5
BP	00-05 cm	#3	T6	value	9.4
BP	00-05 cm		T6	mean	9.1
BP	00-05 cm		T6	SD	0.6
BP	05-10 cm	#1	T6	value	12
BP	05-10 cm	#2	T6	value	9
BP	05-10 cm	#3	T6	value	10
BP	05-10 cm		T6	mean	10
BP	05-10 cm		T6	SD	2
BP	10-20 cm	#1	T6	value	8
BP	10-20 cm	#2	T6	value	6
BP	10-20 cm	#3	T6	value	8
BP	10-20 cm		T6	mean	7
BP	10-20 cm		T6	SD	2
BP	20-40 cm	#1	T6	value	0.65

BP	20-40 cm	#2	T6	value	0.67
BP	20-40 cm	#3	T6	value	0.66
BP	20-40 cm		T6	mean	0.66
BP	20-40 cm		T6	SD	0.01
BP	40-60 cm	#1	T6	value	0.502
BP	40-60 cm	#2	T6	value	0.518
BP	40-60 cm	#3	T6	value	0.518
BP	40-60 cm		T6	mean	0.512
BP	40-60 cm		T6	SD	0.009
BP	60-80 cm	#1	T6	value	0.5
BP	60-80 cm	#2	T6	value	0.47
BP	60-80 cm	#3	T6	value	0.51
BP	60-80 cm		T6	mean	0.49
BP	60-80 cm		T6	SD	0.02
BP	00-05 cm	#1	T7	value	7
BP	00-05 cm	#2	T7	value	10
BP	00-05 cm	#3	T7	value	8
BP	00-05 cm		T7	mean	8
BP	00-05 cm		T7	SD	2
BP	05-10 cm	#1	T7	value	6
BP	05-10 cm	#2	T7	value	8
BP	05-10 cm	#3	T7	value	7
BP	05-10 cm		T7	mean	7
BP	05-10 cm		T7	SD	1
BP	10-20 cm	#1	T7	value	5.9
BP	10-20 cm	#2	T7	value	5.5
BP	10-20 cm	#3	T7	value	4.5
BP	10-20 cm		T7	mean	5.3
BP	10-20 cm		T7	SD	0.7
BP	20-40 cm	#1	T7	value	0.7
BP	20-40 cm	#2	T7	value	0.72
BP	20-40 cm	#3	T7	value	0.77
BP	20-40 cm		T7	mean	0.73
BP	20-40 cm		T7	SD	0.03
BP	40-60 cm	#1	T7	value	0.65
BP	40-60 cm	#2	T7	value	0.67
BP	40-60 cm	#3	T7	value	0.69
BP	40-60 cm		T7	mean	0.68
BP	40-60 cm		T7	SD	0.03
BP	60-80 cm	#1	T7	value	0.65
BP	60-80 cm	#2	T7	value	0.67
BP	60-80 cm	#3	T7	value	0.71
BP	60-80 cm		T7	mean	7.9

BP	60-80 cm		T7	SD	0.5
BP	00-05 cm	#1	T8	value	7.8
BP	00-05 cm	#2	T8	value	8.5
BP	00-05 cm	#3	T8	value	7.5
BP	00-05 cm		T8	mean	7.9
BP	00-05 cm		T8	SD	0.5
BP	05-10 cm	#1	T8	value	8
BP	05-10 cm	#2	T8	value	10
BP	05-10 cm	#3	T8	value	7
BP	05-10 cm		T8	mean	8
BP	05-10 cm		T8	SD	1
BP	10-20 cm	#1	T8	value	6
BP	10-20 cm	#2	T8	value	6.4
BP	10-20 cm	#3	T8	value	5.8
BP	10-20 cm		T8	mean	6.1
BP	10-20 cm			SD	0.3
BP	20-40 cm	#1	T8	value	0.99
BP	20-40 cm	#2	T8	value	0.98
BP	20-40 cm	#3	T8	value	1.01
BP	20-40 cm		T8	mean	0.99
BP	20-40 cm		T8	SD	0.02
BP	40-60 cm	#1	T8	value	0.96
BP	40-60 cm	#2	T8	value	0.99
BP	40-60 cm	#3	T8	value	1.01
BP	40-60 cm		T8	mean	0.98
BP	40-60 cm		T8	SD	0.03
BP	60-80 cm	#1	T8	value	0.96
BP	60-80 cm	#2	T8	value	0.95
BP	60-80 cm	#3	T8	value	1.02
BP	60-80 cm		T8	mean	0.98
BP	60-80 cm		T8	SD	0.04
BP	00-05 cm	#1	T9	value	15.1
BP	00-05 cm	#2	T9	value	15.5
BP	00-05 cm	#3	T9	value	14.3
BP	00-05 cm		T9	mean	14.9
BP	00-05 cm		T9	SD	0.6
BP	05-10 cm	#1	T9	value	23
BP	05-10 cm	#2	T9	value	19
BP	05-10 cm	#3	T9	value	12
BP	05-10 cm		T9	mean	18
BP	05-10 cm		T9	SD	5
BP	10-20 cm	#1	T9	value	13
BP	10-20 cm	#2	T9	value	8

BP	10-20 cm	#3	T9	value	12
BP	10-20 cm		T9	mean	11
BP	10-20 cm		T9	SD	3
BP	20-40 cm	#1	T9	value	1.66
BP	20-40 cm	#2	T9	value	1.63
BP	20-40 cm	#3	T9	value	1.7
BP	20-40 cm		T9	mean	1.67
BP	20-40 cm		T9	SD	0.03
BP	40-60 cm	#1	T9	value	1.67
BP	40-60 cm	#2	T9	value	1.61
BP	40-60 cm	#3	T9	value	1.58
BP	40-60 cm		T9	mean	1.62
BP	40-60 cm		T9	SD	0.05
BP	60-80 cm	#1	T9	value	1.7
BP	60-80 cm	#2	T9	value	1.7
BP	60-80 cm	#3	T9	value	1.9
BP	60-80 cm		T9	mean	1.7
BP	60-80 cm		T9	SD	0.1
BP	00-05 cm	#1	T10	value	20
BP	00-05 cm	#2	T10	value	29
BP	00-05 cm	#3	T10	value	32
BP	00-05 cm		T10	mean	27
BP	00-05 cm		T10	SD	6
BP	05-10 cm	#1	T10	value	31
BP	05-10 cm	#2	T10	value	42
BP	05-10 cm	#3	T10	value	27
BP	05-10 cm		T10	mean	33
BP	05-10 cm		T10	SD	7
BP	10-20 cm	#1	T10	value	23
BP	10-20 cm	#2	T10	value	35
BP	10-20 cm	#3	T10	value	26
BP	10-20 cm		T10	mean	28
BP	10-20 cm		T10	SD	6
BP	20-40 cm	#1	T10	value	2.43
BP	20-40 cm	#2	T10	value	2.44
BP	20-40 cm	#3	T10	value	2.59
BP	20-40 cm		T10	mean	2.49
BP	20-40 cm		T10	SD	0.09
BP	40-60 cm	#1	T10	value	2.5
BP	40-60 cm	#2	T10	value	2.3
BP	40-60 cm	#3	T10	value	2.4
BP	40-60 cm		T10	mean	2.4
BP	40-60 cm		T10	SD	0.1

BP	60-80 cm	#1	T10	value	2.8
BP	60-80 cm	#2	T10	value	2.7
BP	60-80 cm	#3	T10	value	2.9
BP	60-80 cm		T10	mean	25
BP	60-80 cm		T10	SD	3
BP	00-05 cm	#1	T11	value	25
BP	00-05 cm	#2	T11	value	22
BP	00-05 cm	#3	T11	value	27
BP	00-05 cm		T11	mean	27
BP	00-05 cm		T11	SD	6
BP	05-10 cm	#1	T11	value	33
BP	05-10 cm	#2	T11	value	20
BP	05-10 cm	#3	T11	value	28
BP	05-10 cm		T11	mean	29
BP	05-10 cm		T11	SD	6
BP	10-20 cm	#1	T11	value	32
BP	10-20 cm	#2	T11	value	32
BP	10-20 cm	#3	T11	value	22
BP	10-20 cm		T11	mean	13
BP	10-20 cm		T11	SD	6
BP	20-40 cm	#1	T11	value	8
BP	20-40 cm	#2	T11	value	20
BP	20-40 cm	#3	T11	value	12
BP	20-40 cm		T11	mean	6
BP	20-40 cm		T11	SD	4
BP	40-60 cm	#1	T11	value	10
BP	40-60 cm	#2	T11	value	7
BP	40-60 cm	#3	T11	value	3
BP	40-60 cm		T11	mean	6
BP	40-60 cm		T11	SD	4
BP	60-80 cm	#1	T11	value	3
BP	60-80 cm	#2	T11	value	4
BP	60-80 cm	#3	T11	value	10
BP	60-80 cm		T11	mean	6
BP	60-80 cm		T11	SD	4

Ca µg/gsol	Na µg/gsol	K µg/gsol	Sr µg/gsol	site -	depth -	Duplicate
37.8	11.9	120	0.173	SP	00-05 cm	#1
37.8	12.3	123	0.171	SP	00-05 cm	#2
38.3	12.2	123	0.162	SP	00-05 cm	#3
38	12.1	122	0.169	SP	00-05 cm	
0.3	0.2	2	0.006	SP	00-05 cm	
11.56	6	27.4	0.0566	SP	05-10 cm	#1
11.57	6.1	27.7	0.0552	SP	05-10 cm	#2
11.49	6.2	27.1	0.0552	SP	05-10 cm	#3
11.54	6.1	27.4	0.0557	SP	00-05 cm	
0.04	0.1	0.3	0.0008	SP	00-05 cm	
4.9	5.7	19.7	0.0303	SP	10-20 cm	#1
4.7	5.7	18.6	0.0299	SP	10-20 cm	#2
4.7	5.5	18.6	0.0298	SP	10-20 cm	#3
4.8	5.6	19	0.03	SP	10-20 cm	
0.1	0.1	0.6	0.0003	SP	10-20 cm	
3.15	4.25	10	0.0179	SP	20-40 cm	#1
3.21	4.21	10.9	0.018	SP	20-40 cm	#2
3.21	4.17	10.3	0.0188	SP	20-40 cm	#3
3.19	4.21	10.4	0.0182	SP	20-40 cm	
0.03	0.04	0.5	0.0005	SP	20-40 cm	
2.7	5.4	8.67	0.0189	SP	40-60 cm	#1
2.9	5.2	8.61	0.0201	SP	40-60 cm	#2
2.7	5.4	8.54	0.0188	SP	40-60 cm	#3
2.7	5.4	8.61	0.0193	SP	40-60 cm	
0.1	0.1	0.06	0.0007	SP	40-60 cm	
2.1	4.58	6.32	0.0175	SP	60-80 cm	#1
2.4	4.7	6.39	0.0179	SP	60-80 cm	#2
2.3	4.7	6.34	0.0173	SP	60-80 cm	#3
2.3	4.66	6.35	0.0176	SP	60-80 cm	
0.1	0.07	0.03	0.0003	SP	60-80 cm	
21.9	5.6	81	0.091	SP	00-05 cm	#1
21.2	5.6	78	0.085	SP	00-05 cm	#2
22.6	5.8	83	0.089	SP	00-05 cm	#3
21.9	5.7	81	0.089	SP	00-05 cm	
0.7	0.1	2	0.003	SP	00-05 cm	
5.73	2.05	22	0.03	SP	05-10 cm	#1
5.73	2.06	19	0.028	SP	05-10 cm	#2

5.71	1.98	19	0.027	SP	05-10 cm	#3
5.73	2.03	20	0.028	SP	05-10 cm	
0.01	0.04	1	0.001	SP	05-10 cm	
2.62	1.96	15	0.0182	SP	10-20 cm	#1
2.67	2.02	17	0.0191	SP	10-20 cm	#2
2.62	1.93	14	0.0178	SP	10-20 cm	#3
2.64	1.97	16	0.0184	SP	10-20 cm	
0.03	0.05	1	0.0006	SP	10-20 cm	
2.2	1.65	9.4	0.0138	SP	20-40 cm	#1
2.24	1.71	8.8	0.0143	SP	20-40 cm	#2
2.31	1.63	8.5	0.0144	SP	20-40 cm	#3
2.25	1.66	8.9	0.0141	SP	20-40 cm	
0.06	0.05	0.5	0.0003	SP	20-40 cm	
1.71	1.77	6.9	0.0144	SP	40-60 cm	#1
1.84	1.67	7.1	0.0145	SP	40-60 cm	#2
1.74	1.76	7.2	0.0134	SP	40-60 cm	#3
1.76	1.73	7.1	0.0141	SP	40-60 cm	
0.07	0.05	0.1	0.0006	SP	40-60 cm	
1.31	1.52	5.1	0.0113	SP	60-80 cm	#1
1.44	1.44	5.5	0.0115	SP	60-80 cm	#2
1.32	1.43	5.4	0.0107	SP	60-80 cm	#3
1.36	1.46	5.3	0.0112	SP	60-80 cm	
0.07	0.05	0.2	0.0004	SP	60-80 cm	
13.4	3.01	56	0.06	SP	00-05 cm	#1
12.9	2.93	57	0.01	SP	00-05 cm	#2
14.2	3.11	62	0.06	SP	00-05 cm	#3
13.5	3.02	58	0.04	SP	00-05 cm	
0.6	0.09	3	0.03	SP	00-05 cm	
4.72	2.82	26	0.0282	SP	05-10 cm	#1
4.79	2.78	26	0.0279	SP	05-10 cm	#2
4.71	2.85	28	0.028	SP	05-10 cm	#3
4.74	2.82	26	0.0281	SP	05-10 cm	
0.04	0.04	1	0.0002	SP	05-10 cm	
2.09	2.87	22	0.018	SP	10-20 cm	#1
2.05	2.84	24	0.018	SP	10-20 cm	#2
2.12	2.79	20	0.0173	SP	10-20 cm	#3
2.09	2.83	22	0.0178	SP	10-20 cm	
0.04	0.04	2	0.0004	SP	10-20 cm	
1.63	2.33	10.8	0.012	SP	20-40 cm	#1
1.65	2.44	10.8	0.0121	SP	20-40 cm	#2
1.67	2.39	12	0.0122	SP	20-40 cm	#3
1.65	2.39	11.2	0.0121	SP	20-40 cm	
0.02	0.05	0.7	0.0001	SP	20-40 cm	

1.22	1.9	8.9	0.003	SP	40-60 cm	#1
1.28	2.2	9.2	-	SP	40-60 cm	#2
1.28	1.9	8.1	0.011	SP	40-60 cm	#3
1.26	2	8.7	0.007	SP	40-60 cm	
0.03	0.2	0.6	0.006	SP	40-60 cm	
0.94	1.6	8.5	0.0098	SP	60-80 cm	#1
1.04	1.8	8.8	0.0099	SP	60-80 cm	#2
0.93	1.6	8.9	0.0096	SP	60-80 cm	#3
0.97	1.7	8.8	0.0097	SP	60-80 cm	
0.06	0.1	0.2	0.0002	SP	60-80 cm	
10.1	2.3	50	0.05	SP	00-05 cm	#1
9.2	2	44	0.02	SP	00-05 cm	#2
10.2	2.1	45	0.05	SP	00-05 cm	#3
9.8	2.1	46	0.04	SP	00-05 cm	
0.6	0.1	3	0.02	SP	00-05 cm	
3.92	3.7	34	0.0262	SP	05-10 cm	#1
3.83	3.5	29	0.0255	SP	05-10 cm	#2
3.92	3.9	33	0.0268	SP	05-10 cm	#3
3.89	3.7	32	0.0262	SP	05-10 cm	
0.06	0.2	3	0.0007	SP	05-10 cm	
1.7	3.66	25	0.018	SP	10-20 cm	#1
1.66	3.57	23	0.018	SP	10-20 cm	#2
1.7	3.58	26	0.016	SP	10-20 cm	#3
1.69	3.6	24	0.018	SP	10-20 cm	
0.02	0.05	1	0.001	SP	10-20 cm	
1.18	3	13.6	0.0115	SP	20-40 cm	#1
1.2	3	13.9	0.0115	SP	20-40 cm	#2
1.28	3.3	15.1	0.0113	SP	20-40 cm	#3
1.22	3.1	14.2	0.0114	SP	10-20 cm	
0.05	0.2	0.8	0.0001	SP	10-20 cm	
0.91	2.2	11.2	0.006	SP	40-60 cm	#1
0.96	2.7	12	0.012	SP	40-60 cm	#2
0.97	2.5	11.9	0.01	SP	40-60 cm	#3
0.95	2.5	11.7	0.01	SP	40-60 cm	
0.03	0.3	0.4	0.003	SP	40-60 cm	
0.71	2	10.3	0.0092	SP	60-80 cm	#1
0.82	2.2	10.8	0.0094	SP	60-80 cm	#2
0.71	2.1	11.1	0.0089	SP	60-80 cm	#3
0.75	2.1	10.7	0.0091	SP	60-80 cm	
0.07	0.1	0.4	0.0002	SP	60-80 cm	
8.3	1.7	36	0.043	SP	00-05 cm	#1
7.6	1.5	34	0.036	SP	00-05 cm	#2
8.7	1.9	43	0.042	SP	00-05 cm	#3

8.2	1.7	37	0.04	SP	00-05 cm	
0.5	0.2	5	0.004	SP	00-05 cm	
3.15	3.4	32	0.024	SP	05-10 cm	#1
3.25	3.4	30	0.023	SP	05-10 cm	#2
3.31	3.8	34	0.026	SP	05-10 cm	#3
3.24	3.5	32	0.024	SP	05-10 cm	
0.08	0.3	2	0.001	SP	05-10 cm	
1.36	3.41	26	0.018	SP	10-20 cm	#1
1.35	3.44	29	0.018	SP	10-20 cm	#2
1.31	3.39	24	0.015	SP	10-20 cm	#3
1.34	3.41	26	0.017	SP	10-20 cm	
0.03	0.03	3	0.002	SP	10-20 cm	
1.01	2.7	13.5	0.011	SP	20-40 cm	#1
0.96	2.8	13.9	0.0108	SP	20-40 cm	#2
0.98	3.1	14.3	0.0104	SP	20-40 cm	#3
0.98	2.9	13.9	0.0107	SP	20-40 cm	
0.02	0.2	0.4	0.0003	SP	20-40 cm	
0.73	2.1	10.6	0.01	SP	40-60 cm	#1
0.86	2.4	10.7	0.012	SP	40-60 cm	#2
0.75	2.3	11	0.009	SP	40-60 cm	#3
0.78	2.3	10.7	0.011	SP	40-60 cm	
0.07	0.1	0.2	0.002	SP	40-60 cm	
0.51	1.83	9.3	0.0085	SP	60-80 cm	#1
0.6	1.8	9.6	0.0088	SP	60-80 cm	#2
0.49	1.75	10.7	0.0082	SP	60-80 cm	#3
0.54	1.79	9.9	0.0085	SP	60-80 cm	
0.06	0.04	0.8	0.0003	SP	60-80 cm	
8.5	2.1	46	0.056	SP	00-05 cm	#1
8.2	1.8	44	0.043	SP	00-05 cm	#2
9.2	2	46	0.052	SP	00-05 cm	#3
8.6	1.9	45	0.05	SP	00-05 cm	
0.5	0.1	1	0.007	SP	00-05 cm	
2.71	5	59	0.037	SP	05-10 cm	#1
2.77	4.6	45	0.03	SP	05-10 cm	#2
2.61	5.1	51	0.033	SP	05-10 cm	#3
2.7	4.9	52	0.033	SP	05-10 cm	
0.08	0.3	7	0.003	SP	05-10 cm	
1.05	4.9	46	0.024	SP	10-20 cm	#1
1.11	4.4	34	0.019	SP	10-20 cm	#2
1.12	4.8	43	0.023	SP	10-20 cm	#3
1.09	4.7	41	0.022	SP	10-20 cm	
0.04	0.3	7	0.002	SP	10-20 cm	
0.94	3.1	17.2	0.0128	SP	20-40 cm	#1

0.98	3.4	17	0.0134	SP	20-40 cm	#2
0.97	3.6	18.4	0.0133	SP	20-40 cm	#3
0.96	3.4	17.5	0.0132	SP	20-40 cm	
0.02	0.2	0.8	0.0003	SP	20-40 cm	
0.66	2.5	12.7	0.012	SP	40-60 cm	#1
0.68	3	13.8	0.013	SP	40-60 cm	#2
0.69	2.7	13.7	0.011	SP	40-60 cm	#3
0.68	2.7	13.4	0.012	SP	40-60 cm	
0.02	0.2	0.6	0.001	SP	40-60 cm	
0.49	2.28	12	0.00992	SP	60-80 cm	#1
0.55	2.19	12	0.00982	SP	60-80 cm	#2
0.49	2.36	14	0.00982	SP	60-80 cm	#3
0.51	2.28	13	0.00985	SP	60-80 cm	
0.04	0.08	1	0.00006	SP	60-80 cm	
8.6	1.9	35	0.053	SP	00-05 cm	#1
8.8	2.3	48	0.051	SP	00-05 cm	#2
9.6	2	38	0.049	SP	00-05 cm	#3
9	2.1	40	0.051	SP	00-05 cm	
0.5	0.2	7	0.002	SP	00-05 cm	
2.4	5.5	40	0.025	SP	05-10 cm	#1
2.9	6	47	0.029	SP	05-10 cm	#2
2.6	6.2	44	0.026	SP	05-10 cm	#3
2.6	5.9	43	0.026	SP	05-10 cm	
0.2	0.3	3	0.002	SP	05-10 cm	
1	5.96	39	0.023	SP	10-20 cm	#1
1.1	5.84	36	0.021	SP	10-20 cm	#2
1.2	5.83	33	0.019	SP	10-20 cm	#3
1.1	5.88	36	0.021	SP	10-20 cm	
0.1	0.07	3	0.002	SP	10-20 cm	
0.76	4.4	20	0.0125	SP	20-40 cm	#1
0.82	4.5	20	0.0133	SP	20-40 cm	#2
0.81	4.9	22	0.0133	SP	20-40 cm	#3
0.8	4.6	20	0.013	SP	20-40 cm	
0.03	0.3	1	0.0005	SP	20-40 cm	
0.548	3.3	15.9	0.012	SP	40-60 cm	#1
0.561	4	17.2	0.014	SP	40-60 cm	#2
0.565	3.8	17.7	0.011	SP	40-60 cm	#3
0.46	3.1	16.9	0.0109	SP	40-60 cm	
0.03	0.06	0.7	0.0002	SP	40-60 cm	
0.43	3.04	16.2	0.0107	SP	60-80 cm	#1
0.49	3.12	16.7	0.0111	SP	60-80 cm	#2
0.45	3.15	17.7	0.0108	SP	60-80 cm	#3
9.2	2.7	36	0.048	SP	60-80 cm	

0.7	0.2	3	0.002	SP	60-80 cm	
8.8	2.8	36	0.047	SP	00-05 cm	#1
8.8	2.7	39	0.047	SP	00-05 cm	#2
10.1	2.5	33	0.05	SP	00-05 cm	#3
9.2	2.7	36	0.048	SP	00-05 cm	
0.7	0.2	3	0.002	SP	00-05 cm	
2.2	8.2	54	0.028	SP	05-10 cm	#1
2.5	8.6	57	0.03	SP	05-10 cm	#2
2.3	8.4	49	0.028	SP	05-10 cm	#3
2.3	8.4	53	0.029	SP	05-10 cm	
0.2	0.2	4	0.001	SP	05-10 cm	
1.02	8.6	45	0.024	SP	10-20 cm	#1
1.12	8.4	46	0.025	SP	10-20 cm	#2
1.03	8.3	44	0.022	SP	10-20 cm	#3
1.06	8.4	45	0.024	SP	10-20 cm	
0.06	0.2	1	0.001	SP	10-20 cm	
0.73	6.1	25	0.0142	SP	20-40 cm	#1
0.73	6.3	25.4	0.015	SP	20-40 cm	#2
0.75	6.8	26.4	0.0157	SP	20-40 cm	#3
0.73	6.4	25.6	0.015	SP	20-40 cm	
0.01	0.3	0.8	0.0008	SP	20-40 cm	
0.55	4.6	22	0.013	SP	40-60 cm	#1
0.58	5.8	23	0.017	SP	40-60 cm	#2
0.57	5.2	24	0.013	SP	40-60 cm	#3
0.57	5.2	23	0.015	SP	40-60 cm	
0.02	0.6	1	0.002	SP	40-60 cm	
0.48	4.1	21	0.0139	SP	60-80 cm	#1
0.52	4.2	21	0.0142	SP	60-80 cm	#2
0.52	4.6	24	0.0143	SP	60-80 cm	#3
0.51	4.3	22	0.0141	SP	60-80 cm	
0.03	0.2	2	0.0002	SP	60-80 cm	
12.6	4.2	58	0.056	SP	00-05 cm	#1
13.4	4.5	60	0.061	SP	00-05 cm	#2
13.2	4.6	56	0.06	SP	00-05 cm	#3
13.1	4.5	58	0.059	SP	00-05 cm	
0.4	0.2	2	0.003	SP	00-05 cm	
3.3	15.7	117	0.036	SP	05-10 cm	#1
3.2	14.7	99	0.03	SP	05-10 cm	#2
3	14.7	77	0.028	SP	05-10 cm	#3
3.2	15	98	0.031	SP	05-10 cm	
0.2	0.6	20	0.004	SP	05-10 cm	
1.44	13.5	76	0.0244	SP	10-20 cm	#1
1.34	14	62	0.0231	SP	10-20 cm	#2

1.45	14.8	78	0.0249	SP	10-20 cm	#3
1.41	14.1	72	0.0241	SP	10-20 cm	
0.06	0.6	9	0.0009	SP	10-20 cm	
1.01	10.4	38.7	0.02	SP	20-40 cm	#1
1.03	10.8	38.6	0.021	SP	20-40 cm	#2
0.94	10.4	38.4	0.019	SP	20-40 cm	#3
0.99	10.5	38.6	0.02	SP	20-40 cm	
0.05	0.2	0.1	0.001	SP	20-40 cm	
0.71	9.1	36	0.0188	SP	40-60 cm	#1
0.75	8.7	36	0.0189	SP	40-60 cm	#2
0.73	8.6	33	0.0191	SP	40-60 cm	#3
0.73	8.8	35	0.019	SP	40-60 cm	
0.02	0.3	1	0.0002	SP	40-60 cm	
0.65	6.8	34	0.02	SP	60-80 cm	#1
0.74	7.1	35	0.02	SP	60-80 cm	#2
0.72	8	39	0.023	SP	60-80 cm	#3
0.7	7.3	36	0.021	SP	60-80 cm	
0.05	0.6	2	0.002	SP	60-80 cm	
14	7	70	0.1	SP	00-05 cm	#1
16	8	110	0.12	SP	00-05 cm	#2
17	10	121	0.12	SP	00-05 cm	#3
16	8	101	0.12	SP	00-05 cm	
1	1	27	0.01	SP	00-05 cm	
3.1	29	168	0.09	SP	05-10 cm	#1
3.3	30	206	0.1	SP	05-10 cm	#2
2.8	31	154	0.07	SP	05-10 cm	#3
3.1	30	176	0.09	SP	05-10 cm	
0.3	1	27	0.02	SP	05-10 cm	
1.28	26	126	0.11	SP	10-20 cm	#1
1.45	30	180	0.07	SP	10-20 cm	#2
1.31	28	142	0.03	SP	10-20 cm	#3
1.35	28	149	0.07	SP	10-20 cm	
0.09	2	27	0.04	SP	10-20 cm	
0.77	19	54	0.032	SP	20-40 cm	#1
0.77	23	59	0.029	SP	20-40 cm	#2
0.69	20	55	0.034	SP	20-40 cm	#3
0.74	21	56	0.032	SP	20-40 cm	
0.05	2	2	0.002	SP	20-40 cm	
0.7	18	56	0.033	SP	40-60 cm	#1
0.69	17	54	0.032	SP	40-60 cm	#2
0.71	16	53	0.037	SP	40-60 cm	#3
0.7	17	54	0.034	SP	40-60 cm	
0.01	1	2	0.003	SP	40-60 cm	

0.75	13	54	0.04	SP	60-80 cm	#1
0.8	13	53	0.04	SP	60-80 cm	#2
0.79	15	60	0.11	SP	60-80 cm	#3
13.9	9	97	0.11	SP	60-80 cm	
0.4	1	13	0.01	SP	60-80 cm	
13.6	9	92	0.11	SP	00-05 cm	#1
13.6	9	87	0.1	SP	00-05 cm	#2
14.3	10	112	0.12	SP	00-05 cm	#3
2.4	36	166	0.11	SP	00-05 cm	
0.3	4	32	0.02	SP	00-05 cm	
2.7	40	195	0.12	SP	05-10 cm	#1
2.1	32	132	0.08	SP	05-10 cm	#2
2.4	37	170	0.12	SP	05-10 cm	#3
1.18	34	166	0.12	SP	05-10 cm	
0.09	2	25	0.02	SP	05-10 cm	
1.24	36	178	0.13	SP	10-20 cm	#1
1.23	36	182	0.13	SP	10-20 cm	#2
1.08	31	137	0.09	SP	10-20 cm	#3
0.7	31.3	108	0.07	SP	10-20 cm	
0.2	0.8	25	0.03	SP	10-20 cm	
0.6	30.4	85	0.05	SP	20-40 cm	#1
0.9	31.9	135	0.1	SP	20-40 cm	#2
0.6	31.7	103	0.06	SP	20-40 cm	#3
0.66	25	79	0.038	SP	20-40 cm	
0.03	6	18	0.008	SP	20-40 cm	
0.65	30	96	0.047	SP	40-60 cm	#1
0.63	25	82	0.037	SP	40-60 cm	#2
0.7	19	60	0.032	SP	40-60 cm	#3
0.66	25	79	0.038	SP	40-60 cm	
0.03	6	18	0.008	SP	40-60 cm	
0.58	22	74	0.02	SP	60-80 cm	#1
0.57	23	73	0.02	SP	60-80 cm	#2
0.66	25	94	0.04	SP	60-80 cm	#3
0.6	24	81	0.03	SP	60-80 cm	
0.05	2	12	0.01	SP	60-80 cm	

time		Mg µg/gsol	Ca µg/gsol	Na µg/gsol	K µg/gsol	Sr µg/gsol
T1	value	2.9	4	9	58	0.0175
T1	value	3.2	4.3	9.2	60	0.0185
T1	value	3.2	4.3	9.3	60	0.0191
T1	mean	3.1	4.2	9.1	59	0.0184
T1	SD	0.2	0.1	0.2	1	0.0008
T1	value	7.3	13	7.2	42	0.063
T1	value	7.3	12.3	7.2	42	0.058
T1	value	6.4	11.9	7	38	0.055
T1	mean	7	12.4	7.2	41	0.059
T1	SD	0.5	0.5	0.1	2	0.004
T1	value	4.6	5.7	4.8	26	0.036
T1	value	4.4	5.6	4.4	26	0.036
T1	value	4.1	5.4	4.1	24	0.034
T1	mean	4.4	5.6	4.4	25	0.035
T1	SD	0.3	0.1	0.3	1	0.001
T1	value	2.63	5.89	4.9	16.7	0.035
T1	value	2.65	5.82	4.96	16.2	0.038
T1	value	2.66	5.91	4.89	16.7	0.038
T1	mean	2.65	5.87	4.92	16.5	0.037
T1	SD	0.01	0.05	0.04	0.3	0.001
T1	value	2.3	5.5	4.6	19.3	0.0356
T1	value	2.25	5.9	4.7	19.2	0.0354
T1	value	2.31	5.6	4.7	20	0.0356
T1	mean	2.29	5.7	4.7	19.5	0.0355
T1	SD	0.03	0.2	0.1	0.5	0.0001
T1	value	2.03	5.9	3.85	23	0.0341
T1	value	2	6.2	3.92	22.7	0.0335
T1	value	1.93	5.7	3.94	22.6	0.0353
T1	mean	1.99	5.9	3.9	22.7	0.0343
T1	SD	0.05	0.2	0.05	0.2	0.0009
T2	value	2.5	2.46	5.32	48	0.0131
T2	value	3	2.59	5.41	50	0.0137
T2	value	2.6	2.48	5.42	47	0.0129
T2	mean	2.7	2.51	5.38	48	0.0132
T2	SD	0.3	0.07	0.05	2	0.0004
T2	value	4.8	6.7	2.2	31	0.0366
T2	value	4.5	6.5	2.1	29	0.0359

T2	value	4.4	6.4	2	28	0.035
T2	mean	4.6	6.5	2.1	30	0.0358
T2	SD	0.2	0.2	0.1	1	0.0008
T2	value	3.9	3.59	1.4	24	0.028
T2	value	3.7	3.56	1.2	23	0.029
T2	value	2.8	3.43	1.1	18	0.026
T2	mean	3.4	3.52	1.2	22	0.027
T2	SD	0.6	0.08	0.1	4	0.002
T2	value	1.61	3.82	1.19	13.4	0.026
T2	value	1.68	3.72	1.12	13.2	0.026
T2	value	1.67	3.8	1.18	14.1	0.028
T2	mean	1.65	3.78	1.16	13.6	0.027
T2	SD	0.04	0.05	0.04	0.5	0.001
T2	value	1.35	3.4	1.02	15.5	0.0281
T2	value	1.38	3.6	1.1	15.2	0.028
T2	value	1.4	3.7	1.1	15.6	0.0288
T2	mean	1.38	3.6	1.07	15.4	0.0283
T2	SD	0.02	0.1	0.05	0.2	0.0004
T2	value	1.3	3.7	1.01	16.4	0.0255
T2	value	1.22	3.69	0.86	16.9	0.0258
T2	value	1.24	3.53	0.91	15.9	0.026
T2	mean	1.25	3.64	0.93	16.4	0.0258
T2	SD	0.05	0.09	0.08	0.5	0.0002
T3	value	4.4	2.5	3.4	48	0.0156
T3	value	4.6	2.6	3.5	48	0.0159
T3	value	5.1	2.7	3.7	52	0.0159
T3	mean	4.7	2.6	3.5	49	0.0158
T3	SD	0.3	0.1	0.1	2	0.0002
T3	value	7.6	5.74	1.46	46	0.0331
T3	value	6.8	5.63	1.4	41	0.0317
T3	value	8	5.72	1.52	49	0.0328
T3	mean	7.5	5.7	1.46	45	0.0326
T3	SD	0.7	0.06	0.06	4	0.0007
T3	value	5	3.18	1.5	36	0.024
T3	value	5	3.11	1.5	35	0.025
T3	value	7	3.12	1.7	45	0.025
T3	mean	5	3.14	1.5	39	0.025
T3	SD	1	0.03	0.1	6	0.001
T3	value	1.34	2.9	1.4	20	0.021
T3	value	1.3	2.9	1.2	18.8	0.021
T3	value	1.32	2.87	1.2	19.4	0.024
T3	mean	1.32	2.89	1.3	19.4	0.022
T3	SD	0.02	0.02	0.1	0.6	0.002

T3	value	0.94	2.2	1.12	21.6	0.021
T3	value	0.97	2.4	1.11	20.5	0.022
T3	value	1.02	2.7	1.19	21.5	0.025
T3	mean	0.98	2.4	1.14	21.2	0.023
T3	SD	0.04	0.2	0.05	0.6	0.002
T3	value	0.91	2.2	1.26	24.4	0.02
T3	value	0.92	2.23	1.12	24.6	0.021
T3	value	0.93	2.11	1.24	24.4	0.022
T3	mean	0.92	2.18	1.2	24.5	0.021
T3	SD	0.01	0.06	0.07	0.1	0.001
T4	value	6.6	3.58	2.85	58	0.0204
T4	value	5.6	3.54	2.84	52	0.0197
T4	value	5.8	3.56	2.89	54	0.0191
T4	mean	6	3.56	2.86	54	0.0197
T4	SD	0.5	0.02	0.03	3	0.0006
T4	value	8	5	1.55	53	0.0329
T4	value	10	5.2	1.63	61	0.0327
T4	value	8	5	1.56	53	0.0336
T4	mean	9	5.1	1.58	55	0.0331
T4	SD	1	0.1	0.04	5	0.0004
T4	value	6.7	2.57	2.05	54	0.025
T4	value	5.7	2.53	1.89	48	0.028
T4	value	5.4	2.5	1.97	46	0.027
T4	mean	5.9	2.53	1.97	50	0.027
T4	SD	0.7	0.04	0.08	4	0.002
T4	value	1.2	1.88	1.54	26	0.021
T4	value	1.17	1.83	1.48	26	0.022
T4	value	1.2	1.81	1.45	27	0.025
T4	mean	1.19	1.84	1.49	26	0.023
T4	SD	0.02	0.03	0.04	1	0.002
T4	value	0.9	1.3	1.4	28.2	0.023
T4	value	0.94	1.5	1.38	28.2	0.023
T4	value	0.95	1.6	1.41	28.8	0.027
T4	mean	0.93	1.4	1.4	28.4	0.024
T4	SD	0.02	0.2	0.01	0.4	0.003
T4	value	0.956	1.29	1.54	32.3	0.021
T4	value	0.966	1.27	1.56	32	0.022
T4	value	0.95	1.23	1.65	33.2	0.025
T4	mean	0.957	1.26	1.59	32.5	0.023
T4	SD	0.008	0.03	0.06	0.6	0.002
T5	value	7.5	3.42	2.06	57	0.025
T5	value	7	3.43	2.11	54	0.025
T5	value	6.4	3.33	2.09	51	0.023

T5	mean	7	3.39	2.09	54	0.024
T5	SD	0.5	0.06	0.02	3	0.001
T5	value	8.3	4.59	1.41	53	0.0338
T5	value	9.6	4.68	1.5	60	0.0352
T5	value	9.4	4.62	1.55	60	0.0348
T5	mean	9.1	4.63	1.49	58	0.0346
T5	SD	0.7	0.05	0.07	4	0.0007
T5	value	4.3	2.42	1.81	43	0.028
T5	value	5.7	2.5	1.66	49	0.032
T5	value	5.4	2.35	1.81	48	0.029
T5	mean	5.1	2.42	1.76	47	0.03
T5	SD	0.7	0.08	0.08	3	0.002
T5	value	1.18	1.74	1.33	26.9	0.022
T5	value	1.14	1.78	1.24	25.7	0.023
T5	value	1.17	1.63	1.26	27	0.028
T5	mean	1.16	1.72	1.27	26.5	0.024
T5	SD	0.02	0.08	0.05	0.7	0.003
T5	value	1.04	1	1.23	28.3	0.025
T5	value	1.04	1.2	1.3	28.7	0.024
T5	value	1.07	1.4	1.31	29.4	0.03
T5	mean	1.05	1.2	1.28	28.8	0.027
T5	SD	0.02	0.2	0.04	0.6	0.003
T5	value	1.079	1	1.39	31.7	0.023
T5	value	1.083	0.98	1.36	31.3	0.025
T5	value	1.089	0.97	1.31	30.6	0.03
T5	mean	1.084	0.98	1.36	31.2	0.026
T5	SD	0.005	0.02	0.04	0.5	0.003
T6	value	9	3.9	1.62	59	0.028
T6	value	10	4.4	1.78	67	0.033
T6	value	11	4.2	1.76	70	0.033
T6	mean	10	4.2	1.72	65	0.031
T6	SD	1	0.3	0.09	5	0.002
T6	value	13	4.5	1.8	80	0.041
T6	value	13	4.3	1.7	78	0.039
T6	value	15	4.5	2	94	0.044
T6	mean	14	4.4	1.8	84	0.042
T6	SD	1	0.1	0.1	8	0.003
T6	value	8	2.2	2.2	63	0.034
T6	value	9	2.2	2.16	69	0.039
T6	value	10	2	2.26	75	0.037
T6	mean	9	2.2	2.21	69	0.037
T6	SD	1	0.1	0.05	6	0.003
T6	value	1.23	1.3	1.51	29.4	0.021

T6	value	1.13	1.29	1.42	28	0.022
T6	value	1.28	1.28	1.49	29.6	0.029
T6	mean	1.21	1.29	1.48	29	0.024
T6	SD	0.08	0.01	0.05	0.9	0.004
T6	value	1.11	0.8	1.58	30.8	0.024
T6	value	1.08	0.9	1.43	30.3	0.024
T6	value	1.12	1	1.46	32	0.022
T6	mean	1.1	0.9	1.49	31	0.023
T6	SD	0.02	0.1	0.08	0.9	0.001
T6	value	1.18	0.72	1.67	34	0.029
T6	value	1.16	0.71	1.57	34.9	0.023
T6	value	1.16	0.7	1.6	33.7	0.027
T6	mean	1.17	0.71	1.62	34.2	0.027
T6	SD	0.01	0.01	0.05	0.6	0.003
T7	value	8.6	5.01	1.46	58	0.037
T7	value	7.5	4.89	1.47	53	0.033
T7	value	8.4	4.98	1.52	57	0.034
T7	mean	8.2	4.96	1.48	56	0.035
T7	SD	0.6	0.06	0.03	3	0.002
T7	value	12	4.6	2.2	78	0.042
T7	value	9	4.1	2.09	62	0.035
T7	value	10	4.2	2.17	66	0.035
T7	mean	10	4.3	2.15	69	0.037
T7	SD	2	0.2	0.06	8	0.004
T7	value	8	1.9	3	72	0.039
T7	value	5	1.8	2.8	54	0.034
T7	value	6	1.7	2.8	58	0.032
T7	mean	6	1.8	2.9	61	0.035
T7	SD	2	0.1	0.1	9	0.004
T7	value	1.2	1	2.2	35	0.022
T7	value	1.7	1	2.4	39	0.032
T7	value	1.2	0.6	2.2	37	0.023
T7	mean	1.4	0.9	2.2	37	0.026
T7	SD	0.3	0.2	0.1	2	0.005
T7	value	1.4	0.72	2.1	38	0.027
T7	value	1.2	0.7	2	37	0.03
T7	value	1.4	0.58	2.4	42	0.024
T7	mean	1.4	0.67	2.2	39	0.027
T7	SD	0.1	0.08	0.2	3	0.003
T7	value	1.4	0.6	2.3	42	0.025
T7	value	1.4	0.6	2.5	42	0.03
T7	value	1.1	0.9	2	32	0.021
T7	mean	1.3	0.7	2.3	38	0.025

T7	SD	0.2	0.2	0.2	6	0.004
T8	value	8.7	7.1	1.48	58	0.045
T8	value	10.1	7.3	1.65	66	0.047
T8	value	10.3	7.5	1.61	66	0.047
T8	mean	9.7	7.3	1.58	63	0.046
T8	SD	0.9	0.2	0.09	5	0.001
T8	value	11	4.8	3.1	83	0.045
T8	value	13	4.5	3.2	91	0.047
T8	value	10	4.4	3.2	79	0.038
T8	mean	12	4.6	3.2	84	0.043
T8	SD	1	0.2	0.1	7	0.005
T8	value	7	1.8	4.5	76	0.039
T8	value	10	1.8	4.3	92	0.048
T8	value	8	1.6	4.3	80	0.042
T8	mean	8	1.7	4.4	83	0.043
	SD	2	0.1	0.1	8	0.005
T8	value	1.57	0.86	3.25	45	0.025
T8	value	1.55	0.87	3.06	43	0.026
T8	value	1.61	0.84	3.16	46	0.037
T8	mean	1.58	0.85	3.15	45	0.029
T8	SD	0.03	0.02	0.09	1	0.007
T8	value	1.68	0.57	3.22	48.4	0.028
T8	value	1.59	0.66	3.12	48.5	0.028
T8	value	1.61	0.63	3.1	49.3	0.033
T8	mean	1.62	0.62	3.15	48.7	0.03
T8	SD	0.05	0.04	0.07	0.5	0.003
T8	value	1.71	0.54	3.65	53.1	0.026
T8	value	1.8	0.62	3.58	54	0.03
T8	value	1.69	0.55	3.64	52.9	0.033
T8	mean	1.74	0.57	3.62	53.3	0.03
T8	SD	0.06	0.04	0.04	0.6	0.004
T9	value	17	10.7	1.9	94	0.056
T9	value	25	12.1	2.4	131	0.059
T9	value	21	11.8	2.3	114	0.06
T9	mean	21	11.5	2.2	113	0.058
T9	SD	4	0.7	0.2	19	0.002
T9	value	21	5.8	5	138	0.045
T9	value	24	6.2	5	157	0.051
T9	value	27	6	8	171	0.053
T9	mean	24	6	6	156	0.05
T9	SD	3	0.2	2	17	0.004
T9	value	8	1.93	6.2	88	0.06
T9	value	11	1.95	7	111	0.04

T9	value	14	1.81	7.6	131	0.04
T9	mean	11	1.9	6.9	110	0.05
T9	SD	3	0.08	0.7	21	0.01
T9	value	2.05	0.82	4.7	59	0.028
T9	value	2.04	0.8	4.7	60	0.029
T9	value	2.01	0.87	4.3	55	0.035
T9	mean	2.04	0.83	4.6	58	0.03
T9	SD	0.02	0.04	0.2	3	0.004
T9	value	2.35	0.54	4.8	63	0.031
T9	value	2.31	0.57	4.81	66	0.033
T9	value	2.32	0.55	4.87	65	0.03
T9	mean	2.32	0.56	4.83	65	0.031
T9	SD	0.02	0.02	0.04	2	0.002
T9	value	2.39	0.6	5.1	68	0.036
T9	value	2.46	0.59	5.3	70	0.031
T9	value	2.52	0.62	5.7	72	0.032
T9	mean	2.46	0.61	5.3	70	0.033
T9	SD	0.07	0.01	0.3	2	0.002
T10	value	25	14	3	131	0.12
T10	value	24	13.9	3.1	123	0.14
T10	value	31	15.4	3.4	159	0.11
T10	mean	27	14.4	3.2	138	0.12
T10	SD	4	0.8	0.2	19	0.01
T10	value	33	6.5	9.2	214	0.11
T10	value	32	6.4	9.2	214	0.14
T10	value	40	6.8	10.7	252	0.18
T10	mean	35	6.5	9.7	227	0.15
T10	SD	4	0.2	0.8	22	0.03
T10	value	33	1.5	12.7	237	0.13
T10	value	27	1.5	13.7	215	0.13
T10	value	20	1.1	13	170	0.04
T10	mean	27	1.4	13.1	208	0.1
T10	SD	7	0.2	0.5	34	0.05
T10	value	2.6	0.52	8.5	76	0.039
T10	value	2.9	0.49	8.9	80	0.041
T10	value	2.3	0.55	7.7	72	0.038
T10	mean	2.6	0.52	8.4	76	0.039
T10	SD	0.3	0.03	0.6	4	0.002
T10	value	2.154	0.38	9	80.2	0.038
T10	value	2.147	0.36	8.7	81.9	0.037
T10	value	2.166	0.34	9	80.6	0.036
T10	mean	2.156	0.36	8.9	80.9	0.037
T10	SD	0.009	0.02	0.2	0.9	0.001

T10	value	1.84	0.38	9.2	81	0.03
T10	value	1.82	0.35	9.9	84	0.03
T10	value	1.7	0.34	11	84	0.07
T10	mean	1.79	0.36	10.1	83	0.04
T10	SD	0.08	0.02	0.9	2	0.02
T11	value	31	17	4.1	156	0.15
T11	value	21	14	3.3	106	0.11
T11	value	35	18	4.1	176	0.17
T11	mean	29	16	3.8	146	0.14
T11	SD	7	2	0.5	36	0.03
T11	value	32	5.7	11	225	0.15
T11	value	34	5.4	13	243	0.17
T11	value	39	6.1	14	265	0.18
T11	mean	35	5.7	13	244	0.16
T11	SD	4	0.4	1	20	0.02
T11	value	19	1.06	13	163	0.18
T11	value	18	1.07	14	168	0.16
T11	value	33	0.95	20	259	0.28
T11	mean	23	1.02	16	197	0.21
T11	SD	9	0.07	4	54	0.06
T11	value	5	0.42	12.1	102	0.062
T11	value	4	0.34	12.6	97	0.056
T11	value	3	0.37	11.1	88	0.044
T11	mean	4	0.38	11.9	96	0.054
T11	SD	1	0.04	0.8	7	0.009
T11	value	3.7	0.3	14	105	0.06
T11	value	2.4	0.31	9	91	0.04
T11	value	2.7	0.28	12	97	0.04
T11	mean	2.9	0.3	12	97	0.05
T11	SD	0.7	0.02	2	7	0.01
T11	value	3.6	0.39	15	107	0.07
T11	value	2.6	0.33	13	102	0.05
T11	value	3.1	0.36	16	106	0.07
T11	mean	3.1	0.36	15	105	0.07
T11	SD	0.5	0.03	2	2	0.01

Declaration of interests

The authors declare that they have no known competing financial interests or personal relationships that could have appeared to influence the work reported in this paper.

The authors declare the following financial interests/personal relationships which may be considered as potential competing interests:

CRedit author statement

Matthias Oursin: Methodology, validation, Investigation, Formal analysis, writing – original draft.

Marie-Claire Pierret: Conceptualization, validation, Methodology, Investigation, visualization, Project administration, writing – review & editing, Supervision, Funding acquisition, Resources.

Emilie Beaulieu: Software, Formal analysis, Data curation, Methodology, Writing – review & editing, Supervision. **Damien Daval:** Formal analysis, Methodology, software, Writing – review & editing. **Arnaud Legout:** Conceptualization, Methodology, Writing – review & editing, Supervision, Formal analysis, Resources, Supervision.

1 Is there still something to eat for trees in the soils of the Strengbach catchment?

2 Matthias Oursin¹, Marie-Claire Pierret¹, Émilie Beaulieu^{1,2}, Damien Daval³, Arnaud Legout⁴

3

4 ¹ITES Institut Terre et Environnement de Strasbourg - CNRS/Université de Strasbourg - 5 rue
5 Descartes, 67000 Strasbourg. France. Oursin@unistra.fr / marie-claire.pierret@unistra.fr

6 ²ENGEES - École Nationale du Génie de l'Eau et de l'Environnement. 1 quai Koch- 67000
7 Strasbourg. France. beaulieu@engees.unistra.fr

8 ³Damien Daval – ISTERre Institut des Sciences de la Terre – CNRS/Université Grenoble Alpes
9 38000 Grenoble damien.daval@univ-grenoble-alpes.fr

10 ⁴INRAE, BEF, rue d'Amance, 54280 Champenoux. France. arnaud.legout@inrae.fr

11 Corresponding author: Marie-Claire Pierret marie-claire.pierret@unistra.fr

12

13 Supplementary material

14

15 Appendix A. Mineral and chemical composition of soils.

16

	<i>Depth</i>	Kaolinite	Illite	Vermiculite	Smectite	Muscovite	Biotite	Quartz	Orthose	Albite	OM
	<i>cm</i>	%	%	%	%	%	%	%	%	%	%
<i>Beech Plot</i>	0-5	1.4	22.0	1.3	5.2	5.7	0.6	8.3	9.6	6.5	39.4
<i>(BP)</i>	5-10	1.5	10.0	0.0	5.3	8.8	0.8	21.3	27.6	17.5	7.2
	10-20	1.1	7.8	1.3	4.8	10.8	0.7	18.9	25.8	21.4	7.5
	20-40	0.8	6.8	3.7	4.2	15.0	0.6	19.6	21.0	24.0	4.4
	40-60	1.4	6.4	2.5	3.5	20.4	0.6	13.8	23.5	24.0	3.9
	60-80	1.1	4.6	1.2	1.7	20.5	1.1	22.1	19.4	25.5	2.8
<i>Spruce Plot</i>	0-5	1.5	20.1	0.4	8.5	4.7	0.0	16.0	6.6	3.3	39.1
<i>(SP)</i>	5-10	0.5	10.7	0.0	7.7	14.4	0.8	38.9	7.7	5.3	14.0
	10-20	0.2	8.9	0.0	6.1	22.6	0.8	39.4	11.6	6.6	3.7
	20-40	0.2	8.6	1.3	9.3	20.9	0.0	32.9	20.0	4.5	2.2
	40-60	0.2	9.2	1.1	7.3	22.3	0.0	37.8	12.9	7.9	1.3
	60-80	0.1	7.3	1.1	7.5	17.6	0.0	39.0	15.4	11.0	1.0

17

18 Mineral composition of soils from beech and spruce plots, calculated from XRD analyses on
19 bulk soils and clays, and from organic matter content.

20

21

22

23

25 Chemical compositions (expressed in $\mu\text{g/g}$ of soil) for initial and final (after experimentation)
26 bulk soils, compared with the contribution of different reservoirs as clay minerals, initial and
27 final exchangeable pool, organic matter as total cumulated experimental leachate calculated for
28 1 g of soil.

29

30 **Appendix B. Composition of leaching solutions**

31

32 Mean chemical composition and standard deviation (SD) from the three triplicates of the
33 leaching solution at the eleven time-step of each experiment (see Table 1). Chemical
34 compositions are expressed in $\mu\text{g/g}$ of soil. *Data are provided as the excel file containing all*
35 *tables, the table is too big to be copy directly in this document.*

36

37 **Appendix C. Stock of Ca, Mg, Na and K**

Plot	Depth	Ca	Mg	Na	K	Plot	Depth	Ca	Mg	Na	K
-	cm	kg·ha ⁻¹	kg·ha ⁻¹	kg·ha ⁻¹	kg·ha ⁻¹	-	cm	kg·ha ⁻¹	kg·ha ⁻¹	kg·ha ⁻¹	kg·ha ⁻¹
Bulk soils						Clays					
Beech Plot (BP)	00-05	362	391	2375	7017	Beech Plot (BP)	00-05	92	278	795	2640
	05-10	284	575	4246	12615		05-10	33	331	347	2270
	10-20	550	1277	8672	26886		10-20	38	519	438	3231
	20-40	1285	3029	21187	64112		20-40	51	1864	316	10803
	40-60	1013	2423	16183	51389		40-60	57	896	761	5190
	60-80	1226	2793	16313	44682		60-80	37	504	414	2613
Spruce Plot (SP)	00-05	170	381	450	4050	Spruce Plot (SP)	00-05	45	290	161	2059
	05-10	70	601	691	6719		05-10	16	293	86	1979
	10-20	156	1178	1395	14740		10-20	14	472	81	2901
	20-40	341	4220	5253	47760		20-40	93	1333	1035	7840
	40-60	423	4494	6065	54937		40-60	50	1812	285	10301
	60-80	429	3604	4886	43982		60-80	38	1321	205	7516
Ini Exch						OM					
Beech Plot (BP)	00-05	199	34	5	92	Beech Plot (BP)	00-05	614	88	32	288
	05-10	20	6	2	23		05-10	112	16	6	53
	10-20	13	6	3	30		10-20	234	34	12	110
	20-40	22	8	9	53		20-40	328	47	17	154
	40-60	12	3	7	22		40-60	233	34	12	110
	60-80	6	1	6	13		60-80	150	21	8	70
Spruce Plot (SP)	00-05	142	27	5	65	Spruce Plot (SP)	00-05	1422	37	8	117
	05-10	30	6	2	18		05-10	509	13	3	42
	10-20	17	5	3	19		10-20	269	7	2	22
	20-40	39	7	6	46		20-40	446	12	2	37
	40-60	24	5	7	49		40-60	290	7	2	24
	60-80	15	3	4	41		60-80	176	5	1	14
Final Exch											
Beech Plot (BP)	00-05	143	20	4	32						
	05-10	12	3	7	41						
	10-20	10	5	12	70						
	20-40	13	8	18	147						
	40-60	7	3	9	75						
	60-80	6	2	12	69						
Spruce Plot (SP)	00-05	122	23	1	30						
	05-10	24	7	3	37						
	10-20	8	9	3	85						
	20-40	17	17	9	225						
	40-60	11	22	11	255						
	60-80	11	18	8	262						

38

39 Evaluation of the stock of Ca, Mg, Na and K in bulk soil, and in the different reservoirs: initial
40 and final exchangeable cations, clays, and organic matter in each soil layer (expressed in
41 kg/hectare). This calculation considers the proportion of these different reservoirs inside the
42 bulk soils.

43

44

45 **Appendix D. Evaluation and calculation of stocks available and leaching flux in**

46 **Strengbach soils. Fluxes and input-output budgets**

47 - Calculation of the total stock and the exchangeable stock expressed in kg/ha:

48 Element inventories are evaluated in the total soil and in the exchangeable phase based on the
49 concentrations previously measured for each horizon studied. These inventories are expressed
50 in $\text{kg}\cdot\text{ha}^{-1}$.

51 The leaching experiments were carried out with the fraction of the soil $f < 2 \text{ mm}$, thus this
52 fraction is used for the calculations:

$$m_{total\ horizon} \times f_{<2mm} = m_{f<2mm} \quad (0-1)$$

53

54 Each horizon has a defined surface area S of 2 m^2 and a thickness e (5,10 or 20 cm), which give
55 the mass per unit of volume:

$$\rho_{f<2mm} = \frac{m_{f<2mm}}{V_{horizon}} = \frac{m_{f<2mm}}{S \times e} \quad (0-2)$$

56 This density is then used to determine the stocks available on a full hectare ($10,000 \text{ m}^2$). A
57 horizon with a thickness e and with a surface area of 1 ha is considered. The stock for each
58 chemical element i (expressed in $\text{kg}\cdot\text{ha}^{-1}$) was calculated with the elemental concentration C_i .

$$Stock_{i_{f<2mm}} = C_{i_{f<2mm}} \times 10000 \times e \times \rho_{f<2mm} \quad (0-3)$$

59

60 The stocks were calculated for the bulk soil and for the exchangeable pool from the
61 concentration in bulk soil and exchangeable fraction respectively.

62 This calculation is performed for each element and for each horizon of the two plots. To
63 simplify certain calculations, the total stock in the entire profile is also used, which is expressed
64 as the sum of the stocks of each horizon:

$$Stock_{total} = \sum Stock_i \quad (0-4)$$

65

66 - Calculation of total leached concentration expressed in kg/ha:

67 The same equation is used to calculate the total amount A of element leached during the
68 experiment for one ha:

$$A_{leaching}(kg \cdot ha^{-1}) = C_{cumulative\ leaching}(kg \cdot kg_{soil}^{-1}) \times 10000 \times e \times \rho_{f<2mm} \quad (0-5)$$

69

70 With $C_{cumulative\ leaching}$ the cumulative concentration leached during the 11 steps of the 152 days
71 of experimentation.

72

73 - Calculation of the leaching flux:

74 The leaching flux is calculated from the results of the leaching experiments, for each plot. The
75 leaching experiments were carried out with 5 grams of soil. The time of experiment should be
76 converted in corresponding in-situ field time in order to evaluate the leaching flux for each
77 element in $kg \cdot ha^{-1} \cdot yr^{-1}$. The idea is to convert the water/material ratio in quantity or duration of
78 rainfall in the site. The mean annual rainfall at the Strengbach catchment is 1400 mm (Pierret
79 et al., 2018). The interception by vegetation is on average 300 mm/yr (Pierret et al., 2019). Thus
80 the annual water flow infiltrating the soil is 1100 mm (1100 $L \cdot m^{-2}$ per year).

81 During the experiments, a $V_{experimental}$ volume of 440 mL of solution and a $m_{experimental}$ mass of
82 5 g were used. Thus, for a pit of mass m , the amount of rainfall, noted $V_{equivalent}$ required to
83 leach in the same proportions is:

$$V_{equivalent}(L \cdot m^{-2}) = m_{f<2mm}(kg) \times \frac{V_{experimental}(L)}{m_{experimental}(kg)} \times \frac{1}{S(m^2)} \quad (0-6)$$

84 The equivalent time ($t_{equivalent}$ in year) corresponding to the experimental condition i.e. 152 days
85 (Table 1) is then:

$$t_{equivalent} = \frac{V_{equivalent}}{V_{rain}} \quad (0-7)$$

86

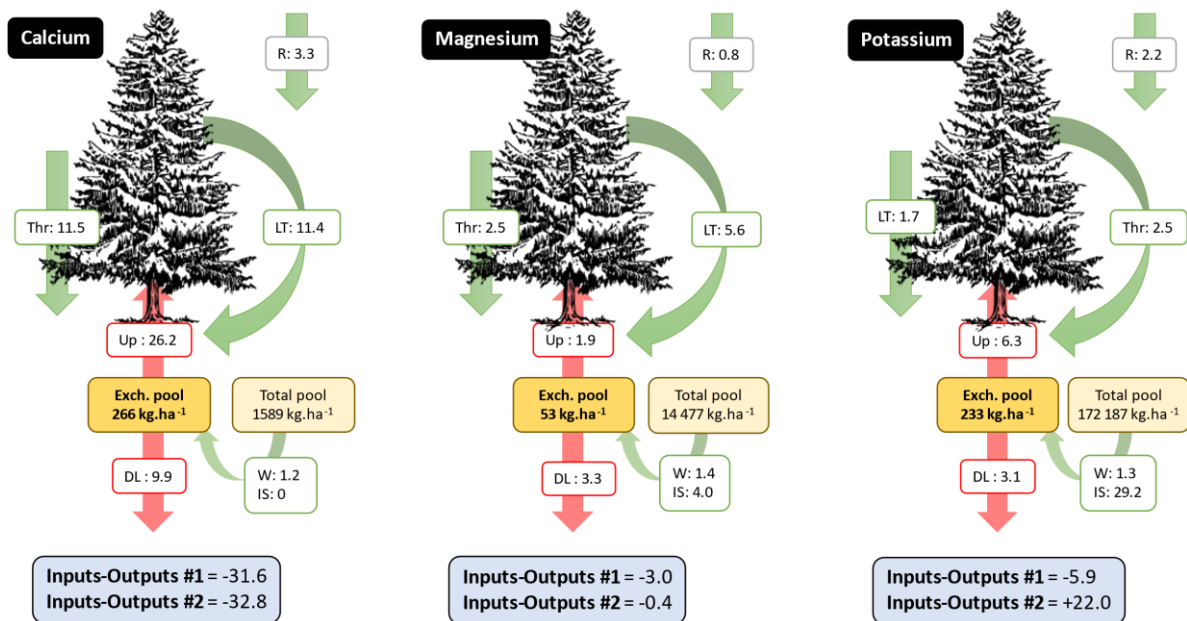
87 The result obtained give 42 years of rain for experiment with soils from the beech plot and 35
 88 years with soils from the spruce plot. This equivalent time allows to calculate the equivalent
 89 annual leaching flow according to:

$$flux_{leaching}(kg \cdot ha^{-1} \cdot yr^{-1}) = IS = \frac{A_{leaching} - Stock_{exchangeable}}{t_{leaching}} \quad (0-8)$$

90

91 If the leaching flux is lower than the initial exchangeable pool, then IS is equal to 0 (see figures)

92



93

94 Fluxes and input-output budgets (in kg·ha⁻¹·yr⁻¹) for calcium, magnesium and potassium at the
 95 SP site. IS is intrinsic flux from soil estimated from our leaching experiments (corrected for the
 96 value of the initial exchangeable pool). W is the weathering flux, R is the atmospheric wet
 97 deposition, Up is the net uptake flux by roots and DL is the deep leaching (see Beaulieu et al.
 98 2020).

99

100 CRediT author statement

101 **Matthias Oursin**: Methodology, validation, Investigation, Formal analysis, writing – original
102 draft. **Marie-Claire Pierret**: Conceptualization, validation, Methodology, Investigation,
103 visualization, Project administration, writing – review & editing, Supervision, Funding
104 acquisition, Resources. **Emilie Beaulieu**: Software, Formal analysis, Data curation,
105 Methodology, Writing – review & editing, Supervision. **Damien Daval**: Formal analysis,
106 Methodology, software, Writing – review & editing. **Arnaud Legout**: Conceptualization,
107 Methodology, Writing – review & editing, Supervision, Formal analysis, Resources,
108 Supervision.

109 Funding

110 ANR HYDROCRIZSTO ANR-15-CE01-0010-02 provided the funding for this study.

111 Acknowledgments

112 We thank OHGE (<http://ohge.unistra.fr/> and Solenn Cotel, Daniel Viville and Sylvain
113 Benarioumlil) for providing all hydro-meteorological data used in this study. We also thank
114 Colin Fourtet, Bernd Zeller and Serge Didier for their generous support during the sampling
115 fieldwork. Thank to Amélie Aubert, Colin Fourtet, René Boutin and Thierry Peronne for
116 technical assistance. The Observatoire Hydro-Géochimique de l'Environnement OHGE is
117 financially supported by INSU-CNRS and is part of the OZCAR French Critical Zone
118 Observatory Network (<https://www.ozcar-ri.org/fr>).

119 This is an EOST - ITES contribution.

120